Dissertation zur Erlangung des Doktorgrades

der Fakultät für Chemie und Pharmazie

der Ludwig-Maximilians-Universität München

Development of sustained release formulations for the intra-articular delivery of a therapeutic antibody

Eva-Maria Ruberg

aus

Speyer

2013

Erklärung

Diese Dissertation wurde im Sinne von § 7 der Promotionsordnung vom 28. November 2011 von Herrn Prof. Dr. Wolfgang Frieß betreut.

Eidesstattliche Versicherung

Diese Disseration wurde eigenständig und ohne unerlaubte Hilfe erarbeitet.

München, 25.01.2013

.....

Eva-Maria Ruberg

Dissertation eingereicht am 25.01.2013

1. Gutachter: Prof. Dr. Wolfgang Frieß

2. Gutachter: Prof. Dr. Gerhard Winter

Mündliche Prüfung am 04.03.2013

Acknowledgements

The present thesis was prepared at the Department of Pharmacy, Pharmaceutical Technology and Biopharmaceutics at the Ludwig-Maximilians-University Munich, Germany under the supervision of Prof. Wolfgang Frieß.

At first, I would like to express my deepest gratitude to Prof. Wolfgang Frieß for giving me the opportunity to be a member of his research group, for his scientific guidance through this interesting project and the personal advices. Thank you for the pleasant working atmosphere and the numerous social activities.

My sincere thanks go to Prof. Gerhard Winter for his dedicated leadership of the chair, the scientific programs and the excellent working conditions. Thank you for kindly being co-referee of this thesis.

Abbott GmbH & Co. KG is greatfully acknowledged for the financial support and the generous drug supply. Especially, I would like to thank Dr. Michael Siedler for the scientific advices, valuable discussions and for giving me the chance to join his group in Worcester, USA for some weeks. Moreover, I would like to express my profound thanks to Dr. Markus Tschoepe for rendering every assistance and scientific support during the project. I am indepted to all other people from Abbott for practical and scientific help.

Moreover, I would like to thank Christian Minke from the Department of Chemistry of the LMU Munich for the SEM measurements and Sabine Barnert from the University of Freiburg for the Cryo-TEM measurements.

I thank my bachelor and master students Maria Amundsen, Florian Prändl, Patrik Kondziella and Constanze Blümel for the great work they did and the friendly discussions.

Dr. Winfried Schlögl, Philipp Matthias, Madeleine Witting and Verena Saller are kindly acknowledged for the IT support. Thanks are also extended to Imke Leitner for the outstanding help at any time.

Futhermore, all my present and former colleagues are kindly acknowledged for the every day coffee breaks, the warm and friendly working atmosphere, the weekly running group and the great time we spent together. Particularily, I want to thank Kerstin Höger, Dr. Sarah Claus, Dr. Julia Kasper, Kristine Berkenhoff, Dr. Winfried Schlögl, Tim Menzen, Philipp Matthias, Verena Saller, Madeleine Witting, Dr. Sarah Küchler, Sarah Zölls, Stefanie Funke, Kay Strüver, Cihad Anamur, Christian Neuhofer, Martina Sprengholz, Thomas Bosch,

Sebastian Hertel, Raimund Geidobler, Yibin Deng, Dr. Katja Schmid, Dr. Miriam Printz, Dr. Lars Schiefelbein, Dr. Johannes Mathes, Dr. Frank Schaubhut and Dr. Sebastian Fuchs. Special thanks go to my room mates Julia, Sarah and Kerstin. Thank you for the great time, the numerous chats and chocolate breaks in our “Teestube” and your friendship.

Hermann Röder and Cathy Gohdes are kindly acknowledged for proof reading parts of my thesis.

Above all, I want to thank my parents and Florian for their great support, the never ending encouragement and for their love.

Für meine Eltern

TABLE OF CONTENTS

CHAPTER 1

GENERAL INTRODUCTION AND OBJECTIVES OF THE THESIS

CHAPTER 2

DEVELOPMENT OF AN *IN SITU* FORMING POLY(LACTIDE-CO-GLYCOLIDE)-BASED FORMULATION FOR THE INTRA-ARTICULAR DELIVERY OF A THERAPEUTIC ANTIBODY

CHAPTER 3

THE USE OF POLYSACCHARIDES AS CARRIERS FOR THE INTRA-ARTICULAR DELIVERY OF A THERAPEUTIC ANTIBODY

CHAPTER 4

DEVELOPMENT OF A PHOSPHOLIPID-BASED FORMULATION FOR THE INTRA-ARTICULAR DELIVERY OF A THERAPEUTIC ANTIBODY

CHAPTER 1

GENERAL INTRODUCTION AND OBJECTIVES OF THE THESIS

1 GENERAL INTRODUCTION

1.1 Current management of arthritic diseases

Arthritic diseases are considered as one of the leading causes for progressive and irreversible joint degeneration resulting in reduced quality of life and/or disability [1]. Osteoarthrits (OA) and rheumatoid arthritis (RA) are the most common forms, affecting predominantly weight bearing joints such as knees, hips and ankles [1, 2]. The main symptoms are joint inflammation, pain and cartilage destruction. Due to a high prevalence in the elderly population, the number of affected patients in the US is expected to reach 60 millions by the year 2020, thus presenting an enormous social and economical burden [3]. As no curative therapy has been developed so far, the medical disease management is focused on the reduction of pain and inflammation in order to maintain mobility and prevent joint degeneration [4, 5]. According to the guidelines of the American College of Rheumatology and Osteoarthritis Research Society International, the current treatment of OA includes the systemic and intra-articular (IA) application of non-biologic drugs such as corticosteroids, analgetic and anti-inflammatory agents. The treatment of RA includes additional systemic administration of disease-modifying anti-rheumatic drugs (DMARDs), such as methotrexate, sulfasalazine, cyclosporine, hydroxychloroquine, penicillamine or azathioprine, and biologic agents like interleukine-1 receptor antagonists or TNF-α antagonists [5-7]. The long-term systemic application of these therapeutics frequently results in substantial side-effects [8]. Moreover, oftentimes high doses are required to achieve adequate therapeutic drug levels in the affected joint which makes therapies with e.g. biologic agents highly expensive [9]. The local direct targeting of the affected site by IA application of the drug presents an attractive approach from both the economic and the patient´s perspective. It offers the possibility to achieve high drug concentrations at the site of

application with limited systemic exposure leading to overall dose reduction and therefore minimization of side-effects and costs. Furthermore, drugs with low bioavailability can be administered [10]. However, the IA route of application is accompanied by pain for the patient and bears the risk of joint infections and cartilage damage. Therefore, the IA injection frequency should be limited (see section 1.3) [11].

1.2 Anatomy and physiology of the joint

Joints can be classified into amphiathroses, synarthroses and diarthroses (synovial joints). Synovial joints, most often affected by OA and RA, are enclosed by a fibrous capsule and ligaments providing joint stability and mobility. The surfaces of the bone endings are covered by hyaline cartilage contributing to an almost frictionless mobility of the joint. The cartilage is an avascular tissue, composed of chondrocytes embedded in a matrix of collagen, proteoglycans and water [12]. It is supplied with nutritiens by the synovial fluid (SF), a viscous liquid with similar composition to plasma. In comparison to plasma, SF comprises additional amounts of hyaluronic acid and lubricin, both providing lubricating functions [13]. Moreover, lower total protein concentrations, e.g. albumin, are found in SF [13, 14]. In normal joints, the SF volume is approximately 0.5-2 mL whereas in RA affected joints, it can be increased up to 100 mL [13, 15]. The inner layer of the joint capsule is lined by the vascularized synovial membrane (synovium) consisting of type A and B synoviocytes and capillaries. Type A synoviocytes have macrophage-like properties whereas type B cells secrete hyaluronic acid and lubricin [15]. Both the synovial membrane and the capillary endothelium are highly fenestrated. Due to the little diffusion barrier provided by the synovial membrane, a high synovial turnover is observed with a complete SF replacement within 2 hrs [13]. Small molecules with a molecular weight (MW) below 10 kDa are in equilibrium between SF and plasma as diffusion through the intercellular gaps of the synovial membrane and across the capillary walls is enabled. The synovial entrance of higher MW molecules, such as proteins, is limited by the endothelial fenestration and presents therefore a size dependent process. In comparison, clearance of higher MW species is reported to occur via lymph drainage in the subsynovial tissue [15]. Rodnan *et al.* investigated the clearance of IA injected molecules of different size and albumin (67 kDa) and γ-globulin (150 kDa) left the joint space within the same time of 72 hrs [16]. These data indicate that the synovial clearance presents a size-independent mechanism for molecules within the size range of plasma molecules. Instead of diffusion, clearance via passive bulk flow of the lymphatic drainage presents the predominant mechanism [17]. Upon joint inflammation, permeability of

the capillary walls is enhanced leading to an increase of volume and protein concentration in SF, but also to an accelerated synovial clearance rate.

1.3 The intra-articular route of application

The IA route of application offers the possibility to target the localized affected tissue of the joint while circumventing high systemic drug exposure that it is typically observed upon systemic dosing. The IA adminstration is characterized by direct injection of the drug into the joint cavity. Due to the risk of serious infections and cartilage damage induced by incorrect needle placement, sterile conditions and application from experienced physicians are of utmost importance [18]. The number of injections per joint and year should be limited to 3-4 [11]. According to clinical studies, a post-injection rest of 24 hrs is recommended in order to increase the residence time of the drug at the site of application [11]. Aspiration of SF prior to administration of the drug is suggested as it reduces dilution of the injected drug and oftentimes relieves pain [11, 18]. Because of the rapid clearance from the synovial space, the IA delivery of therapeutic drugs presents a challenging approach with respect to the maintenance of therapeutic concentrations for prolonged periods of time. For paracetamol and diclofenac mean terminal half-lives of 1.1 and 5.2 hrs were reported respectively [19]. IA application of anakinra, a recombinant interleukine-1 receptor antagonist, in patients suffering of OA, revealed a slight improvement of the symptoms until day 4 in comparison to placebo. Afterwards, no significant difference was detectable suggesting that IA injection does no lead to depot formation in the joint [20]. These examples emphasize the need for injectable depot systems that facilitate prolonged therapeutic action at the site of application.

1.4 Requirements on formulations for intra-articular administration

The IA route of application presents a special form of the parenteral way of administration. Therefore, the pH of the formulation should be isohydric or exhibit a pH close to 7.4. Isotonicity is desirable to provide high physiological compatibility. In order to avoid joint infection and further inflammation, sterility is of major importance [13]. Therefore, the use of pre-filled syringes is advantageous since critical preparation steps, such as formulation transfer from vial into syringe, entails the risk of contamination [11, 13]. In order to allow a rapid and easy application through thin syringe needles, an adequate formulation viscosity needs to be provided. It is known from literature that the maximal injection force should not exceed 25 N [21]. The syringe needle size is reported to differ depending on the affected

joint and the patient´s constitution. Commonly recommended needle sizes for knee or shoulder treatment are in the range of 18 G to 25 G. Smaller joints, e.g. interphalangeal joints, require smaller needle sizes in the range of 25-30 G [22]. Compatibility of the formulation components with both the injection site and the incorporated drug has to be assured as activation of unwanted immune responses may amplify the inflammatory conditions [13]. After injection, the formulation should allow preservation of the entire joint mobility. Therefore, a semi-solid consistency is beneficial in order to avoid joint blockage or cartilage friction. On account of the limited injection frequency, the restricted injection volume and the rapid clearance of injected drugs, a high drug load and a prolonged residence time at the injection site present central formulation aspects.

1.5 Intra-articular drug delivery systems

Several attempts were made with respect to prolongation of the drug residence time at the site of application. On the German market, mainly glucocorticoid products can be found that are formulated as (crystal-) suspensions (table 1-1). As they show poor aqueous solubility continuous dissolution occurs upon IA administration, leading to prolonged drug concentrations over several days [13, 23]. Also an emulsion formulation, containing dexamethasone-21-palmitate, has received approval for IA administration. This formulation provides a mean residence time in the joint of 8 days [24]. Besides the drug containing formulations, several hyaluronic acid formulations can be found on the market. The use of hyaluronic acid gels for the treatment of arthritic diseases can be attributed to its viscosupplememententative effect, as the lubricating properties of SF are typically reduced in arthritic joints [25]. Moreover, anti-inflammatory properties of HA are discussed in literature [26].

Besides the formulations available on the market, intensive research has been focused on the development of other drug delivery systems for sustained drug release. Most of the drug delivery systems in literature are based on microparticles or microspheres. The use of semi-solid formulations is also reported. The group of Liang analyzed the pharmacokinetic profile of 30-100 µm polylactide microparticles containing methotrexate after IA administration in healthy rabbits. In comparison to the free drug, significantly higher methotrexate levels were found in the SF 6 hrs after injection and in the synovial tissue after 24 hrs [27]. Thakkar *et al.* investigated the effect of chitosan microparticles containing celecoxib in arthritic rats over an observation period of 18 days. A continuous anti-inflammatory effect was demonstrated. In comparison, after IA administration of the free drug, an initial reduction of the joint

inflammation was observed that increased again until the end of the study [28]. Mierisch *et al.* proposed calcium alginate beads as carrier system for the IA delivery of transforming growth factor-β (TGF-β). *In vitro* experiments revealed a slow release rate of 0.25 % per hour. The results were underlined by *in vivo* experiments in rabbits where an improved effect on osteochondral defects was demonstrated [29]. The studies mentioned above emphasize the potential of drug-loaded microparticles to prolong the therapeutic effect after IA administration. In patent literature, the use of HA based injectable microparticles for the sustained release of proteins or peptides is described. Even though the IA application is not described by the authors, the IA use of this drug delivery system would present an interesting approach due to the physiological presence of HA in the SF [30, 31].

Table 1-1 IA formulations on the German market, derived from [13] and [32].

Active pharmaceutical ingredient	Exemplary product name	Formulation
Betamethasone hydrogenphosphate disodium/ Betamethasone acetate	Celestan Depot®	Solution
Dexamethasone hydrogenphosphate disodium	Dexabene®, Fortecortin® Inject	
Gadopentic acid	Magnevist®	
Gadoteric acid	Artirem®	
Hyaluronic acid	Curavisc®	
Hyaluronic acid, cross-linked	Synvisc®	
Hyaluronate sodium	Viscoseal®	
Prednisolone acetate	Prednigalen®	
Betamethasone hydrogenphosphate disodium / Betamethasone dipropionate	Diprosone® Depot	Suspension
Dexamethasone acetate / lidocaine-HCl	Supertendin®	
Prednisolone acetate	Predni H injekt®	
Triamcinolone acetonide	Volon A®	
Triamcinolone-16, 21-diacetate	Delphicort®	
Triamcinolone hexacetonide	Lederlon®	
Dexamethasone-21-palmitate	Lipotalon®	Emulsion

Besides the use of polymer-based formulations, numerous studies can be found dealing with the liposomal drug encapsulation. The concept of IA administration of drug-loaded liposomes for the treatment of inflammatory joint diseases was first described by Shaw *et al.* in 1976 [33]. Dingle *et al.* reported a significant reduction of joint inflammation, temperature and

diameter in arthritic rabbits during an observation period of 6 days after IA injection of cortisol containing liposomes. Upon administration of the free drug an anti-inflammatory response was only detectable at higher concentrations during the first 24 hrs [34]. Comparable studies can be found on the IA administration of liposomally encapsulated drugs, such as dexamethasone palmitate [35], methotrexate [36], lidocaine [37], lactoferrin [38], iohexol [39], triamcinolone acetonide [40] or the radionuclide [^{99m}Tc]pertechnetate [41]. The successful IA injection of liposomal Verteporfin® for the photodynamic therapy of RA as an alternative to surgical or radiation synvectomy was demonstrated by Chowdhary *et al.* in arthritic rabbits. High accumulation of the liposomes in the synovial tissue without recovery in plasma was observed 3 hrs after IA injection. Upon intravenous (IV) application, liposomes were recovered both in the synovial tissue and in plasma [42]. Tanaka *et al.* presented an interesting approach to extend IA drug residence time using magnetic liposomes containing TGF-β. Prior to injection of the liposomal formulation, magnetic implants were inserted into the articular cartilage of rabbits. Upon administration of the TGF-β liposomes containing Fe_3O_4 as magnetic agent, cartilage defects were continuously reduced within the observation period of 12 weeks. This effect was attributed to the magnetic induced accumulation of the liposomes at the target site [43]. Instead of magnet implantation, Butoescu *et al.* reported about the use of a local external magnetic field leading to IA retention of dexamethasone acetate-loaded PLGA microparticles that contain superparamagnetic iron oxide nanoparticles (SPIONs) [44].

1.6 Drug delivery systems for therapeutic proteins

Despite the numerous promising studies found in literature, IA delivery approaches for therapeutic proteins are rare at present. Concomitantly with the tremendous advances in biotechnology, which have revolutionized the therapies of chronic and life-threatening diseases, the demand for the development of injectable protein delivery systems has increased in recent years [45] due to the oftentimes short drug plasma half-lives and thus high injection frequencies [46]. Numerous research groups have been focused on this topic, however, no sustained release formulation for a therapeutic protein can be found on the market which emphasizes the challenge of this approach [47]. Delivery strategies for proteins have been extensively reviewed in literature [9, 48-52]. The protein stability within the delivery system and upon release presents an important aspect as the native three-dimensional macromolecular structure strongly correlates with biological activity [53] and protein denaturation is known to provoke immunological repsonses in the body [54].

In literature, microparticles, solid or *in situ* forming implants, liposomes or hydrogels are mainly reported as potential carrier systems for the sustained release of proteins. These systems primarily consist of synthetic or natural polymers or lipids. The most frequently used synthetic polymers in this context are polylactide (PLA) and poly(lactide-co-glycolide) (PLGA), formulated as microparticles or *in situ* forming implants [55-58]. The extensive use can be attributed to the high biocompatibility and safety which led to approval by the Food and Drug Administration [59]. But also natural polymers such as gelatin [60], chitosan [61], alginate [62] or hyaluronic acid [30], formulated as microparticles or hydrogels, were demonstrated to present suitable carrier materials. Microparticle systems suffer from the major disadvantage that only low amounts of drug can be loaded [48]. Moreover, in case of PLGA-based microparticles, harsh preparation conditions are required. The formation of organic/water interfaces is reported to bear the risk of protein unfolding and thus presents a major drawback for the incorporation of susceptible proteins [48, 63]. In contrast, the *in situ* depot formation based on e.g. PLGA is an attractive alternative. Although protein instability related to PLA and PLGA degradation has been discussed [64, 65], promising release studies can be found in literature [57, 58]. Hydrogels reveal a highly protein-compatible environment due to the hydrophilic character of the matrix. The drug release velocity can be tailored by variation of the concentration and MW of the polymer. Chemical or physical cross-linkage of hydrogels is a frequently applied method to decelerate drug release due to the formation of a dense hydrogel network [49, 66]. However, cross-linkage of hydrogels might compromise protein stability [66]. Apart from the above mentioned formulation approaches, lipid derived protein delivery systems have been in the focus of several research groups [67-69]. Besides the development of solid lipid implants [70] or solid lipid particles [71], drug encapsulation into lipid vesicles was demonstrated to provide protein release over prolonged periods of time [68, 69] and high protein stability [68, 72].

As the IA route of application presents a special form of the parenteral route of administration, the current knowledge concerning the controlled parenteral release strategies for therapeutic proteins can be adopted and form the basis of the present project. However, the prevailing physiologic conditions in the joint, such as clearance mechanism and velocity, pH and composition of SF have to be taken into consideration. Moreover, formulation aspects, like injectable volume, release window, type and viscosity of the formulation are important parameters that have to be included.

2 OBJECTIVES OF THE THESIS

The aim of the present project was the development of sustained release formulations for the IA application of a therapeutic monoclonal antibody (mAb). Within this scope, four formulations were to be developed which should provide different release profiles and depot forming mechanisms. On account of the characteristics of the IA route of application and the physiological conditions in the joint, the formulations to be developed were intended to fulfill a variety of requirements. In order to avoid critical preparation steps that might introduce the risk of contamination, the formulations were envisaged to show a convenient and easy handling. An adequate viscosity was required to allow injectability through thin syringe needles. The syringe needle size commonly used for IA injection depends on the joint to be treated. In order to assure adequate injection even into small joints, injectability was primarily evaluated by using 26 G syringe needles. This needle size is representative for the lower needle size limit. With regards to the formulation consistency after injection, the focus was on the development of a semi-solid depot enabeling entire mobility of the joint and providing prolonged residence time in the joint cavity. Due to the restricted injection volume and the limited injection frequency, a high drug load was desirable. The mAb-loaded formulation was intended to provide a constant drug release over a prolonged period of time. Besides the physical characterization of the carrier systems, a detailed understanding concerning the protein´s conformational stability upon incorporation into the formulation and release was within the focus of this project. *In vitro* mAb release from the formulations was to be investigated by using adequate release models that simulate well the physiological conditions present in the joint. Based on the most promising *in vitro* release profiles, the pharmacokinetic characteristics should be evaluated *in vivo* by making use of a rat model.

The first objective of this work was the development of an *in situ* forming PLGA formulation, suitable for the IA administration of mAb (Chapter 2). Into a non-aqueous PLGA solution, mAb was to be suspended as spray-dried powder. Upon contact with aqueous body fluid, PLGA precipitation occurs on account of the solvent exchange which leads to entrapment of the mAb particles. As PLGA is a hydrolytically unstable polymer, sustained mAb release occurs simultaneously with polymer degradation. A suitable formulation composition was to be evaluated with respect to mAb stability and *in vitro* mAb release. Therefore, the PLGA type and content as well as the choice, type and concentration of the non-aqueous organic PLGA solvents were to be varied. Based on *in vitro* and *in vivo* data, the efficiency of this formulation for the IA delivery of mAb was to be assessed.

The suitability of polysaccharides as carrier for the local IA delivery of mAb was investigated in Chapter 3. Hyaluronic acid (HA) was used as gel forming agent for the preparation of a highly-concentrated mAb-containing gel. Besides the detailed formulation characterization, it was an additional aim to investigate the presence of electrostatic interactions between negatively charged HA and slightly positively charged mAb at physiological pH. Within this scope, sodium alginate, a polysaccharide with a higher charge density than HA, was additionally used to study the conditions at which insoluble charge complexes with mAb are formed that could contribute to enhanced mAb retention within the joint cavity.

In Chapter 4 the development of phospholipid (PL)-based mAb containing formulations is presented. Two different formulations were within the scope of this study. In a first approach, an *in situ* forming PL-mAb formulation was to be developed, consisting of spray-dried mAb particles suspended within a non-aqueous PL solution. Upon contact with SF, the formulation was envisaged to spontaneously transfer into a vesicular formulation, causing the dissolution of the incorporated mAb particles and mAb entrapment into the vesicles. The second approach comprised the development of a vesicular PL-mAb formulation that was intended to be prepared *ex vivo* by mixing of a non-aqueous PL solution with a highly-concentrated mAb solution. After being administered into the joint cavity, both formulations were expected to provide prolonged residence time and thus sustained synovial mAb concentration and therapeutic effects.

CHAPTER 2

DEVELOPMENT OF AN *IN SITU* FORMING POLY(LACTIDE-CO-GLYCOLIDE)-BASED FORMULATION FOR THE INTRA-ARTICULAR DELIVERY OF A THERAPEUTIC ANTIBODY

1 INTRODUCTION

Since the first approval by the FDA as carrier material for the application of therapeutic drugs in humans, poly(lactide-co-glycolide) (PLGA) has received enormous interest because this polymer shows complete biodegradability, high biocompatibility and the potential to release incorporated drugs in a controlled manner over a period of days to months [59, 73, 74]. PLGA is a co-polymer of lactic and glycolic acid and belongs to the group of hydrolysable synthetic polyesters. In aqueous environment, its ester bonds are cleaved into shorter chains and ultimately into α-hydroxy acids which makes surgery for removal of PLGA carriers unnecessary [59]. PLGA degradation has been studied intensively and is reported to be influenced by the polymer properties (molecular weight (MW) [75], co-polymer ratio [59], esterification of the end-group functionality [76]), formulation components (organic solvents [77], pH regulating excipients [78]), sterilization techniques [79, 80] as well as by the properties of the release medium (temperature [81], pH, solvent [82]). PLGA has been mainly used as carrier material for the preparation of drug loaded solid implants and microparticles. Despite the presence on the market, solid implants suffer from low patient acceptance due to painful administration as large trochars are required [83]. Drug loaded microparticles present a more attractive way for the delivery of small molecules and peptides. The microparticle-based delivery of high MW drugs such as proteins, however, is reported to be challenging due to manufacturing related instabilities comprising the emulsification and the exposure to water-organic phase interfaces that might induces protein aggregation [47, 63, 84]. Dunn and co-workers introduced *in situ* forming PLGA implants as attractive option [85]. This approach encompasses the dissolution of the polymer in a biocompatible water-miscible solvent in which the drug is dispersed or dissolved. Upon contact with aqueous body fluid, polymer

precipitation takes place on account of the solvent exchange, leading to entrapment of the drug and depot formation at the injection site. Based on this so called Atrigel® technology, several products can be found on the market, such as Eligard® (Medigene), Atridox® (Atrix Laboratories) and Atrisorb®-D Free Flow™ (Zila). Among the used solvents, *N*-methyl-2-pyrrolidone (NMP), 2-pyrrolidone and dimethylsulfoxide (DMSO) were preferred due to their rather good compatibility [86]. However, as shown by several research groups, the use of hydrophilic solvents leads to a higher drug burst which can be attributed to the rapid solvent exchange accompanied by the formation of a highly porous matrix [58, 82, 87]. In contrast, the Alzamer® Depot™ technology by ALZA Corp. is based on the use of poorly water-miscible solvents such as benzyl benzoate, in order to minimize drug burst and modify formulation morphology [88]. These product examples indicate that, besides the factors mentioned above, the choice of the organic solvents has a major impact on the overall drug release and therefore has to be carefully selected with respect to the intended purpose.

Concomitantly to the expansion of therapeutic proteins, the interest in *in situ* forming depot systems has emerged [45]. The main requirements for these systems are that the burst upon injection is limited and the drug is continuously released over a longer period of time in native conformation [58]. Eliaz and co-workers found out that with increasing protein load the release rate from *in situ* hardening PLGA/glycofurol systems increased due to rapid dissolution of the protein particles situated at the surface of the matrix followed by the formation of a porous network that enables drug diffusion out of the matrix. Moreover, with increasing PLGA content a significant burst reduction was achieved [59]. A reduction in burst and release rate was also found in other studies where the impact of polymer MW on the release of the model peptide leuprolide acetate was studied [75, 89]. The influence of a variation in solvent, testing NMP, triacetin and ethyl benzoate, on the *in vitro* release of lysozyme was investigated by Brodbeck *et al.*. The use of triacetin and ethyl benzoate, both showing low water-miscibility, revealed a slow phase inversion and thus low burst intensity. Moreover, after contact with aqueous medium the formulation exhibited a semi-solid consistency [82].

Due to the potential to form a local depot system at the site of injection, PLGA-based *in situ* forming systems present a promising vehicle for the intra-articular (IA) sustained delivery of therapeutic proteins. With respect to IA administered PLGA-based drug delivery systems, microspheres are the most studied vehicles [90]. However, the *in vivo* release tests were typically performed with small molecules such as diclofenac sodium [91], ibuprofen [92], methotrexate [93], paclitaxel [94] or dexamethasone [95]. Only a few studies report about the successful release of peptides or proteins [55, 56]. As mentioned previously, the use of

PLGA-based microparticles for the delivery of proteins faces some drawbacks. The application of an *in situ* forming PLGA-based system for the delivery of proteins could be advantageous with respect to protein stability. A semi-solid consistency might be beneficial for the administration into the joint cavity.

The aim of this part of the thesis was the development of a PLGA-based *in situ* forming formulation for the IA delivery of a therapeutic monoclonal antibody (mAb). With respect to the rapid clearance of drugs from the synovial cavity, a continuous drug release over a prolonged period of time was envisaged. Based on prior knowledge about spray drying of proteins, the mAb was used as spray-dried powder to be suspended in an injectable PLGA/organic solvent mixture. In a next step, it was the aim to evaluate a suitable formulation composition with regards to PLGA type and content, protein drug load, type and concentration of organic solvents. Moreover, the formulation consistency upon injection into aqueous medium, the injectability, the protein stability and the *in vitro* drug release were to be evaluated. After having identified a suitable formulation composition, the *in vivo* pharmacokinetic profile upon IA injection into healthy rats was intended to be analyzed. Based on these results, a final formulation for a larger preclinical trial was to be selected.

2 MATERIALS AND METHODS

2.1 Materials

2.1.1 Monoclonal antibody (mAb)

The mAb (IgG1) with a MW of 148 kDa was formulated at 100 mg/mL, pH of 5.4 with trehalose (201.6 mM), histidine (15 mM) and polysorbate 80 (0.01 %). The bulk solution was stored at -80 °C until use. Prior to use, protein solutions were filtered through an Acrodisc® 0.2 µm PVDF syringe filter (Pall, Dreieich, Germany). For *in vivo* experiments, instead of the human mAb, the murine variant was used, which was formulated in histidine buffer (15 mM) at pH 6.0 and a concentration of 24.5 mg/mL.

2.1.2 Biodegradable polymers

All polymers listed in table 2-1 were purchased from Boehringer Ingelheim (Ingelheim, Germany) and were stored at 2-8 °C in a desiccator under exclusion of light.

Table 2-1 List of PLGA 50:50 qualities used.

Name of polymer	**End-group functionality**	**Inherent viscosity (0.1% in $CHCl_3$, 25°C) [dL/g]**	**Article number/ batch number**
Resomer® RG 502H	Free carboxylic acid	0.16-0.24	60640802/1040446
Resomer® RG 503H	Free carboxylic acid	0.32-0.44	60640660/RES-0281
Resomer® RG 502	Endcapped	0.16-0.24	60640667/1039274
Resomer® RG 503	Endcapped	0.32-0.44	60640661/1002249

2.1.3 Excipients, reagents and chemicals

Table 2-2 lists the excipients, reagents and chemicals used throughout this chapter. All substances were of analytical grade. Ultrapure water for all buffers was used from a PureLab UV/UF system (Elga LabWater, Celle, Germany).

Table 2-2 List of excipients, reagents and chemicals.

Excipients, reagents, chemicals	Source
Calcium chloride	Merck, Darmstadt, Germany
Citric acid monohydrate	Carl Roth, Karlsruhe, Germany
Cobalt nitrate hexahydrate	Sigma-Aldrich Laborchemikalien, Seelze, Germany
Dibasic potassium phosphate	AnalaR Normapur, VWR international, Leuven, Belgium
Dibasic sodium phosphate dihydrate	Merck, Darmstadt, Germany
Ethanolamine	Sigma-Aldrich Laborchemikalien, Seelze, Germany
Ethyl acetate	Merck, Darmstadt, Germany
Glycine	Sigma-Aldrich Laborchemikalien, Seelze, Germany
L-histidine	Merck, Darmstadt, Germany
Hydroxyethyl cellulose 400	Merck, Darmstadt, Germany
L-isoleucine	Fluka Chemie, Buchs, Switzerland
Mannitol	Riedel-de Haen, Seelze, Germany
Monobasic sodium phosphate dihydrate	Merck, Darmstadt, Germany
N-ethyl-*N*9-(dimethylaminopropyl) carbodiimide	Sigma-Aldrich Laborchemikalien, Seelze, Germany
N-hydroxy succinimide	Sigma-Aldrich Laborchemikalien, Seelze, Germany
ortho-phosphoric acid	Zentrale Versorgung LMU München, Germany
Polyethylene glycol 300	Sasol, Marl, Germany
Polysorbate 80	Merck, Darmstadt, Germany
Potassium chloride	Caelo, Hilden, Germany
Potassium thiocyanate	Sigma-Aldrich Laborchemikalien, Seelze, Germany
Sodium alginate, viscosity 350-550 mPas (1 %, 20 °C)	AppliChem, Darmstadt, Germany
Sodium azide	Acros organics, Geel, Belgium
Sodium citrate	Caelo, Hilden, Germany
Sodium chloride	AnalaR Normapur, VWR international, Leuven, Belgium
Sodium hydroxide, 1M	Merck, Darmstadt, Germany

Trehalose	Merck, Darmstadt, Germany
Triacetin	Fluka Chemie, Buchs, Switzerland

2.2 Methods

2.2.1 Spray drying with the Mini Spray Dryer B-290

Spray drying experiments with the mAb were performed on a Mini Spray Dryer B-290 (Büchi Labortechnik, Flawil, Switzerland). The instrument consisted of a heating system with inlet temperature (T_{in}) sensor for the drying air, a spray nozzle, a drying chamber with outlet temperature (T_{out}) sensor, a high efficiency cyclone for separation of the dried powder, a collection vessel and an aspirator with particle filter. For atomization of the spray drying solution, a two fluid nozzle (tip Ø 0.7 mm, cap Ø 1.5 mm) or a three fluid nozzle (inner tip Ø 0.7 mm, outer tip Ø 2.0 mm, cap Ø 2.8 mm) were used with compressed air from an in-house supply. The use of a LT Mini dehumidifier (Deltatherm® Hirmer, Much, Germany) ensured a constant low residual moisture (RM) within the system. Cooling water was circulated through a jacket around the nozzle. The T_{in}/T_{out} was 130 °C/64 °C, the aspirator flow rate was 38 m^3/hr or 100 % and the atomizing air flow rate was 667 L/hr. The spray drying solution was pumped with a liquid feed rate of 3 mL/min by means of an internal pump. In case that the three fluid nozzle was employed, an external pump was used (Minipuls 3, Gilson, Middleton, USA). All liquid samples were filtered through an Acrodisc® 0.2 µm PVDF syringe filter (Pall, Dreieich, Germany) prior to spray drying. After the process, the resulting powder was collected in glass vials, closed and stored in a desiccator at ambient atmosphere. The yield was calculated from the amount of powder recovered in the collection vessel in relation to the solid content of the used spray drying solution.

2.2.2 Spray drying with the Nano Spray Dryer B-90

Spray drying experiments with the murine mAb were performed on a Nano Spray Dryer B-90 (Büchi Labortechnik, Flawil, Switzerland), comprising a heating system with T_{in} sensor for the drying air, an inbuilt peristaltic pump for the drying solution, a spray head with vibrating mesh for generation of small droplets, a spray tower where a laminar air flow is generated, an electric particle collector for efficient separation of the dried particles and an particle filter with T_{out} sensor. The T_{in}/T_{out} was 55 °C/28 °C, the drying air was used from an in-house supply at a flow rate of 115 L/min and a mesh size of 5.5 µm was employed for droplet generation. Spray solutions were filtered through an Acrodisc® 0.2 µm PVDF syringe filter prior to spray

drying. During the spray drying process, spray solutions were kept on ice. Dried particles were collected in glass vials, closed and stored in a desiccator at ambient temperature.

2.2.3 Karl-Fischer analysis

The RM content of the spray-dried (sd) powder was determined by coulometric Karl-Fischer titration using an Aqua 40,00 titrator with headspace module (Analytik Jena, Jena, Germany). Therefore, 10-20 mg of the respective powder were accurately weighed into a 2 R glass vial, sealed with rubber stopper and heated up to 100 °C. For determination of the RM content, the evaporated water was transferred into the titration solution. As reference, a standard with defined RM was used (apura® water standard oven 1 %, Merck, Darmstadt, Germany).

2.2.4 Scanning electron microscopy (SEM)

Scanning electron microscopy was performed on a JSM-6500F JEOL scanning electron microscope (JEOL, Eching, Germany). Samples were attached on a sample holder by means of double-sided tape and sputtered with carbon. SEM was used for morphology analysis of sd particles and vacuum dried PLGA specimens.

2.2.5 Preparation of formulations

The respective amount of PLGA was accurately weighed into a glass vial. After addition of the respective volumes of the organic solvents, the vials were closed by a rubber stopper and shortly vortexed in order to disperse the PLGA powder. Samples were heated up to 40 °C in a beaker until complete dissolution of PLGA was achieved. After cooling down to room temperature, the respective amount of sd mAb powder was added and dispersed in the PLGA solution by means of a spatula. Directly prior to injection, the PLGA-mAb suspensions were transferred into syringes.

2.2.6 Injectability

The maximal injection force, required for injection of 0.4 mL of the formulation into air, was determined by means of a TA.XTplus texture analyzer (Stable Micro Systems, Surrey, UK) at ambient temperature. This value was defined as the highest force measured before the plunger reached the end of the syringe after having overcome the plunger-stopper

breakloose force. Therefore, 1 mL Luer-Lock syringes (VWR International, Ismaning, Germany) connected to 23 G syringe needles (Terumo, Leuven, Belgium) were clamped in a tripod underneath the punching tool of the instrument. The crosshead velocity was set to 1 mm/s, a representative velocity for the manual syringe delivery [96]. After 30 s, the measurement stopped automatically.

2.2.7 Mechanical testing

For determination of the mechanical properties of *in situ* hardened PLGA specimens, approximately 100 µL of the respective formulation were placed into a 96-well plate (Nunc®, Sigma-Aldrich Laborchemikalien, Seelze, Germany). The well plate was submersed for 24 hrs in PBS in order to allow solvent exchange and PLGA precipitation. The buffer medium was heated-up to 37 °C and agitated by means of a magnetic stirrer. After incubation, the hardness of the samples was investigated using a TA.XTplus texture analyzer (Stable Micro Systems, Surrey, UK) at ambient temperature. Therefore, a cylindrical stainless steel punching tool (Ø 4 mm) penetrated into the specimens with a velocity of 0.05 mm/s. The required maximal forces to achieve a penetration depth of 1 mm were recorded and used for comparison.

2.2.8 Rheometry

The viscosity of *in situ* hardened PLGA formulations was studied on a plate-cone rheometer (Physica MCR 100, Anton Paar, Ostfildern, Germany) with logarithmically increasing shear rate (10^{-3}-500 s^{-1}, 500-10^{-3} s^{-1}) at a gap position of 0.042 mm. A cone with a diameter of 50 mm and an angle of 1 ° was used and measurements were performed at 20 °C. Approximately 600 mg of the sample were used. For formulation comparison the viscosity at 500 s^{-1} was utilized.

2.2.9 Protein extraction from non-aqueous PLGA formulations

In order to analyze the structural integrity of mAb after dispersion in non-aqueous PLGA solutions, approximately 250 mg of freshly prepared non-aqueous PLGA-mAb formulation were accurately weighed into a 2 mL Eppendorf cup. Ethyl acetate was added up to the 2 mL mark and the sample was incubated for 15 min. As reference, approximately 44 mg sd mAb were accurately weighed into an Eppendorf cup and treated in the same way. Samples were

centrifuged for 10 min at 12,000 rpm. Afterwards, approximately 1.5 mL ethyl acetate was replaced and the pellet was resuspended. This washing step was repeated twice. After the last centrifugation step the supernatant was removed and the residual sediment was dried in a vacuum chamber at ambient temperature. After one hour, the dried protein was reconstituted with 1 mL water. The obtained solutions were used for HP-SEC and HP-IEC analysis.

2.2.10 Protein extraction from PLGA matrices after release experiments

Protein extraction from hardened PLGA matrices was performed after lyophilzation of the PLGA matrices in an Epsilon 2-6 D freeze dryer (Christ, Osterode, Germany) in the vials used for the *in vitro* release experiments. The vials were frozen to -50 °C at 0.45 °C/min and held for 2 hrs. Primary drying was performed at a shelf-temperature of -15 °C and 0.045 mbar within 20 hrs. Secondary drying was carried out at a shelf-temperature of 40 °C within 10 hrs and 0.045 mbar. Lyophilized vials were closed manually. After drying, protein extraction was performed according to 2.2.9.

2.2.11 *In vitro* mAb release tests

2.2.11.1 Vial model

In vitro mAb release experiments from *in situ* hardened PLGA formulations were performed by injection of approximately 400 mg of the non-aqueous PLGA-mAb suspensions into 6 R glass vials (Schott, Mainz, Germany) filled with 6 mL PBS containing 0.01 % NaN_3. If possible, formulations were manually injected. At higher formulation viscosities, injection through syringe needles was carried out with the help of a custom made manual injection aid consisting of a syringe holder and a screw as syringe plunger substitute. After injection, the vials were sealed with rubber stopper, stored at 37 °C in a convection oven and agitated at 40 rpm on a shaker. At predefined time points the complete release medium was carefully replaced by fresh buffer and analyzed for protein concentration via UV spectroscopy or fluorimetry.

2.2.11.2 Mechanical stress model

In order to simulate the mechanical conditions present in the joint, *in situ* hardening formulations were subjected to mechanical treatment during *in vitro* release experiments.

Therefore, approximately 50 mg of non-aqueous PLGA-mAb formulations were injected into HPLC vials (VWR international, Ismaning, Germany) filled with 750 µL PBS containing 0.01 % NaN_3. Directly after injection, the *in situ* hardening PLGA formulations were kneaded with 20 penetration cycles of a plane stainless steel punching tool (Ø 4 mm) by means of a TA.XTplus texture analyzer (Stable Micro Systems, Surrey, UK) at ambient temperature (figure 2-1). Meanwhile, the vial was manually rotated in order to avoid indentation at the same position. After mechanical stressing, the vials were tightly sealed and incubated at 37 °C. At predefined time points, the complete release medium was carefully replaced by fresh buffer and the mechanical treatment of the remaining PLGA matrix was repeated. Protein release was determined via UV spectroscopy or fluorimetry.

Figure 2-1 Mechanical stress model for simulation of IA conditions during mAb release. After injection of 50 mg of the PLGA formulation a punching tool penetrates into the *in situ* formed matrix with 20 indentation cycles.

2.2.12 UV spectroscopy (OD 280, second derivative, absorbance at 350 nm)

Protein concentrations were determined photometrically on an Agilent 8453 UV-Vis spectrometer (Agilent Technologies Deutschland, Böblingen, Germany) equipped with a Peltier temperature controller (Agilent Technologies Deutschland, Böblingen, Germany) at λ=280 nm and 25 °C in quartz UV cuvettes with a path length of 1 cm. An extinction coefficient of either 1.39 $mL \cdot mg^{-1} \cdot cm^{-1}$ (mAb) or 1.40 $mL \cdot mg^{-1} \cdot cm^{-1}$ (murine mAb) was applied. Samples were diluted to a concentration ranging from 0.1 to 0.7 mg/mL prior to analysis. Corresponding blank spectra were subtracted from the protein spectra. Second derivative protein spectra were calculated between 240 and 350 nm by means of the ChemStation software. Turbidity of undiluted protein containing samples was determined at 350 nm and 25 °C. Concentrations of smaller sample volumes were analyzed undiluted with a NanoDrop ND-2000 spectrometer (PEQLAB Biotechnologie, Erlangen, Germany).

2.2.13 Fluorimetry

Protein concentrations below 0.1 mg/mL were determined with a Varian Carry Eclipse fluorimeter (Varian, Darmstadt, Germany). Solutions were measured at 20 °C either in 3.0 mL (Sarstedt, Nümbrecht, Germany) or 0.5 mL (Brand, Wertheim, Germany) cuvettes, depending on the available volume. Excitation occurred at a wavelength of 280 nm with an excitation slit of 5 nm. The emission spectrum was recorded from 280 nm to 600 nm. For protein quantification a calibration curve, ranging from 0.002 to 0.1 mg/mL at the emission maximum at 334 nm, was used.

2.2.14 Fourier transform infrared spectroscopy (FTIR)

FTIR spectra were recorded with a Tensor 27 FTIR spectrometer (Bruker Optics, Ettlingen, Germany) using a Bio-ATR unit (attenuated total reflection) connected to a thermostat tempered to 20 °C (DC30-K20, Thermo Haake, Dreieich, Germany). Corresponding blank spectra were subtracted from the protein spectra. After a 120-scan measurement, the second derivative spectra were generated (OPUS, Bruker Optics, Ettlingen, Germany). For investigation of changes in secondary protein structure, the vector normalized second derivative spectra between the wavenumbers of 1720 and 1580 cm^{-1} were compared with the spectra of the native, untreated protein.

2.2.15 High performance size exclusion chromatography (HP-SEC)

HP-SEC was used for quantification of soluble aggregates, monomer and fragments of the mAb. The measurement was performed on a HPLC 1100 chromatograph (Agilent Technologies Deutschland, Böblingen, Germany) using a Superose® 6 10/300 GL column (GE Healthcare, Uppsala, Sweden) with UV detection at 214 and 280 nm. The mobile phase consisted of 0.15 M sodium chloride in 0.02 M sodium phosphate, adjusted to pH 7.5 with *ortho*-phosphoric acid. The flow rate was 0.5 mL/min. Samples were diluted with mobile phase to a target concentration of 1 mg/mL and centrifuged for 10 min at 12,000 rpm (Sigma 1-15, Sigma Laborzentrifugen, Osterode am Harz, Germany) in order to remove insoluble aggregates. Chromatograms were integrated manually by means of the ChemStation software Rev. B.02.01 (Agilent Technologies Deutschland, Böblingen, Germany). For quantification, the area under the curve was used. Protein concentrations were calculated based on a calibration curve.

2.2.16 High performance ion exchange chromatography (HP-IEC)

HP-IEC was performed for detection of oxidized protein species after protein extraction from non-aqueous PLGA formulations. The experiment was performed on a HPLC 1200 chromatograph (Agilent Technologies Deutschland, Böblingen, Germany) with a ProPac-WCX-10 column and a ProPac-WCX-10G-precolumn (Dionex, Sunnyvale, USA). Mobile phase A consisted of 0.01 M sodium phosphate, pH 7.5, mobile phase B of 0.01 M sodium phosphate and 0.5 M sodium chloride at pH 5.5. The binary gradient listed in table 2-3 was applied with a flow rate of 1.0 mL/min. Protein detection occurred at 280 nm.

Table 2-3 Binary gradient used for HP-IEC measurements.

Time	Solvent
0 min	94 % A, 9 % B
20 min	84 % A, 16 % B
22 min	0 % A, 100 % B
28 min	94 % A, 6 % B

2.2.17 Bright-field microscopy

In order to visualize large insoluble protein aggregates, protein samples were filtered through a 0.2 µm polypropylene membrane filter (Pall, Dreieich, Germany). Protein on the filter surface was stained with 1 mL of a protein detection kit as described by the supplier (Sigma-Aldrich Laborchemikalien, Seelze, Germany). After 5 min, protein aggregates were washed with 10 mL PBS. The filter membrane was analyzed on a Keyence digital VHX-500F bright-field microscope (Keyence Deutschland, Neu-Isenburg, Germany).

2.2.18 Surface plasmon resonance (SPR) measurements

Analysis of the binding capacity of *in vitro* released mAb was performed at the Abbott Bioresearch Center, Worcester, USA using a BIACORE T100 instrument (GE Healthcare, Uppsala, Sweden) connected to the BIAevaluation® software. Release experiments were performed with the murine mAb. Goat anti-murine mAb antibody was immobilized on a carboxy methylated (CM5®) chip according to the standard immobilization procedures described by Biacore Life Science. The sensor chip surfaces of sample and reference cells were first activated by a 6-min injection of a solution containing 0.4 M *N*-ethyl-*N*9-

(dimethylaminopropyl) carbodiimide and 0.1 M *N*-hydroxy-succinimide. After anti-murine mAb antibody immobilization in the sample cell via amine linkage of lysine residues, residual activated carboxymethyl groups of both sample and reference cell were deactivated with ethanolamine. In order to verify that the immobilized mAb was still intact, the binding capacity was determined with a murine mAb antigen solution, carried through the sample cell. MAb containing samples obtained from *in vitro* release experiments were diluted with the running buffer to a concentration of 0.5 µg/mL. The experiment was performed at 25 °C with a flow rate of 50 µL/min. After injection of the mAb samples and capture by the covalently bound goat anti-murine mAb antibody, murine TNFα solution was carried through the cell in order to determine the binding capacity of murine mAb. As reference a mAb standard solution at same concentration was used. Dissociation of captured murine mAb was performed with 10 mM glycine (pH=1.5) in order to regenerate the sensor surface for the next experiment.

2.2.19 *In vivo* experiments

An *in vivo* study was performed at the Abbott Bioresearch Center in Worcester, USA according to the granted animal test proposal in order to assess the pharmacokinetic profile of PLGA-mAb formulations upon IA injection. The study was performed with healthy male Lewis rats weighing approximately 275 – 300 g at the start of the study. Instead of the human mAb, the murine variant was used. For generation of protein particles, the mAb solution, formulated in 15 mM histidine, was admixed with excipients (201.6 mM trehalose, 0.01 % polysorbate 80) and spray-dried as described in section 2.2.2. Selection of PLGA formulation composition was based on *in vitro* release data. In order to cover a broad release window, three formulations showing “long”, “intermediate” and “short” *in vitro* mAb release profiles were selected. Besides the IA administration, the PLGA-mAb formulation with the “long” *in vitro* release profile was additionally administered subcutaneously (SC) in order to assess the impact of the mechanical exposure in the knee joint on the *in vivo* release.

Prior to injection, animals were anaesthetized in an anesthesia chamber using isoflurane (5 %) and oxygen. Once the rats were completely anesthetized, the right knee was shaved. Animals were dosed either IA or SC with 50 µL of the respective PLGA-mAb formulation. IA injection was carried out by injection through the patella into the knee joint using a 21 G needle. At predefined time points (1 hr, 2 hrs, 4 hrs, 6 hrs, 12 hrs, 1 d, 2 d, 3 d, 7 d) blood samples were collected from the tail nick of the animals and stored at -80 °C until analysis. At day 7, animals were sacrificed in an anesthesia chamber using CO_2. Blood samples were

analyzed in regard to mAb concentration via ELISA according to the Abbott standard protocol.

3 RESULTS AND DISCUSSION

3.1 Spray drying of mAb and powder characterization

At first, sd mAb particles had to be generated for preparation of the non-aqueous PLGA-mAb suspension. The recovery of the sd mAb powder prepared on a Mini Spray Dryer B-290 was between 60 and 74 % and the RM ranged from 3.4 to 4.9 %. SEM analysis revealed a broad particle size distribution in the low µm-range and the presence of particles of round and doughnut-like shape (figure 2-2 A). Reconstitution with water resulted in clear solutions and HP-SEC showed that the monomer recovery was unchanged compared to prior to spray drying (99.5 ± 0.03 % (sd mAb), vs. 99.6 ± 0.1 % (mAb before spray drying)).

Generation of sd murine mAb particles for *in vivo* experiments was carried out on a Nano Spray Dryer B-90 on account of the possibility to dry the minute volumes of restricted murine mAb solutions while achieving high yields [97]. Dried particles were prepared with a recovery of 86 % and a RM content of 7.3 %. In order to reduce the RM content, the powder was subjected to an additional vacuum drying step by incubation of the powder at 100 mbar and 32 °C for 40 hrs. This led to a slight reduction of RM to 6.4 %. SEM images revealed the presence of spherical particles in the size range of 0.5 µm to 6 µm (figure 2-2 B). Again, HP-SEC analysis after reconstitution showed an unchanged monomer recovery (98.4 % ± 0.7 % (sd murine mAb), vs. 98.6 % ± 0.5 % (murine mAb before spray drying)). Thus it was possible to generate the mAb powder necessary for formulation preparation at high quality and adequate yields.

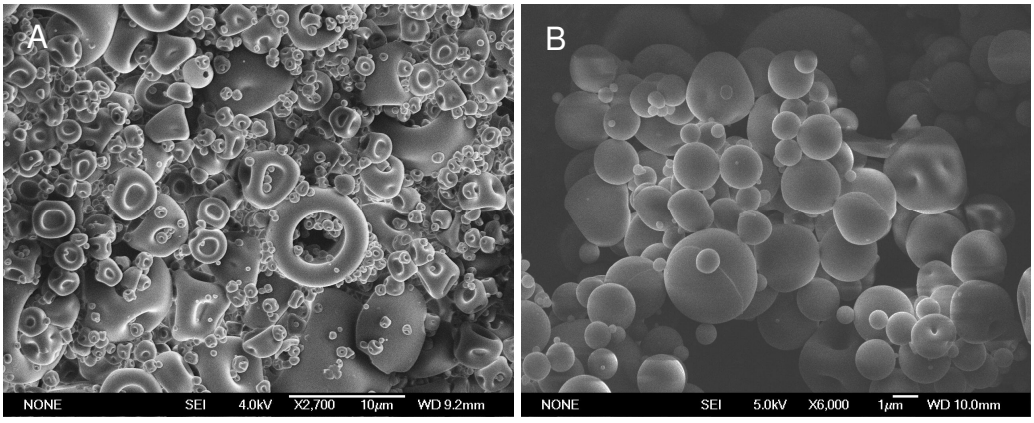

Figure 2-2 SEM images of sd mAb particles generated on a Mini Spray Dryer B-290 (A) and of sd murine mAb particles prepared on a Nano Spray Dryer B-90 (B).

3.2 Pre-screening experiments

3.2.1 Initial screening of different PLGA and organic solvent concentrations

PLGA-based drug containing formulations intended for IA administration have to meet several requirements including injectability through thin syringe needles and drug release in the desired time frame. In order to guarantee the preservation of the entire joint mobility, a semi-solid consistency after contact with synovial fluid (SF) and subsequent hardening needs to be provided as joint blockage or cartilage friction have to be avoided. In general, the polymer content plays an important role in controlling the release window. But it also needs to be considered that high polymer content leads to an increase in viscosity of the formulations which limits injectability. Besides the polymer content, also the PLGA MW and the end-group functionality have a major influence on solvent exchange after contact with aqueous medium and initial hardening. Furthermore, the choice of the organic solvents used for preparation of PLGA solutions plays a crucial role: the use of hydrophilic solvents accelerates water influx and subsequent PLGA precipitation but commonly ends up in a rapid drug burst. In contrast, the addition of hydrophobic solvents is reported to decelerate solvent exchange accompanied with a significant reduction of drug burst. As hydrophobic solvents are known to act as plasticizer, the resulting *in situ* formed matrix exhibits a mellow consistency. Various organic solvents such as PEG 400, NMP, DMSO, triacetin, triethyl citrate, 2-pyrrolidone and benzyl alcohol have been investigated as solvents for *in situ* forming PLGA systems [77, 98]. Strickley reviewed organic solvents that are commonly used in commercially available injectable products [99]. According to that, the water-miscible solvents PEG 300 and PEG 400 are considered as safe and highly compatible. The hydrophobic solvent triacetin is affirmed as generally recognized as safe (GRAS) by the FDA [77]. It can be used as parenteral nutrient [100] and is employed in oral dosage forms. In order to evaluate a suitable formulation composition with adequate consistency after incubation in aqueous medium, different PLGA-organic solvent placebo mixtures were prepared. As PLGA component for the initial evaluation Resomer® RG 503H was chosen based on prior knowledge about precipitation and degradation behavior. PEG 300 was used as hydrophilic solvent for PLGA and triacetin served as hydrophobic solvent and formulation plasticizer. The placebo samples were tested with respect to injectability through a 23 G needle and consistency after incubation for one day at 37 °C in PBS. PLGA was employed at 5 to 25 % (w/w) and triacetin concentrations ranged from 10-30 % (w/w).

In the preliminary study, only formulations with polymer content up to 10 % were easily injectable through a 23 G syringe needle. A polymer content above 10 % led to such a high formulation viscosity that manual injection through the 23 G syringe needle was hardly possible. Formulations comprising triacetin contents of 20-30 % revealed a semi-solid consistency after incubation which was in accordance to the initial idea about the formulation consistency. Consequently, a formulation composition with 10 % PLGA, a triacetin content of 20-30 % and 60-70 % PEG 300 were determined as suitable starting point for further investigations with respect to injectability and formulation consistency.

3.2.2 Investigation of the influence of PEG 300 and triacetin on mAb conformational stability

One basic requirement concerning the selection of formulation components is the compatibility with the incorporated protein. In the following the influence of PEG 300 and triacetin at the aforementioned concentration ranges on mAb conformational stability were analyzed via turbidity measurements, second derivative UV and FTIR spectroscopy and HP-SEC. Therefore, the sd mAb was incubated for 1 hr in 1 mL PEG 300 as well as in 1 mL of a mixture of PEG 300 and triacetin (PEG 300/triacetin (P/T) ratio 80 %/20 % and 70 %/30 %). After incubation, 3 mL PBS were added to the suspensions, respectively, in order to redissolve the sd mAb.

Turbidity measurements after redissolution of sd mAb revealed a slight increase of turbidity with raising triacetin content (figure 2-3). The tertiary protein structure was studied by analysis of the second derivative UV spectra. This method allows the detection of changes in the microenvironment polarity of the aromatic amino acids phenylalanine (Phe), tyrosine (Tyr) and tryptophane (Trp) [101, 102]. The native mAb showed five characteristic peaks that can be attributed to the aromatic amino acids as follows: 249 nm (Phe), 259 nm (Phe), 276 nm (Tyr/Trp), 284 nm (Tyr/Trp) and 292 nm (Trp) [103]. Since no peak shifts were detectable in the samples compared to the reference, it was assumed that the organic solvents in the used concentration ranges have no detrimental impact on the tertiary protein structure (figure 2-4 A). In order gain futher insight into the impact of the organic solvents on the secondary mAb structure, FTIR measurements were performed. The results shown in figure 2-4 B underline the findings of the UV measurements as also no effects on the secondary protein structure by the addition of the organic solvents were seen. Additional HP-SEC analysis demonstrated that the monomer recovery was not reduced significantly by the incubation of the protein particles in the solvent systems (P/T 100 %/0 % 99.8 ± 3.2 %, P/T 80 %/20 % 99.2 ± 3.4 %,

P/T 70 %/30 % 96.7 ± 1.7 %, reference 96.5 ± 2.1 %). According to these results, it was concluded that PEG 300 and triacetin present suitable solvents for the preparation of a mAb containing PLGA formulation since at the analyzed concentration ranges no destabilizing effects on the protein were detectable.

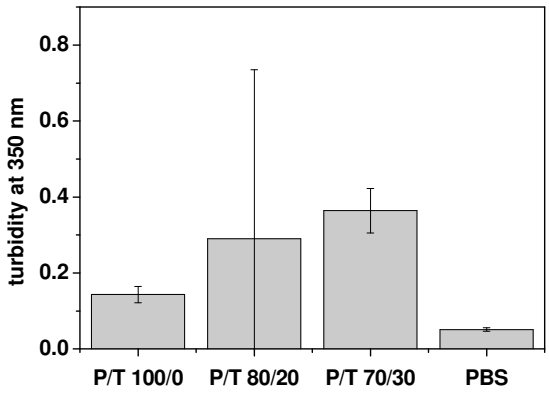

Figure 2-3 Blank corrected results of turbidity measurements at 350 nm of sd mAb incubated in different PEG 300/triacetin (P/T) mixtures (P/T 100 %/0 %, 80 %/20 % and 70 %/30 %) for 1 hr and redissolution in 3 mL PBS in comparison to sd mAb in PBS.

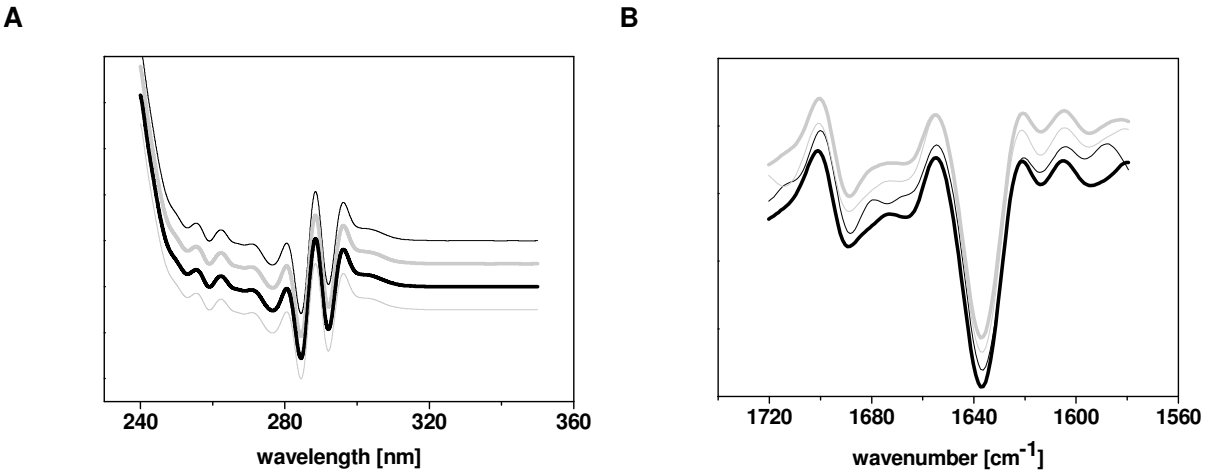

Figure 2-4 Second derivative UV (A) and FTIR (B) spectra of sd mAb incubated in different PEG 300/triacetin (P/T) mixtures (P/T 100 %/0 % (gray, thick), 80 %/20 % (black, thick) and 70 %/30 % (gray, thin) for 1 hr and subsequent addition of 3 mL PBS in comparison to untreated mAb (black, thin). Artificial offset for clarity.

3.2.3 Evaluation of a suitable drug load

Subsequently, a suitable drug load was to be found which has to balance the high protein load necessary for pharmacological reasons, a potential effect on burst release as well as a potential increase in viscosity with high particle concentration. At first, the viscosity and the injectability of the formulation were studied. In order to evaluate the highest drug load possible, the required maximal injection force using a 23 G syringe needle was determined. Moreover, the viscosity prior to injection was studied. As basic formulation composition a PLGA content of 10 % (Resomer® RG 503H) in P/T 70 %/30 % was chosen to evaluate a protein content of 5 %, 7 % and 10 %.

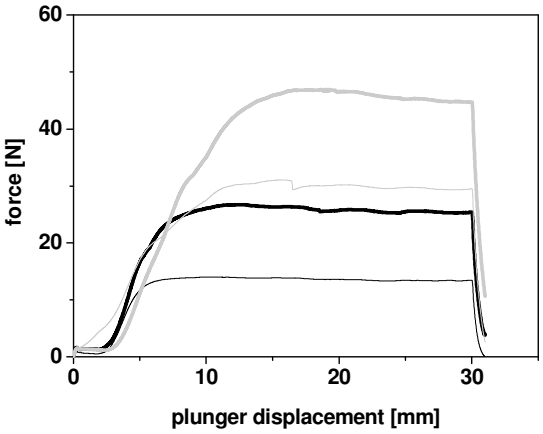

Figure 2-5 Injection force-plunger displacement diagram of injectability measurements using a 23 G needle and formulations with 10 % Resomer® RG 503H, a P/T ratio of 70 %/30 % and a mAb content of 0 % (black, thin line), 5 % (black, thick line), 7 % (gray, thin line) and 10 % (gray, thick line).

Figure 2-5 shows the results of the injectability measurements using a 23 G syringe needle. With increasing drug load, the injection force increased from 27 N (mAb 5 %) up to 47 N (mAb 10 %). In literature, formulations which require injection forces up to 25 N *in vivo* are declared as easy to inject [21]. As the experiment was performed by injection into air, a slight increase of the forces after injection *in vivo* is expected due to a higher resistance and the limited physiological space [21]. To overcome high injection forces, the use of syringe needles with bigger inner diameter could be used. According to the law of Hagen-Poiseuille, the use of a 21 G syringe needle would lead to an injection force of 15 N for the formulation with 10 % drug load which is easy to handle. However, an increase in needle size is known to influence the patient compliance due to injection pain [96]. Therefore, thin needle sizes should always be aspired. Rheometry measurements confirmed that with increasing drug load also the viscosity increases (1.5 ± 0.1 Pa·s (0 % drug load), 2.7 ± 0.1 Pa·s (5 % drug

load), 3.4 ± 0.2 Pa·s (7 % drug load), 4.9 ± 0.2 Pa·s (10 % drug load) at a shear rate of 500 s^{-1}). In order to keep both the injection forces and the viscosity of the formulations as low as possible, a drug load of 5 % was chosen for further experiments. At this drug load, the amount of formulation to be administered to the joint would be 280 mg, presuming a release period of 28 days with a complete drug release and an envisaged daily mAb release of 500 µg.

3.2.4 Studies on the *in vitro* release of mAb from PLGA formulations and characterization of the formulations

In situ forming PLGA-based drug containing formulations are generally described to show a triphasic release pattern. The first phase is characterized by a burst release of the drug due to the lag between injection and solidification. Drug particles that are deposited on or close to the surface are easily accessible by the incubation medium, leading to rapid dissolution and diffusion out of the matrix [87]. The second phase is governed by a diffusion controlled sustained release of the drug that is entrapped in the solidified PLGA matrix. In the third phase, drug release occurs concomitantly with PLGA erosion [104]. For orientation, mAb *in vitro* release experiments were performed by injection of approximately 0.4 g of a formulation composed of 10 % Resomer® RG 503H, a P/T ratio of 70 %/30 % and a mAb content of 5 % into 6 R glass vials filled with 6 mL release medium at 37 °C. For this preliminary experiment 20 G needles were employed in order to allow easy manual injection. A strong burst effect of 85 ± 11 % during the first 5 hrs was observed with no further release within the next 40 hrs (figure 2-6). This almost complete burst release can be ascribed to the rapid PEG 300 exchange accompanied by an influx of the surrounding aqueous medium into the formulation.

The role of solvent exchange in this context was investigated by Brodbeck *et al.* who reported a strong initial burst release from *in situ* forming PLGA formulations when solvents with a high hydrophilicity were used. The burst effect was reduced when using solvents with a lower water affinity due to slower solvent exchange causing the formation of a less porous structure with hampered water influx and subsequent protein dissolution [82]. Besides by the use of less hydrophilic solvents, the burst intensity can be reduced by increasing the polymer MW as longer polymer chains induce the formation of a more entangled network that hinders protein release [89]. Shively *et al.* pointed out that with increasing polymer content the drug release from *in situ* forming implants can be significantly reduced [105]. This effect might be explained by the fact that both the hydrophobicity and the density of the system increase,

leading to a decreased water influx rate and the formation of a less porous structure [106]. Moreover, the polymer type is reported to influence the drug release. In the present study, a polymer type with free carboxylic acid end-group was employed. The use of an end-capped polymer variant is known to increase the hydrophobicity [107] and therefore the water influx into the *in situ* forming system is reduced.

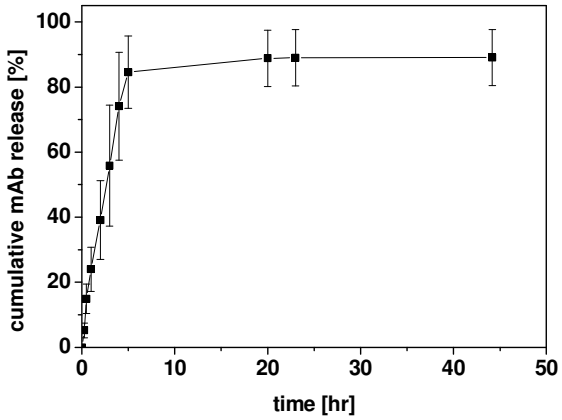

Figure 2-6 Cumulative mAb release from a formulation composed of 10 % Resomer® RG 503H, a P/T ratio of 70 %/30 % and a mAb content of 5 %; injection of approximately 0.4 g through a 20 G needle into PBS at 37 °C.

To study whether the burst release could be suppressed by the use of significantly higher polymer content, the formulations with the highest polymer content possible were to be tested independent of injectability of the formulation and consistency of the formed matrices. Resomer® RG 503H showed a maximal solubility of 33 % (w/w) in both pure PEG 300 and triacetin. In order to test if a polymer with lower MW than Resomer® RG 503H shows a higher solubility, Resomer® RG 502H was also dissolved at various concentrations in both solvents (MW range Resomer® RG 503H 24-38 kDa vs. Resomer® RG 502H 7-17 kDa). It became obvious that Resomer® RG 502H has a maximal solubility of 50 % (w/w) in both solvents. Consequently, this polymer was used for following *in vitro* release experiments as higher polymer content was achieved. As the handling of the formulation after addition of 5 % sd mAb was hardly possible, the polymer content was slightly reduced from 50 % to 45 % for further *in vitro* mAb release experiments.

Even at a PLGA content of 45 % the PEG 300 containing formulation still exhibited a burst of 70 ± 10 %. A phase of continuous drug release of 0.1 % per day followed. Beginning on day 9 the release was slightly enhanced and the incubation medium turned slightly turbid with the presence of white flakes pointing towards enhanced PLGA degradation and erosion. Opposite to that, the triacetin containing formulation did not show any burst. Until day 6 only 1.3 % of mAb were released. After day 6, a significant increase in mAb release up to 30 % at

day 26 in a sigmoidal release pattern was identified (figure 2-7). The observed differences in mAb release rate confirm the findings of Brodbeck *et al.* [82]. The impact of the hydrophilic solvent on the formation of an interconnecting highly porous structure was clearly underlined by SEM analysis of the vacuum dried PEG 300 containing PLGA matrix (figure 2-8). The triacetin containing formulation could not be analyzed via SEM analysis as this formulation showed a mellow consistency indicating that PLGA was not completely precipitated. In contrast to triacetin, the PEG 300 containing formulation was of hard consistency after incubation that enabled vacuum drying and SEM analysis.

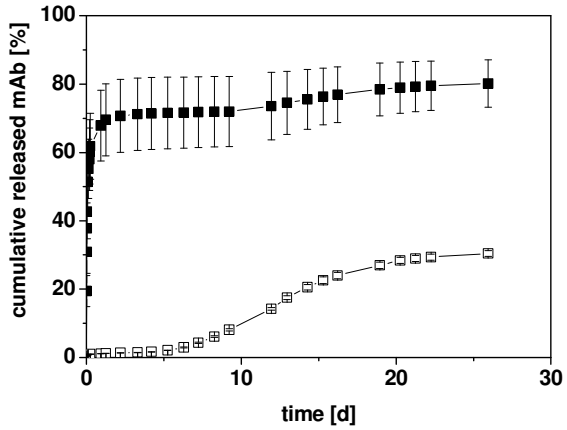

Figure 2-7 Cumulative mAb release from formulations composed of 45 % Resomer® RG 502H, 5 % mAb and either PEG 300 (filled square) or triacetin (opened square). Approximately 0.4 g of the formulations was injected without syringe needle into 6 R vials filled with PBS at 37 °C.

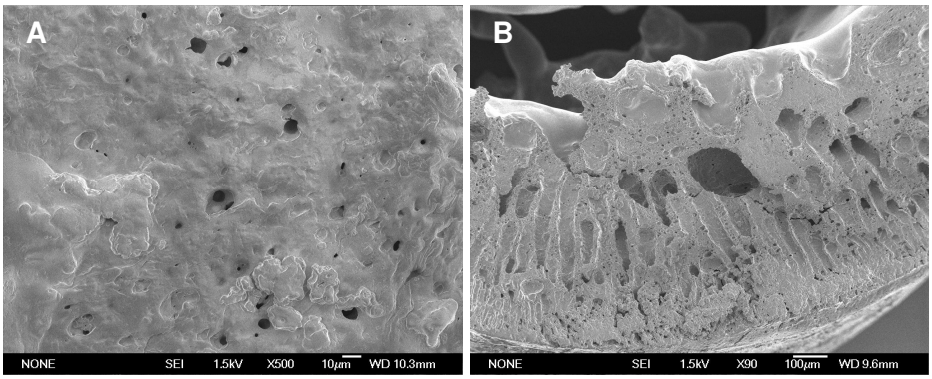

Figure 2-8 SEM images of side view (A) and cross section (B) of a formulation composed of 45 % Resomer® RG 502H, 5 % mAb and PEG 300 after incubation for 1 day.

The above findings indicate that the used solvent has a major influence on both the consistency of the *in situ* formed matrix and the *in vitro* mAb release. Concerning the formulation consistency, the PEG containing formulation is expected be too hard for IA

application as it might lead to friction in the joint and restricted joint mobility, whereas the consistency of the triacetin containing formulation seems to be applicable. However, regarding the mAb release behavior, the release rate from the triacetin formulation might be too low for the intended purpose. In order identify a formulation showing a release profile in between the two formulations analyzed, the impact of various P/T ratios on the *in vitro* mAb release as well as on the formulation consistency was studied. MAb containing formulations based on 45 % Resomer® RG 502H and different P/T ratios were prepared. As the viscosity of the prepared formulations was too high for an injection through syringe needles, injection into the release medium was carried out without syringe needle.

The visual inspection of the formulations one day after incubation revealed that with more than 15 % triacetin, the *in situ* formed matrices exhibited a mellow consistency and flowed down to the bottom of the vial (figure 2-9). With PEG 300 contents of equal or more than 95 %, the implant solidified immediately upon contact with release medium due to the rapid solvent exchange and the injected matrix shape was maintained.

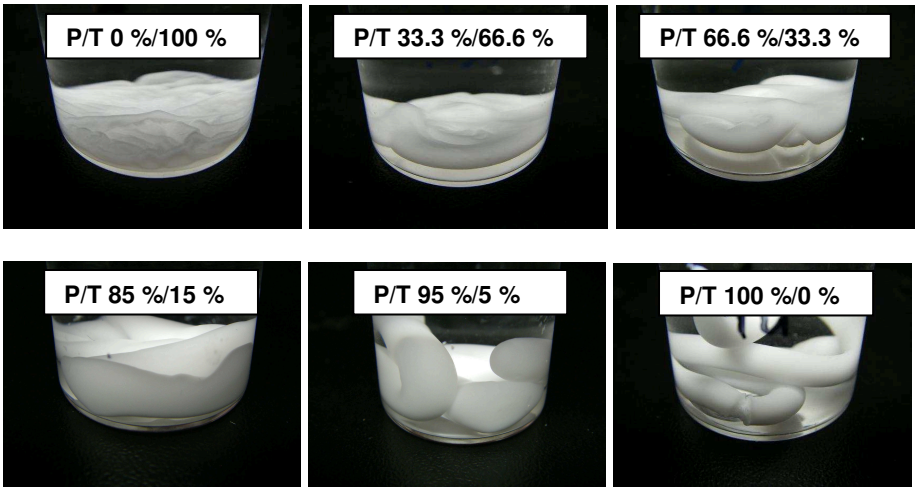

Figure 2-9 Visual appearance of mAb containing formulations consisting of 45 % Resomer® RG 502H and P/T ratios as indicated after one day of incubation in PBS at 37 °C. Injection occurred without syringe needle.

In vitro release experiments demonstrated that a triacetin content of only 5 % leads to a 3-fold reduction of the burst from 67.9 ± 10.3 % to 23.8 ± 1.8 % (figure 2-10). A further increase in triacetin content did not change the initial release profiles drastically. All formulations revealed the same release pattern as described above. Thus, after one day the release profile in the triacetin containing formulations was identified to be independent of the P/T ratio.

Mechanical strength measurements of the incubated matrices after 24 hrs confirmed that the mechanical strength decreased with increasing triacetin content (figure 2-11). The addition of only 5 % triacetin led to a reduction of the mechanical strength by factor 3. A further increase in triacetin content altered the mechanical strength only slightly.

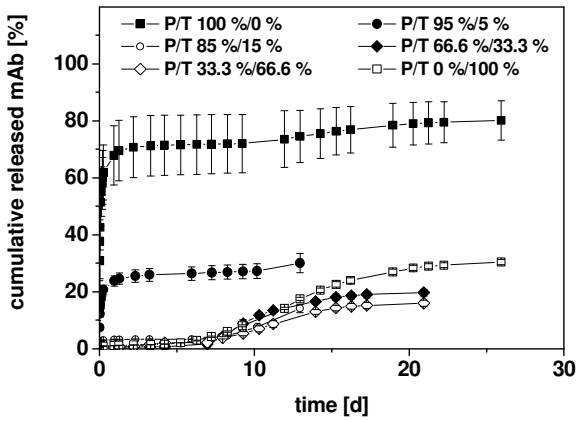

Figure 2-10 *In vitro* release profiles of mAb from formulations composed of 45 % Resomer® RG 502H, 5 % mAb and P/T ratios as indicated. Approximately 0.4 g of the formulations was injected without syringe needle into 6 R vials filled with PBS at 37 °C.

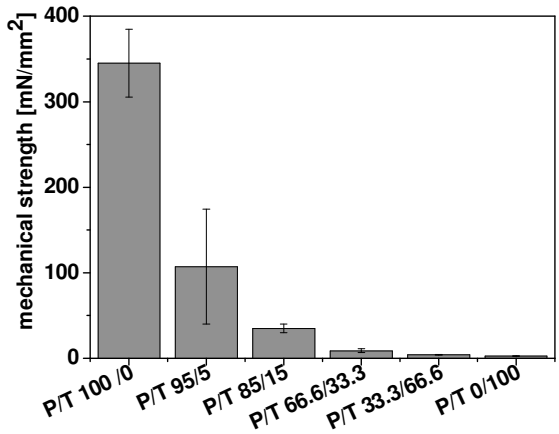

Figure 2-11 Mechanical characteristics of mAb containing formulations based on Resomer® RG 502H, a mAb content of 5 % and P/T ratios as indicated after one day of incubation in PBS at 37 °C.

The results of these pre-screening experiments demonstrate that mAb entrapment into an *in situ* forming PLGA-based matrix at high polymer content in general is possible. The initial burst can be controlled by the P/T ratio employed. So far, formulations were not injectable. In a further step the formulations were intended to be modified with respect to injectability. Moreover, the protein stability after release was to be investigated.

3.3 Investigation of mAb stability in non-aqueous PLGA formulations and after *in vitro* release

So far, formulation development was performed with the focus on the impact of the P/T ratio on the mAb release behavior and the mechanical characteristics of the formulation after incubation. Another aspect of major importance is the preservation of the mAb stability upon formulation preparation and subsequent release. In literature, several degradation reactions and mechanisms are described that might occur when proteins are incorporated into PLGA, such as deamidation, amide bond hydrolysis or acylation induced by the polymer itself or its acidic degradation products. Moreover, protein aggregation is described as a consequence of pH drop during polymer hydrolysis or adsorption on the hydrophobic polymer surface [65]. At first, the physical and chemical stability of mAb dispersed in the non-aqueous PLGA formulation was intended to be analyzed. As PLGA is non-miscible with water, extraction necessitates the use of organic solvents. There are three major requirements on the used solvent for this purpose: (i) it should present a solvent for PLGA but a non-solvent for mAb, (ii) it should be volatile for easy removal after extraction of the protein and (iii) the solvent should be compatible with the mAb. Körber *et al.* successfully used ethyl acetate for extraction of lysozyme from non-aqueous PLGA solutions [108]. Based on this study, the suitability of ethyl acetate for the present purpose was evaluated. In a second step, mAb stability after extraction was assessed via HP-SEC and HP-IEC. In order to exclude any detrimental impact of ethyl acetate on mAb conformational stability, sd mAb was dispersed in ethyl acetate and incubated for 20 min. For separation of sd particles, samples were centrifuged. The supernatant was removed and the sediment was dried under vacuum atmosphere. The dried sediment was reconstituted in water, leading to a clear solution which was analyzed by HP-SEC and HP-IEC measurements.

Dispersion of sd mAb particles in ethyl acetate did not lead to any increase in HP-SEC aggregate or fragment formation (99.2 ± 0.7 % monomer recovery (sd mAb + ethyl acetate) vs. 99.4 ± 0.1 % monomer recovery (sd mAb)). Also HP-IEC measurements did not show any changes induced by ethyl acetate. Thus, ethyl acetate was selected for mAb extraction from the PLGA formulations. For this purpose, an exemplary PLGA formulation composed of 30 % Resomer® RG 502H, 5 % mAb and a P/T ratio of 85 %/15 % was used. Upon mAb separation, drying and reconstitution, a clear solution was obtained that was used for further analysis. HP-SEC monomer recovery after extraction of mAb from the PLGA formulation did not significantly differ from the reference (figure 2-12 A). Similar to HP-SEC, HP-IEC did not show any indications of protein degradation (figure 2-12 B). Based on these results it was

concluded that mAb is initially unaffected by the incorporation into a non-aqueous PLGA solution.

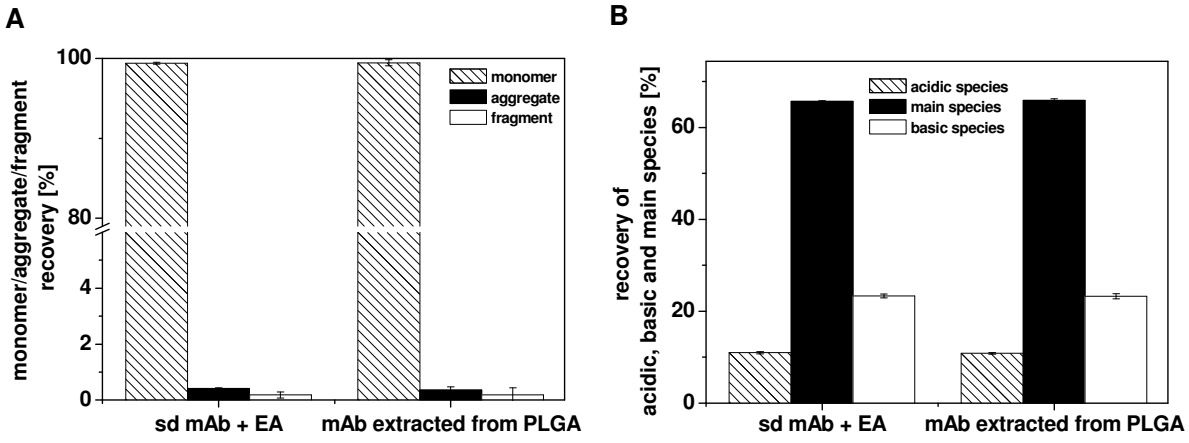

Figure 2-12 (A) HP-SEC recovery of monomer, aggregates and fragments and (B) HP-IEC recovery of acidic, main and basic species of reconstituted mAb extracted from a non-aqueous PLGA formulation (30 % Resomer® RG 502H, 5 % mAb and a P/T ratio of 85 %/15 %) using ethyl acetate (EA), compared to equally treated sd mAb.

In a further step, mAb stability after release from *in situ* formed PLGA matrices was investigated. Therefore, the release fractions were analyzed in regard to monomer content and the presence of soluble aggregates or fragments via HP-SEC. Tertiary protein structure was elucidated via secondary UV spectroscopy. Moreover, large insoluble protein aggregates were intended to be identified via bright-field microscopy after protein staining on a filter membrane.

Due to the low mAb release rate and therefore the low mAb concentration in the release medium after day 1, release fractions could only be analyzed during the burst phase. At these time points, PLGA degradation had not started yet and a pH drop that might induce protein degradation is therefore not expected. However, protein aggregation induced by e.g. interaction with the precipitated polymer could be identified. HP-SEC analysis revealed that additional soluble aggregates or fragments were not present in the release fractions and the total AUC was not reduced. Figure 2-13 shows an exemplary second derivative UV spectrum of released mAb at day 1 in comparison to native mAb. As no peak shifts were detectable, it was concluded, that the tertiary protein structure was essentially preserved upon release from the PLGA matrix.

As mentioned in section 3.2.4, release fractions after day 9 turned slightly turbid with the presence of white flakes. This turbidity was observed in both mAb containing and placebo

samples. In order to tell whether this turbidity is accompanied by protein aggregation, release fractions were filtered through a 0.2 µm membrane filter and stained with a protein detection kit. In presence of protein that is retained by the membrane, purple colorization can be detected by bright-field microscopy. The analysis of the release fractions revealed that the slight turbidity was not exclusively related to PLGA degradation as protein particles or protein carrying PLGA particles in the lower µm range were detected (figure 2-14).

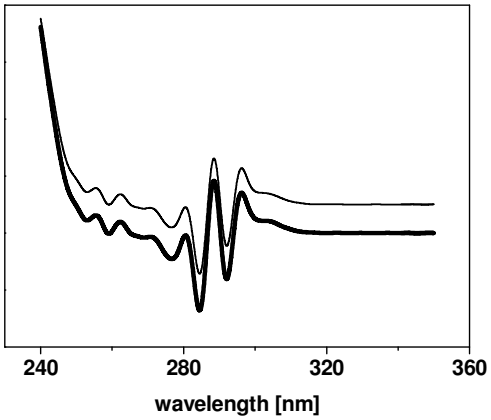

Figure 2-13 Second derivative concentration normalized UV spectrum of mAb containing release fractions at day 1 (thick line) in comparison to native mAb (thin line). Artificial offset for clarity.

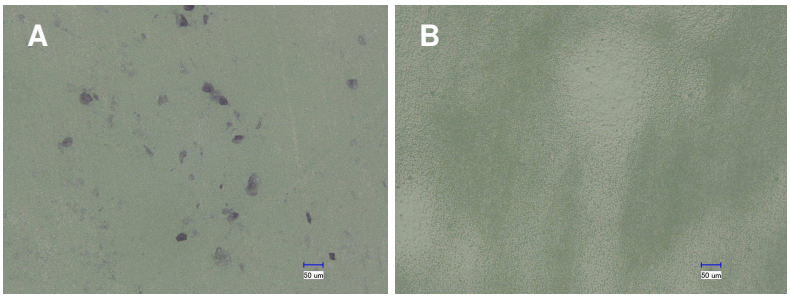

Figure 2-14 Bright-field microscopy images after staining with protein detection kit of release fractions at day 14 from a formulation composed of 45 % Resomer® RG 502H, a P/T ratio of 100 %/0 % and a mAb content of 5 % (A) in comparison to the corresponding placebo sample (B).

The exact mechanism for the detected protein instability is difficult to identify. On the one hand, protein aggregates could be formed already at earlier time points but they initially remain entrapped in the dense PLGA matrix. Release and subsequent detection of these aggregates might occur during PLGA degradation and matrix erosion. On the other hand, it could be the case that protein is adsorbed on the matrix surface during or after release which can be detected upon PLGA degradation and erosion.

The findings of the above study indicate that mAb prior to incubation as well as initially released mAb shows excellent stability. However, the stability of mAb that remains in the degrading PLGA matrix might be a critical aspect.

3.4 Modification of PLGA formulation in regard to injectability and analysis of the resulting release profile

The formulations containing 45 % Resomer® RG 502H had to be tested without syringe needle due to their high viscosity so far. In a next step, the formulations with 5 % mAb and P/T ratios ranging from 85 %/15 % to 33.3 %/66.6 % were intended to be modified in regard to injectability by reducing the polymer content to 30-35 % and the impact of the use of 26 G syringe needles on mAb release was studied. As the viscosity of the formulations was still too high for a manual injection, an injection aid was applied.

The addition of only 15 % triacetin to the formulation still led to a high burst effect of 96 % (figure 2-15). The burst suppression by small amounts of triacetin that was detected at 45 % polymer and injection without needle could not be shown upon injection of a 30 % polymer containing formulation through a 26 G needle. Hence, both the reduction of PLGA content and the use of syringe needles apparently have a tremendous impact on the release profile. However, an increase in triacetin content up to 66 % led to a suppression of the burst effect and incorporation of the mAb in the precipitated matrix could be achieved. Due to high standard deviations, a significant difference between formulations with a P/T ratio between 66.6 %/33.3 % and 33.3 %/66.6 % at a Resomer® RG 502H content of 30 % could not be identified. An increase of the PLGA content from 30 % to 35 % significantly reduced the initially released mAb amount from approximately 50 % to 8 % at a P/T ratio of 33.3 %/66.6 %. The formulation with PLGA content of 35 % revealed the slowest mAb release profile with overall total mAb release of only 28 % after day 16. The effect of the polymer content on the release rate was also reported by Shively *et al*. and Eliaz *et al*. who found out that an increase in PLGA content reduces the overall drug release which might be attributed to an enhanced hydrophobicity and therefore reduced water uptake [59, 105]. A change in formulation consistency could also be hypothesized. Furthermore, it is expected that higher polymer content leads to the formation of a highly dense matrix and thus more efficient mAb incorporation. The high standard deviations can be attributed to differences in shape upon injection induced by the consistency of the formulations causing different initial release rates. Similar to experiments in section 3.2.4, the addition of high amounts of

triacetin led to a moldable formulation consistency (figure 2-16). Triacetin content of 15 % induced the formation of matrices that maintained the structure after injection. The results of the present study demonstrate that formulations based on Resomer® RG 502H were successfully modified with regards to injectability and the burst can be controlled by the addition of triacetin.

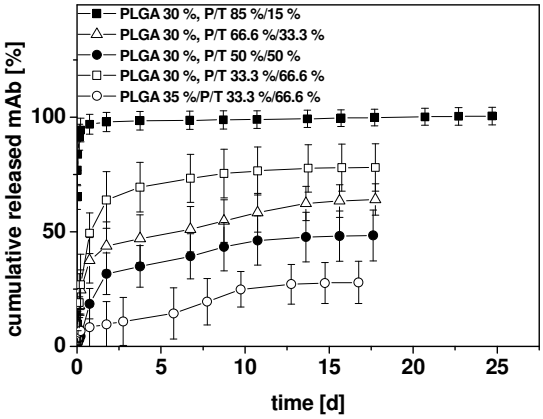

Figure 2-15 *In vitro* release profiles of mAb from formulations composed of 30 % to 35 % Resomer® RG 502H, a mAb content of 5 % and P/T ratios as indicated; injection through 26 G needles.

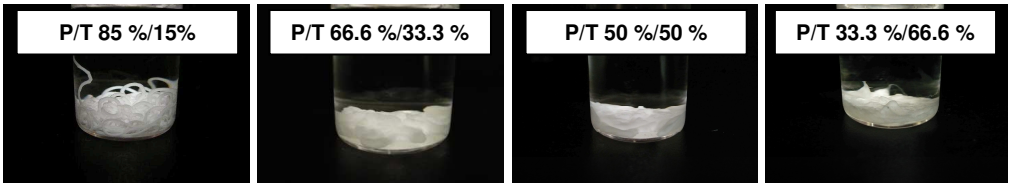

Figure 2-16 Visual appearance of formulations with 30 % Resomer® RG 502H, a mAb content of 5 % and P/T ratios as indicated; injection through 26 G needles.

3.5 *In vitro* release experiments of murine mAb from PLGA formulations and characterization of released mAb

In order to gain insight into the pharmacokinetic profile of selected formulations, an *in vivo* study in rats was envisaged. As this study was intended to be performed with the murine mAb variant, the *in vitro* mAb release experiments performed with the human mAb were to be confirmed with the murine mAb first. Three formulations showing “long” (35 % Resomer® RG 502H and P/T ratio of 33.3 %/66.6 %), “intermediate” (30 % Resomer® RG 502H and a P/T ratio of 66.6 %/33.3 %) and “short release” (30 % Resomer® RG 502H and a P/T ratio of 85 %/15 %) were selected. The murine mAb content was reduced to 2.5 % due to pharmacological reasons. Injection occurred by means of 21 G

syringe needles. This needle size was the largest possible needle size allowing IA injection in rats.

Murine mAb release was studied during one week. A high burst of 62 % was observed in the "short release" formulation but not for the "intermediate" and "long release" formulations (figure 2-17). The obtained release profiles are overall comparable to the release profiles achieved with the human mAb. Slight differences concerning the total mAb release can be seen: while the "short release" formulation revealed a murine mAb release of 66 ± 4 % after 7 days, complete release of the human mAb was observed in foregoing experiments. Regarding the "intermediate" and "long release" formulations, an overall significant slower murine mAb release was identified. After 7 days, only 5.2 ± 1.6 % ("intermediate") and 2.1 ± 1.9 % ("long") were recovered in the release fractions. The observed differences can be ascribed to the use of different needle size in both experiments: while the experiment with the human mAb was performed with 26 G needles, the murine mAb formulations were injected through 21 G needles. Moreover, differently produced sd powders were employed and the drug load in the murine mAb formulations was reduced by factor 2 which might contribute to the observed release differences. However, overall three different release profiles were seen with both the human and the murine mAb variant which presents an essential aspect for the intended *in vivo* study.

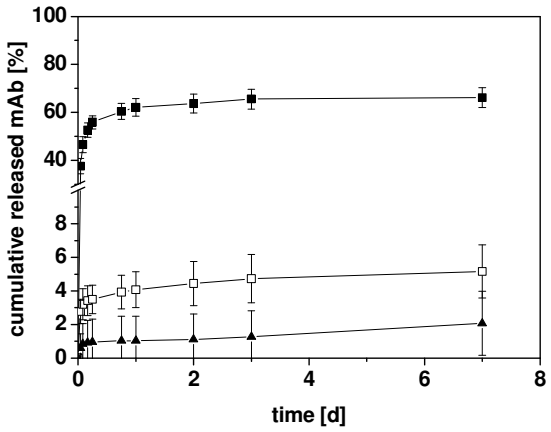

Figure 2-17 *In vitro* release profiles of murine mAb (2.5 %) from "short release" (30 % Resomer® RG 502H, P/T 85 %/15 %, filled square), "intermediate release" (30 % Resomer® RG 502H, P/T 66.6 %/33.3 %, opened square) and "long release" formulations (35 % Resomer® RG 502H, P/T 33.3 %/66.6 %, triangle). Injected through 21 G syringe needles.

HP-SEC analysis of release fractions revealed that the monomer content of murine mAb slightly decreased during the release experiment (figure 2-18). After 3 days, a reduction of

the monomer recovery to 86 ± 1.7 % (“short release” formulation) was detected. Incubation of murine mAb at 37 °C in PBS for the same period of time also led to a slight reduction in monomer recovery from 97 ± 0.4 % to 94 ± 0.4 % after 7 days. Only samples from “short” and “intermediate release” formulations up to day 3 could be analyzed. In all other samples the protein content was too low.

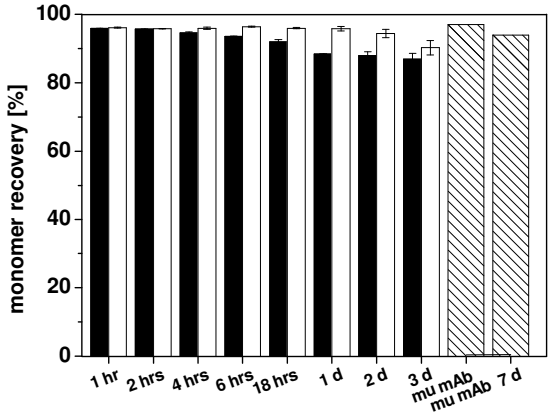

Figure 2-18 Monomer recovery of murine mAb (mu mAb) upon release from “short release” (black) and “intermediate release” formulation (white) at different time points compared to mu mAb standard solution and mu mAb solution incubated for 7 days at 37 °C in PBS / NaN_3 (striped).

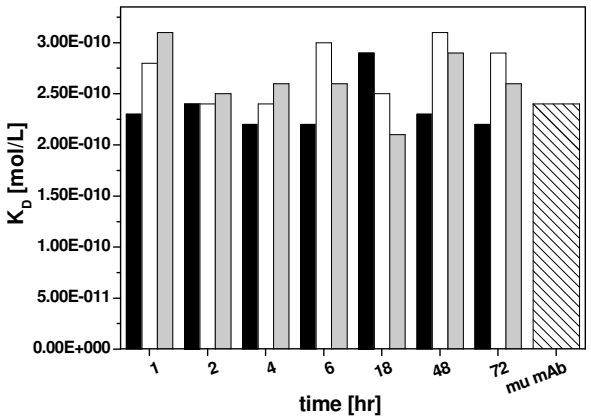

Figure 2-19 K_D as determined by SPR of murine mAb (mu mAb) released from “short release” (black), “intermediate release” (white) and “long release” formulation (gray) at different time points compared to mu mAb standard solution (striped).

Additionally, SPR analysis of the released murine mAb was performed in order to investigate its binding activity by determination of the dissociation constant (K_D) of bound murine mAb antigen upon binding to the murine mAb. This value reflects the binding strength between two binding partners and is calculated by the quotient of association rate constant and dissociation rate constant of the complex. A strong binding is reflected by a low K_D value.

Changes in K_D values indicate structural and thus functional disorder of one of the reaction partners [109]. Released murine mAb fractions showed comparable K_D values compared to murine mAb standard solution (figure 2-19) thus indicating that the binding activity of the murine mAb released from different PLGA formulations was preserved.

3.6 *In vivo* study of mAb release from PLGA formulations after IA application

In order to study the pharmacokinetic profile of the PLGA formulations upon IA administration *in vivo*, an animal study was performed. The previously characterized murine mAb containing PLGA formulations showing “long”, “intermediate” and “short release” profiles were analyzed. Moreover, the release of murine mAb from “long release” PLGA formulation and a murine mAb solution upon SC administration was tested in order to highlight the difference between the two application sites IA and SC.

Serum analysis upon IA administration of the formulations at predefined time points revealed an increase in mAb concentration during the first 72 hrs (figure 2-20). During the time between 72 hrs and 168 hrs, a significant decrease in mAb concentration was observed. However, no significant difference in serum mAb concentration between “long”, “intermediate” and “short release” formulation could be seen.

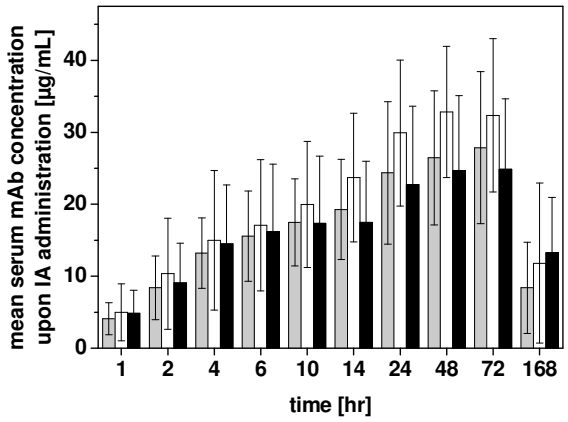

Figure 2-20 Mean serum concentrations of murine mAb after IA administration of 50 µL of “short release” (30 % Resomer® RG 502H, P/T ratio 85 %/15 %, black), “intermediate release” (30 % Resomer® RG 502H, P/T ratio 66.6 %/33.3 %, white) and “long release” formulation (35 % Resomer® RG 502H, P/T ratio 33.3 %/66.6 %, gray) determined via ELISA.

In table 2-4 the c_{max} and t_{max} values of the formulations are summarized. The PLGA formulations reached similar c_{max} values. While the "long release" and "short release" formulation showed a t_{max} of 72 hrs, the "intermediate release" formulation reached the highest serum level already after 48 hrs. In contrast, IA injected murine mAb solution revealed an approximately 50 % higher c_{max} which was reached already after 12 hrs. However, it has to be taken into account that the results of the mAb solution were obtained with a slightly higher dose. From other studies performed by the Abbott Bioresearch Center, it is known that a lower dosing leads to lower c_{max} but same t_{max} values. Therefore, it is expected that c_{max} of mAb solution after IA administration should be rather similar to the ones of the PLGA formulations at same dose.

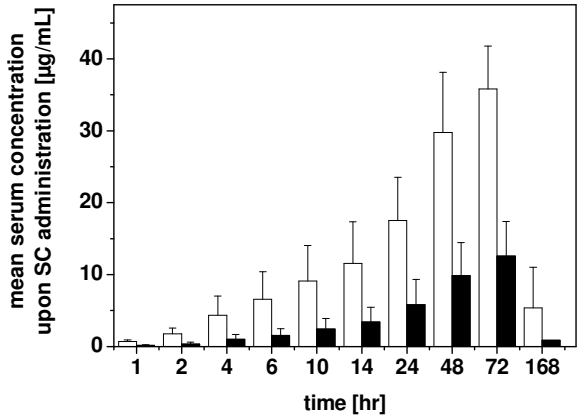

Figure 2-21 Mean serum concentrations of murine mAb after SC administration of 50 µL of "long release" formulation (35 % Resomer® RG 502H, P/T ratio 33.3 %/66.6 %, 2.5 % murine mAb, black) compared to murine mAb solution at same concentration (white).

Different results were obtained after SC administration. As shown in figure 2-21, the "long release" PLGA formulation revealed significantly lower serum mAb concentrations compared to the mAb solution at same concentration. Both formulations showed the same t_{max} of 72 hrs. The formation of anti-drug antibodies was observed in some animals that were dosed with the PLGA formulation. These animals were removed from the calculation. Concerning the impact of the application site, a significant influence on the mAb release rate was identified (table 2-4). The c_{max} of the "long release" formulation after IA administration was by a factor of 2.2 higher compared to the c_{max} after SC application. This effect might be ascribed to the exposure of the formulation to stronger mechanical manipulation in the knee joint compared to the subcutaneous space leading to enhanced mAb release. The mechanical influence would also explain the fact that no differences in serum levels between "short",

Table 2-4 Dose, c_{max} and t_{max} of different formulations upon IA and SC administration.

	Dose [mg/kg]	**c_{max} [µg/mL]**	**t_{max} [hr]**
"long release", IA	4.5	27.9 ± 10.6	72
"intermediate release", IA	4.5	32.8 ± 9.1	48
"short release", IA	4.5	24.9 ± 9.8	72
mAb solution, IA	6.5	46.5 ± 12.0	12
"long release", SC	4.5	12.6 ± 4.8	72
mAb solution, SC	4.5	35.8 ± 6.0	72

"intermediate" and "long release" formulation were seen. Besides the mechanical exposure it has to be taken into account that the absorption half-life of SC administered drugs is described to be longer than that of IA injected drugs. For the SC administration an absorption half-life of 1.4 day is reported for mAbs in general [110] while the synovial half-life of mAb upon IA injection was determined to be 0.5 days (data generated by Abbott). The physiological differences of the application sites might contribute to the detected higher mAb serum concentrations upon IA administration of the "long release" formulation compared to the SC application. The main reason for the short residence time of IA administered drugs in general is the rapid turnover of the SF within few hours. This effect is known to be even more accelerated in patients suffering from rheumatoid arthritis [13]. Due to this fact, the incorporation of the drug into a depot system for prolongation of the residence time at the site of application presents a promising approach. *In vitro* release experiments clearly revealed differences in mAb release profile between the different PLGA formulations tested. But these differences could not be seen *in vivo*. Even in comparison to a non-retarded mAb solution, no significant difference in c_{max} was observed. This poor *in vitro – in vivo* correlation might be ascribed to the high mechanical stress within the knee joint. This leads to spreading and kneading of the formulation with animal movement and consequently changes in shape, reduced diffusion path lengths of incorporated mAb and exposure of otherwise internal structures. These effects are strongly related to an increase in mAb release rate. Based on these findings, it can be concluded that the observed formulation differences *in vitro* are not sufficient to result in differences *in vivo* upon IA administration. Upon SC administration, however, the retardation effect was more pronounced which points to the impact of the mechanical conditions at the application site on the pharmacokinetic. From these findings it was concluded that the *in vitro* release model needs to be modified with respect to simulation

of the joint conditions in order to be able to predict the *in vivo* mAb release from PLGA formulations.

3.7 PLGA formulation screening with the mechanical stress model

The use of an *in vitro* release model that simulates well the physiological conditions is essential to predict *in vivo* drug release behavior. Up to now, no regulatory approved standard methods are available for *in vitro* release testing of sustained release parenteral formulations [111, 112]. In general, besides the presence of sink conditions, the appropriate *in vitro* model should induce the same drug release mechanism as *in vivo* [111]. This includes in the present case the simulation of the mechanical conditions in the joint that lead to spreading and kneading of the *in situ* forming matrix. This mechanical effect was to be implemented by the use of a punching tool that repeatedly penetrates into the incubated PLGA matrix. In order to assess the suitability of the model, the three formulations tested *in vivo* were analyzed. The injected volume of the formulations was reduced to 50 mg in analogy to the *in vivo* study. Directly after injection through a 21 G needle into PBS, the formulations were subjected to 20 penetration cycles by the punching tool. After 24 hrs of incubation at 37 °C the released mAb amount was quantified.

All formulations revealed a high mAb release of equal or more than ~50 % (“short release” formulation 74.9 ± 4.1 %, “intermediate release” formulation 49.3 ± 7.7 %, “long release” formulation 54.4 ± 12.0 %). Comparing these results with the burst intensities of foregoing *in vitro* release experiments (section 3.4, “short release” formulation 96.8 ± 4.4 %, “intermediate release” formulation 37.5 ± 9.9 %, “long release” formulation 8.4 ± 8.9 %), the impact of mechanical treatment becomes obvious. Based on these results this model was applied in the following for further formulation screening.

In order to identify a PLGA formulation that provides sufficient mAb retention, the PLGA content was increased up to 50 % irrespectively to injectability and the P/T ratio was varied from 40 %/60 % to 100 %/0 % at 5 % mAb content. Injection into the incubation medium was performed without syringe needle. After each sample draw, the formulations were subjected to mechanical manipulation with the punching tool. Significant differences in the release rates between the formulations were only observed at day 1 (figure 2-22). Until day 3, an intensive mAb release of more than 55 % was observed for all formulations. Subsequently, the release rate decreased for all formulations leading to a plateau formation.

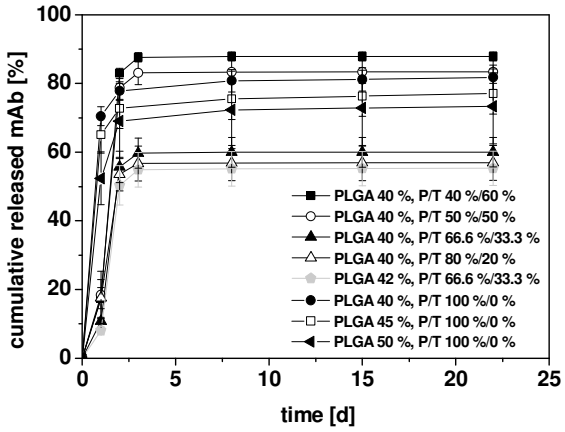

Figure 2-22 *In vitro* release profiles of mAb from formulations composed of 40 % to 50 % Resomer® RG 502H, a mAb content of 5 % and P/T ratios as indicated; injection without syringe needle.

A clear relation between burst intensity and P/T content and/or polymer content could not be identified as indicated by previous experiments. Compared to the experiments performed without mechanical treatment (section 3.4) the mAb release rate in all formulations was significantly accelerated at day 1 and 2 which can be explained by a substantially enhanced matrix swelling due to water uptake which was visually detectable by an increase in matrix volume. The water uptake led to dissolution of sd mAb particles incorporated in the matrix. During the second mechanical treatment, after the first sample draw at day 1, the swollen matrices were compressed and the dissolved mAb solution was squeezed out. The experiment was terminated after 22 days as no further mAb release was noticed despite visually detectable PLGA degradation. Analysis of the non-released mAb amount after lyophilization, extraction of PLGA with ethyl acetate and redissolution indicated that large protein particles had formed (see figure 2-23).

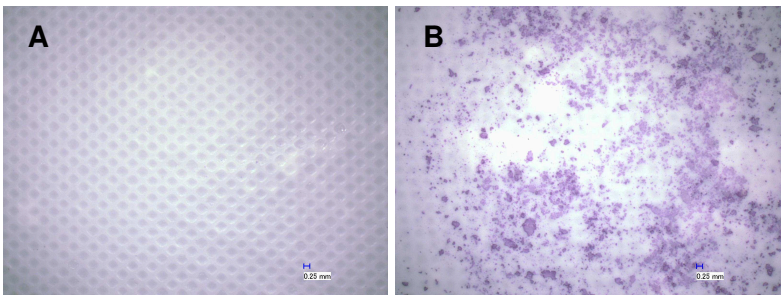

Figure 2-23 Bright-field microscopy images after staining with protein detection kit of mAb extracted from PLGA matrices (42 % Resomer® RG 502H, P/T 66.6 %/33.3 %, mAb 5 %) at day 22. (A) placebo formulation, (B) active formulation.

Besides the incomplete release, fractions at day 1 and 2 exhibited a high turbidity. This was most pronounced in formulations with a P/T ratio of 100 %/0 % and these fractions were investigated for monomer recovery by HP-SEC. It could be shown that the relative monomer recovery was unchanged (figure 2-24). However, the total AUC was reduced from 90 % to 70 % at day 2 indicating the presence of insoluble aggregates reflected by the sample turbidity. In conclusion, with the help of the mechanical treatment model a rapid mAb release and strong protein aggregate formation was observed which leads to the fact that after the initial burst, no further mAb release could be seen.

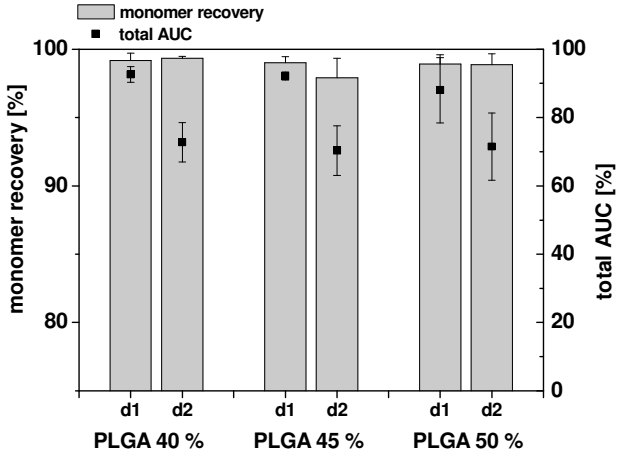

Figure 2-24 Results of HP-SEC analysis of release fractions at day 1 (d1) and day 2 (d2) of selected formulations composed of 40-50 % Resomer® RG 502H, a P/T ratio of 100 %/0 % and a mAb content of 5 %.

Despite the successful incorporation of proteins in PLGA systems, the occurrence of protein instabilities and incomplete protein drug release is recognized as challenging [47, 64, 65, 84]. Protein instabilities include deamidation, chain cleavage and acylation by the polymer as well as protein aggregation induced by the acidic microclimate pH occurring during polymer degradation, the use of organic solvent in formulation preparation or protein adsorption phenomena to hydrophobic polymer surfaces or water/organic solvent interfaces [64, 65]. On the one hand, instabilities occurring at the beginning of a release experiment can be ascribed to formulation preparation and/or storage as well as to unfolding induced by water/organic phase interfaces. On the other hand, instabilities detected after the burst release are likely induced by polymer degradation, interactions between protein and polymer or protein adsorption to the solid PLGA matrix [64]. In the present study, both instabilities at the beginning and upon extraction at the end of the release experiment were identified. As mAb stability upon formulation preparation (see paragraph 3.3) and incubation in the organic solvents (see paragraph 3.2.2) has been demonstrated, the aggregate formation can be

attributed to mAb-polymer interactions such as adsorption on the hydrophobic surface and unfolding on water/organic phase interfaces after incubation in aqueous medium. As foregoing release experiments, performed with the vial model, rendered clear release fractions but incomplete overall release, it can be presumed that insoluble aggregates were retained inside the PLGA matrix. In opposite to that, application of the mechanical stress model led to release of both soluble and partly aggregated protein. These protein instabilities may be prevented by the addition of excipients such as surfactants, HSA, cyclodextrins, L-arginine and/or pH modifying additives [65, 84]. However, the addition of excipients could have an impact on the protein release kinetic and complete suppression of aggregate formation due to stabilizing excipients might be challenging, as demonstrated by Morlock *et al.* [84]. Irrespective of protein instability, the experiments also demonstrate that the burst release could not be controlled by the formulation components.

3.8 Modification of the reconstitution time of mAb powder and analysis of the impact on mAb release from PLGA formulations

Previous experiments demonstrated that the burst release could not be controlled by formulation components when applying the mechanical stress model as *in vitro* release system. In order to achieve drug release over an extended period of time, a high mAb incorporation and thus low burst release is mandatory. To avoid rapid dissolution of mAb particles during the lag between formulation injection and PLGA hardening, the sd mAb powder was to be modified. This was to be achieved by adding either gel forming excipients or hydrophobic additives to the mAb solution which is dried. The gel forming excipient hydroxyethyl cellulose 400 (HEC) was expected to decelerate mAb dissolution by formation of a gel matrix. The addition of the hydrophobic amino acid isoleucine (ile) was presumed to reduce the particle hydrophilicity and prolong particle dissolution.

Addition of 4 % HEC to the 10 % mAb spray drying solution and subsequent lyophilization of the highly viscous gel, milling on dry ice under nitrogen atmosphere and sieving of the powder through a 90 µm mesh led to prolongation of the reconstitution time to 62.1 ± 2 min vs. 3.2 ± 0.1 min (sd mAb without HEC). Ile at a concentration of 3 % (w/v) was added to the 10 % mAb spray drying solution in a volumetric ratio of 1:2.3. After spray drying, the resulting powder showed a reconstitution time of 23.1 ± 13.4 min.

In order to study whether the addition of dissolution modifying excipients could reduce the mAb burst release from PLGA formulations, HEC-mAb particles generated by lyophilization

as well as ile-mAb particles obtained by spray drying were dispersed in a PLGA formulation (40% Resomer® RG 502H, P/T ratio 40 %/60 %, 5% mAb content) respectively and the release was tested. Compared to a formulation without dissolution modifying agent, the use of HEC led to a more rapid and complete mAb release (figure 2-25). Instead of delaying the release by a gel matrix formation, the presence of HEC seemed to induce enhanced water influx into the system and swelling due to the hygroscopic character of the excipient. The overall release profile of the ile containing formulation was similar to the reference formulation with an even higher burst at day 1. In conclusion, it was not possible to achieve higher mAb retention in the solidifying PLGA matrix by modifying the dissolution rate of the mAb particles using HEC or ile.

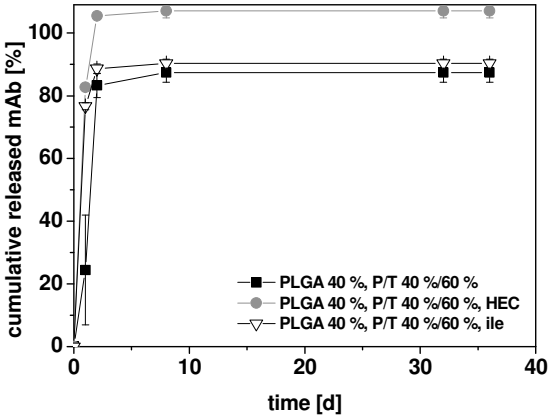

Figure 2-25 *In vitro* release profiles of mAb from PLGA formulations (40 % Resomer® RG 502H, P/T ratio 40 %/60 %, mAb content 5 %) using HEC or ile as dissolution modifying excipients of the incorporated mAb particles in comparison to a formulation with non-modified sd mAb.

In conclusion, the present study revealed that the development of an *in situ* forming PLGA-based depot system for the sustained release of mAb is particularly challenging. This can be primarily ascribed to the high mechanical exposure of the formulation in the joint cavity that induces high mAb release during the lag between injection and PLGA hardening. As no promising formulation with the use of PEG 300 and triacetin could be indentified and protein aggregation during formulation incubation was observed, this formulation approach has limited suitability for the IA administration of mAb.

4 SUMMARY AND CONCLUSIONS

The aim of this part of the thesis was the development and characterization of a PLGA-based formulation for the IA delivery of a therapeutic antibody. This concept encompassed the dispersion of the sd mAb in a non-aqueous PLGA solution that precipitates *in situ* upon contact with SF leading to a solidified matrix with entrapped mAb particles. Drug release was intended to take place concomitantly to polymer degradation. The formulation to be developed was meant to provide adequate injectability through thin syringe needles and mAb release over a prolonged time in order to reduce injection frequency. Moreover, the formulation was intended to provide a semi-solid consistency with adequate mechanical strength in order to resist the high mechanical impact present in the knee joint but avoid friction and restricted joint mobility. Additionally, the formulation components had to be highly compatible with the incorporated mAb and the application site. As these formulation characteristics are strongly dependent on the formulation components and the used concentrations, it was the first task to evaluate a suitable formulation composition and drug load with respect to the aforementioned prerequisites. Therefore, Resomer® RG 503H was used as polymer component. PEG 300 and triacetin were identified as suitable biocompatible polymer solvents. Analysis of the compatibility of the chosen solvents with the sd mAb did not show any instabilities detectable via turbidity measurements, HP-SEC, second derivative UV and FTIR spectroscopy. However, *in vitro* release experiments that were performed by injection of the formulations into PBS filled vials showed a nearly complete mAb release during the first 5 hrs indicating that mAb was not retained by the precipitating polymer. As a proof of principle, the polymer content was increased to 45 % and dissolved in either PEG 300, triacetin or in mixtures of both solvents. Instead of Resomer® RG 503H, Resomer® RG 502H, a polymer with lower MW and intrinsic viscosity was employed as higher concentrated polymer solutions were achieved. This experiment pointed out that mAb retention in the solidifying matrix in general is possible and that the initial burst und subsequent drug release are strongly reduced when higher concentrations of the hydrophobic polymer solvent triacetin are used. The reduced burst effect was explained by the high hydrophobicity of triacetin and therefore high affinity to the polymer leading to reduced water influx and mAb dissolution as well as by the change in formulation consistency. However, the addition of small amounts of triacetin drastically reduced the mechanical strength of the *in situ* formed matrix and therefore a balance between initial drug release and formulation consistency had to be found. In a further step, the formulation was

modified with respect to injectability. Therefore, the PLGA content was reduced and formulations were injected through 26 G syringe needles into the release medium. It could be shown that these modifications had a significant impact on the mAb release pattern. Due to injection through the syringe needle, the surface area of the solidifying formulations increased drastically leading to an overall enhanced burst effect. However, it was clearly detectable, that with increasing triacetin as well as polymer content, the burst intensity was reduced. Based on these data, three formulations showing “long”, “intermediate” and “short” release profiles were selected for an *in vivo* study with rats using a murine mAb variant. Murine mAb analysis of the *in vitro* release fractions revealed a slight decrease in monomer recovery, detected via HP-SEC but unchanged binding affinity as identified by SPR. In accordance to these findings, unchanged tertiary protein structure as well as monomer recovery were observed for the human mAb upon release. Results of *in vivo* experiments clearly displayed that IA mAb retention was only marginal. No differences in serum mAb concentrations between “long”, “intermediate” and “short” release formulation were observed indicating that the mechanical impact induced by movement of the animals leads to unexpected high mAb release rates. In comparison to that, SC application of the “long release” formulation showed drastically lower serum mAb concentrations compared to SC administered mAb solution and to IA injected “long release” formulation which emphasizes the mechanical impact on mAb release. Based on these findings, the *in vitro* release model was modified by incorporation of mechanical manipulation at each sampling time point performed by formulation kneading with a punching tool. Formulations with various polymer contents and P/T ratios were investigated, but insufficient mAb retention resulted using this modified *in vitro* release model. This suggested that mAb dissolution occurs more rapidly than polymer precipitation. Finally, in an effort to reduce the burst release, HEC 400 and the hydrophobic amino acid ile were added to the mAb particle formulation respectively, in order to prolong the particle dissolution. Both modifications led to prolonged reconstitution times of the powders, but the mAb release from the PLGA formulation was not significantly delayed by the additives. Besides the insufficient mAb retention in the PLGA matrix, protein containing release fractions obtained during *in vitro* release experiments with the mechanical stress model were turbid. MAb analysis via HP-SEC did not show a reduction in monomer recovery but a significant decline of the total AUC. From these results it could be concluded, that substantial amounts of insoluble protein aggregates were formed already early during drug release in the course of solvent exchange, PLGA precipitation and formation of hydrophilic-hydrophobic interfaces. These instabilities were not detected in earlier studies as the insoluble aggregates were entrapped within the PLGA matrix and release of insoluble aggregates was only possible upon squeezing of the matrix by applying a punching tool.

The present study clearly demonstrates that the IA administration of *in situ* forming PLGA-based mAb depots is particularly challenging due to the exposure to mechanical load and the rapid SF exchange that makes drug retention at the site of application difficult. Due to movement of the joints, the injected formulation is subjected to kneading effects that lead to increase of the formulation surface accompanied by a reduction of the diffusion path length of incorporated mAb followed by release. In order to avoid enhanced mAb release during joint movement, form-stable matrices with short lag phase between injection and hardening appear necessary that resist the high mechanical exposure. The development of a formulation with high mechanical strength and low burst effect was shown to be highly challenging as the use of high amounts of PEG 300 led to form-stable matrices but was accompanied by a high burst. In contrast, the addition of small amounts of triacetin reduced the burst but simultaneously drastically reduced the mechanical strength. A compromise between consistency and drug release might be possible by using the dispersion or solution of the drug in a polymer solution which is subsequently dispersed in a second oil phase [113]. Upon SC or intra muscular injection, microparticles are reported to be formed due to influx of aqueous body fluids and/or diffusion of the solvent out of the polymer droplets leading to polymer precipitation and thus incorporation of the drug that can be released in a controlled manner. Moreover, preformed drug-loaded small size PLGA implants could be used to overcome the burst release.

CHAPTER 3

THE USE OF POLYSACCHARIDES AS CARRIERS FOR THE INTRA-ARTICULAR DELIVERY OF A THERAPEUTIC ANTIBODY

1 INTRODUCTION

Natural polymers, such as polysaccharides, are considered as attractive carrier materials for the delivery of drugs due to their excellent biocompatibility, biodegradability, abundant availability in nature and low costs [114, 115]. They provide unique physico-chemical properties as well as gelation characteristics that can be beneficial when drugs are envisaged to be released in a controlled way [116]. Depending on their functional groups, polysaccharides are divided into non-polyelectrolytes and polyelectrolytes at physiological pH. The group of polyelectrolytes can be further categorized into positively charged (e.g. chitosan) and negatively charged polysaccharides, such as alginate, hyaluronic acid (HA), heparin or chondroitin sulphate [114]. Some of the functional groups are able to be derivatized by e.g. esterification [117] or acrylation [118]. This is of advantage if improved viscoelastic properties, enhanced resistance towards enzymatic degradation, reduced solubility or prolonged residence time upon injection are desired. Apart from that, these functional groups are reported to interact ionically with charged drug substances, such as proteins [119, 120], to affect drug delivery.

Remarkable attention has been drawn to the use of HA as carrier material in drug delivery. Besides its biocompatibility and biodegradability, it exhibits excellent viscoelastic properties and the ability to create a dense network in which a drug can be incorporated. Especially, the development of HA based formulations for therapeutic proteins and peptides has been in the focus of various research groups. Due to the hydrophilic nature, HA based drug delivery systems provide a protein- and peptide-compatible environment [121]. Concerning non-parenteral drug delivery, studies can be found dealing with the enhanced nasal bioavailability of insulin, released from HA ester microspheres in sheep [122]. More intensively, the

parenteral protein delivery from HA based systems was investigated. Prisell *et al.* analyzed the release of human recombinant insulin-like growth factor-I from HA gels (0.5 – 2 %) in rats. Upon subcutaneous (SC) injection, a significantly slower release was demonstrated compared to the HA-free formulation [123]. Meyer *et al.* investigated the *in vitro* stability and *in vivo* release profile of recombinant human granulocyte colony stimulating factor (rHG-CSF) from viscous HA solutions (2 %) after SC injection in hamsters. No significant protein aggregation upon storage for 6 weeks at 37 °C was detected. *In vivo*, prolonged elevated rHG-CSF plasma levels were observed [124]. In another study, the release of growth hormone (GH) from HA-poly(acrylic acid) sponges was monitored *in vitro.* It could be shown that this delivery system appears to be highly suitable to achieve a sustained drug release [125]. Tian *et al.* investigated the release of an IgG antibody from a HA based gel that was covalently linked with the antibody via a hydrolytically unstable hydrazine linker. Upon hydrolysis the antibody was continuously released over a period of 400 hrs [126]. Despite the numerous *in vitro* and *in vivo* drug release studies found in literature, only little emphasis has been placed on the input in detailed analysis of protein conformational stability after incorporation into the carrier matrix [47]. The preservation of the protein´s conformational stability presents a crucial aspect as its bioactivity largely depends on the native folding. Moreover, protein denaturation is known to induce immunologic reactions [127] and presents therefore a critical parameter.

Especially in the local treatment of joint diseases the use of HA as a carrier for disease modifying drugs presents a promising approach. It combines the beneficial viscosupplementative properties of HA with the pharmacologic effects of the incorporated drug. Various studies are reported in literature dealing with the concept of local intra-articular (IA) delivery. Lyons *et al.* combined a viscous HA gel with triamcinolone crystals that are discussed to dissolve slowly in presence of HA and thus provide a sustained release effect. Moreover, the risk for crystal induced joint inflammation is reported to be reduced by the protective gel [128]. Another patent deals with the incorporation of an antimicrobial agent into a HA gel intended for the treatment or prevention of joint infections upon IA injection [129]. Furthermore, studies about the IA application of HA gels containing a hyaluronidase inhibitor, such as xylose sulphate, dextran sulphate or heparin sulphate, are reported. The incorporated enzyme inhibitor is meant to prevent HA degradation by hyaluronidase and therefore provides a long-lasting therapeutic effect [130]. These studies, however, were only performed with low molecular weight drugs. The applicability of this concept to high molecular weight drugs like therapeutic proteins, however, is not highlighted in literature and is therefore the basis for the present project.

In this study the suitability of HA as a carrier for the local IA delivery of a therapeutic monoclonal antibody (mAb) was investigated. Local IA delivery of a drug presents an attractive approach to generate high drug concentrations at the site of application while reducing the systemic exposure. Especially for expensive drugs with low oral bioavailability, such as therapeutic proteins, this way of application is of enormous interest. However, because of the potentially rapid clearance from the joint cavity, the need for drug delivery systems with prolonged residence time arises [90]. As the IA injection is accompanied by a certain risk of joint infections, the injection frequency has to be limited. Therefore, a high drug load per injection is aspired. In the present study, a highly-concentrated HA-based mAb formulation was to be developed first. In order to achieve a high residence time upon injection, the formulation was meant to provide a high viscosity but acceptable injectability. Different HA materials with various molecular weights and concentrations were to be evaluated. In a subsequent step, the compatibility with the used mAb was assessed by a bundle of analytical methods. This should provide a detailed understanding concerning the protein´s stability upon incorporation into the HA matrix. Additionally, the presence of interactions between HA and mAb as well as the *in vitro* and *in vivo* release behavior were investigated.

Another promising approach for prolongation of the residence time of a therapeutic protein at the site of injection is the use of polysaccharides with a high charge density that induce the formation of insoluble complexes with the protein via charge interactions. The tendency to interact electrostatically with positively charged proteins at physiological pH is described to be enhanced with increasing negative charge density of the polysaccharide [131]. As sodium alginate is known to possess a higher charge density than e.g. HA, it was used in this study. The conditions at which mAb precipitation occurs were intended to be indentified. Interestingly, sodium alginate is used in food industry for purification of whey solutions via precipitation of proteins and subsequent separation [132]. The use of freeze-dried collagen-alginate complexes, cross-linked via multivalent cations, presents a medical application of protein-alginate precipitates. In this context, the precipitates are used as soft tissue implants, wound dressings or prosthesis [133]. The concept of protein precipitation by sodium alginate in the field of drug delivery, however, has not been reported in literature and was to be tested for the IA delivery of mAb.

2 MATERIALS AND METHODS

2.1 Materials

2.1.1 Monoclonal antibody (mAb)

The mAb (IgG1) with a molecular weight (MW) of 148 kDa was formulated at 70 mg/mL, pH 5.2 with sodium chloride (105.5 mM), monobasic sodium phosphate dihydrate (5.5 mM), dibasic sodium phosphate dihydrate (8.6 mM), sodium citrate (1.16 mM), citric acid monohydrate (6.19 mM), mannitol (65.9 mM) and polysorbate 80 (0.1 %). The bulk solution was stored at -80 °C until use. Prior to use, protein solutions were filtered through an Acrodisc® 0.2 µm PVDF syringe filter (Pall, Dreieich, Germany). For *in vivo* experiments, instead of the human mAb, the murine variant was used, which was formulated in histidine buffer (15 mM) at pH 6.0 and a concentration of 24.5 mg/mL.

2.1.2 Hyaluronic acid (HA)

For gel preparation, four different HA qualities were used, as summarized in table 3-1.

Table 3-1 Description of HA powders used.

HA batch No.	Source	MW [MDa]	Residual moisture content [% w/w]
006	Shiseido (Japan)	~1.07	7.4
A07A		~1.50	4.5
TP0711-1		~2.19	6.1
PHI 923	HTL Bio (France)	~1.2	10.4

2.1.3 Excipients, reagents and chemicals

Table 3-2 lists the excipients, reagents and chemicals used throughout this chapter. All substances were of analytical grade. Ultrapure water for all buffers was used from a PureLab UV/UF system (Elga LabWater, Celle, Germany).

Table 3-2 List of excipients, reagents and chemicals used in this chapter.

Excipients, chemicals, reagents	**Source**
Calcium chloride	Merck, Darmstadt, Germany
Citric acid monohydrate	Carl Roth, Karlsruhe, Germany
Dibasic potassium phosphate	AnalaR Normapur, VWR international, Leuven, Belgium
Dibasic sodium phosphate dihydrate	Merck, Darmstadt, Germany
Ethanolamine	Sigma-Aldrich Laborchemikalien, Seelze, Germany
Glycine	Merck, Darmstadt, Germany
L-histidine	Merck, Darmstadt, Germany
Mannitol	Riedel-de Haen, Seelze, Germany
Monobasic sodium phosphate dihydrate	Merck, Darmstadt, Germany
N-ethyl-*N*9-(dimethylaminopropyl) carbodiimide	Sigma-Aldrich Laborchemikalien, Seelze, Germany
N-hydroxy succinimide	Sigma-Aldrich Laborchemikalien, Seelze, Germany
ortho-phosphoric acid	Zentrale Versorgung LMU München, Germany
Polysorbate 80	Merck, Darmstadt, Germany
Potassium chloride	Caelo, Hilden, Germany
Sodium alginate, viscosity 4-12 mPas (1 %, 25 °C)	Sigma-Aldrich Chemie, Steinheim, Germany
Sodium alginate, viscosity 350-550 mPas (1%, 20 °C)	AppliChem, Darmstadt, Germany
Sodium azide	Acros organics, Geel, Belgium
Sodium citrate	Caelo, Hilden, Germany
Sodium chloride	AnalaR Normapur, VWR international, Leuven, Belgium
Sodium hydroxide, 1M	Merck, Darmstadt, Germany

2.2 Methods

2.2.1 Preparation of formulations

HA powder was filled into a Luer-Lock syringe (VWR International, Ismaning, Germany). Into a second syringe the appropriate amount of mAb buffer, pH 5.2, was filled. The two syringes were connected by a syringe adapter (Braun, Melsungen, Germany). Both components were mixed by moving the syringe plungers back and forth until a homogeneous gel was obtained. The received HA gel with a concentration of 3.5 % was filled into one of the two syringes and was allowed to swell overnight at low temperature (storage at 2-8 °C). For final formulation preparation, the HA gel was further mixed with the 2.5-fold amount of either mAb solution, 70 mg/mL (active), or mAb buffer (placebo) by means of the previously described dual-syringe system. This aimed at a HA-mAb gel with a HA concentration of 1 % and a mAb concentration of 50 mg/mL (active).

2.2.2 Characterization of HA bulk material by Karl-Fischer analysis

The residual moisture (RM) content of the HA bulk material was determined by coulometric Karl-Fischer titration using an Aqua 40,00 titrator with headspace module (Analytik Jena, Jena, Germany). Therefore, 10-20 mg of the respective HA powder were accurately weighed into a 2 R glass vial, sealed with rubber stopper and heated up to 100 °C. For determination of the RM content, the evaporated water was transferred into the titration solution. As reference, a standard with defined RM was employed (apura® water standard oven 1 %, Merck, Darmstadt, Germany).

2.2.3 Characterization of HA gels

2.2.3.1 Rheometry

The rheological properties of prepared gels were studied on a plate-cone rheometer (Physica MCR 100, Anton Paar, Ostfildern, Germany) with exponentially in- and decreasing shear rate (0.01-500 s^{-1}, 500-0.01 s^{-1}) at a gap position of 0.042 mm. The applied cone exhibited a diameter of 50 mm and an angle of 1 °. Analysis was performed at 6, 20 and/or 35 °C using 600 mg of the respective gel. The viscosity at 1 s^{-1} was used for comparison.

2.2.3.2 Turbidity

The turbidity of diluted HA gels in formazine nephelometric units (FNU) was determined with a NEPHLA turbidimeter (Dr. Lange, Düsseldorf, Germany), based on light scattering in an 90 ° angle at λ=860 nm. The system was calibrated with a formazine standard. Prior to analysis, the gels were diluted 1:5 with mAb buffer and centrifuged in order to remove air bubbles (10 min, 10,000 rpm). Approximately 2 mL of each sample were used for analysis.

2.2.3.3 Injectability

The maximal force, required for injection of 0.4 mL of the gel into air, was determined by means of a TA.XTplus texture analyzer (Stable Micro Systems, Surrey, UK) at ambient temperature. This value was defined as the highest force measured before the plunger reached the end of the syringe after having overcome the plunger-stopper breakloose force. For this purpose, 1 mL Luer-Lock syringes (VWR International, Ismaning, Germany) connected to 26 G or 23 G syringe needles (Terumo, Leuven, Belgium) were clamped in a tripod underneath the punching tool. The crosshead velocity was set to 1 mm/s, a representative velocity for the manual injection [96]. After 20 s, the measurement stopped automatically.

2.2.4 Characterization of mAb

2.2.4.1 UV spectroscopy (OD 280, second derivative, absorbance at 350 nm)

Protein concentrations were determined photometrically on an Agilent 8453 UV-Vis spectrometer (Agilent Technologies Deutschland, Böblingen, Germany) equipped with a Peltier temperature controller (Agilent Technologies, Böblingen, Germany) at λ=280 nm and 25 °C. Quartz UV cuvettes with a path length of 1 cm were employed. An extinction coefficient of either 1.39 $mL \cdot mg^{-1} \cdot cm^{-1}$ (mAb) or 1.4 $mL \cdot mg^{-1} \cdot cm^{-1}$ (murine mAb) was used. Samples were diluted to a concentration of 0.1 to 0.7 mg/mL prior to analysis. Corresponding blank spectra were subtracted. Smaller sample volumes were analyzed undiluted with a NanoDrop ND-2000 spectrometer (PEQLAB Biotechnologie, Erlangen, Germany). Second derivative protein spectra were calculated between 240 and 350 nm by means of the ChemStation software. Determination of turbidity of protein containing samples was performed with a UV plate reader (FLUOstar Omega, BMG LABTECH, Ortenberg, Germany)

in 96-well plates (Nunc®, Sigma-Aldrich Laborchemikalien, Seelze, Germany) at a filling volume of 300 µL.

2.2.4.2 Fourier transform infrared spectroscopy (FTIR)

FTIR spectra were recorded with the Tensor 27 FTIR spectrometer (Bruker Optics, Ettlingen, Germany) using a Bio-ATR unit (attenuated total reflection) connected to a thermostat at 20 °C (DC30-K20, Thermo Haake, Dreieich, Germany). Corresponding blank spectra were subtracted from the protein spectra. After a 120-scan measurement, the second derivative spectrum was generated (OPUS, Bruker Optics, Ettlingen, Germany). For investigation of changes in secondary protein structure, the vector normalized second derivative spectra between the wavenumbers of 1720 and 1580 cm^{-1} were compared with the spectra of the native, untreated protein.

2.2.4.3 Differential scanning calorimetry (DSC)

A DSC 821^e (Mettler Toledo, Giessen, Germany) was used for determination of the melting temperature (T_m) of the protein in presence and absence of HA. Approximately 60 mg of the respective sample was weighed into a 100 µL aluminium crucible and sealed with caps. Analysis was performed with a heating rate of 1.0 °C/min from 25-90 °C. T_m was calculated by evaluating the midpoint of the endothermic transition peak of the protein.

2.2.4.4 High performance size exclusion chromatography (HP-SEC)

Size exclusion chromatography was applied for quantification of soluble aggregates, monomer and fragments of the mAb. The measurement was performed on a HPLC 1100 chromatograph (Agilent Technologies Deutschland, Böblingen, Germany) using a Superose® 6 10/300 GL column (GE Healthcare, Uppsala, Sweden) with UV detection at 214 and 280 nm. The mobile phase consisted of 0.15 M sodium chloride and 0.02 M sodium phosphate, adjusted to pH 7.5 with *ortho*-phosphoric acid. The flow rate was 0.5 mL/min. Samples were diluted with mobile phase to a target concentration of 1 mg/mL and centrifuged for 10 min at 12,000 rpm (Sigma 1-15, Sigma Laborzentrifugen, Osterode am Harz, Germany) in order to remove insoluble aggregates. Chromatograms were integrated manually by means of the ChemStation software Rev. B.02.01 (Agilent Technologies Deutschland, Böblingen, Germany). For quantification, the area under the curve was used. Protein concentrations were calculated based on a calibration curve.

2.2.4.5 MAb bioassay

The biological activity of the mAb after incorporation into the HA formulation was assessed by a cell based bioassay performed at Abbott, Ludwigshafen according to the Abbott standard protocol. This assay is based on the determination of cell viability upon neutralization of cytotoxic recombinant human TNF (rhTNF) by the mAb. Mouse L-929 cells were incubated with defined amounts of rhTNF and various concentrations of mAb. After incubation for 48 hrs at 37 °C the survived cells were stained with crystal violet and their color intensity was determined photometrically at 620 nm. The relative bioactivity [%] was then calculated in comparison to a reference mAb solution. HA-mAb samples were diluted to a mAb concentration of 1 mg/mL with formulation buffer. As reference, a mAb solution at same concentration was employed. A placebo sample (HA solution, 0.02 %) was used as negative control. Samples were analyzed in duplicate.

2.2.4.6 Surface plasmon resonance (SPR) measurements

Binding between HA and mAb was monitored by SPR on a BIACORE-3000 instrument (GE Healthcare, Uppsala, Sweden) using BIAevaluation® software. The experiments were performed at the Abbott Bioresearch Center in Worcester, USA. The mAb was immobilized on a carboxy methylated (CM3®) chip according to the standard immobilization procedures described by Biacore Life Science. The sensor chip surfaces of sample and reference cells were first activated by a 6-min injection of a solution containing 0.4 M *N*-ethyl-*N*9-(dimethylaminopropyl) carbodiimide and 0.1 M *N*-hydroxy-succinimide. After mAb immobilization in the sample cell via amine linkage of lysine residues, residual activated carboxymethyl groups of both sample and reference cell were deactivated with ethanolamine. In order to verify that the immobilized mAb is still intact, the binding capacity was determined with a TNFα solution, carried through the sample cell. As running buffer, 10 mM phosphate buffer, pH 7.4 with an ionic strength of 125 mM was used, representative for the ionic strength (I) of the mAb formulation. Furthermore, in a second experiment, a buffer, consisting of 15 mM histidine (I<1 mM, pH 7.4) was used in order to exclude shielding effects induced by the running buffer. HA gels (3.5 %) were diluted with running buffer to a concentration of 0.05 %. This dilution step was necessary as the viscosity of undiluted samples was too high for injection into the highly sensitive cells. After a 100 µL injection, HA samples were carried through the cell with a flow rate of 10 µL/min. The experiment was performed at 25 °C.

To distinguish between electrostatic interactions and binding events related to the specific binding site of mAb, a TNF-unspecific human IgG1 (pI=7.2) was immobilized in a third flow-cell. Regeneration of the sensor surface for the next experiment was performed using a 10 mM glycine solution at a pH of 1.5.

2.2.5 *In vitro* mAb release tests

In vitro mAb release experiments were carried out using flow-through cells, illustrated on figure 3-1. Approximately 1 g of HA-mAb gel was accurately weighed into the lower donor compartment. The donor compartment was separated from the upper acceptor compartment by a 0.2 µm pore size polyethersulfone membrane (Supor®-200, Pall Corporation, Michigan, USA) in order to avoid rapid dissolution of the gel and simulate the mAb release from the synovial cavity. The contact area between both compartments was 240 mm^2. The tightly closed cells were placed in a water bath, heated up to 37 °C (Thermomix 1441, B. Braun Biotech International, Melsungen, Germany). PBS containing 0.01 % sodium azide was pumped through the acceptor compartment of the cell with a flow rate of 1.5 mL/hr by means of silicon tubes and 60 mL syringes (Terumo, Leuven, Belgium), clamped into a syringe pump (Kd Scientific, Holliston, USA). The flow rate was chosen in accordance to the synovial turnover within a healthy knee joint [13]. At predefined time points, the released fraction were collected in 50 mL-centrifuge tubes (VWR International, Ismaning, Germany) and analyzed photometrically for protein concentration.

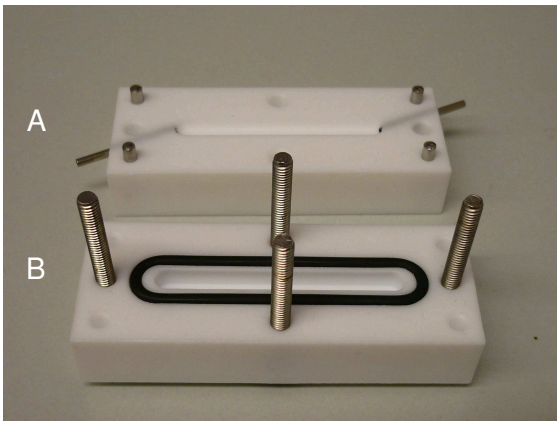

Figure 3-1 Opened diffusion flow-through cell used for mAb *in vitro* release experiments consisting of upper acceptor compartment (A) and lower donor compartment (B).

2.2.6 *In vivo* experiments with HA-mAb gel

An *in vivo* study was performed at the Abbott Bioresearch Center in Worcester, USA for assessment of the pharmacokinetic profile of the HA-mAb formulation upon IA injection. The study was carried out according to a granted animal test proposal in healthy Lewis rats. Instead of the human mAb, the murine mAb variant was used. As the murine mAb was formulated in histidine buffer (15 mM) at a concentration of 24.5 mg/mL, buffer exchange and up-concentration to 50 mg/mL was performed using Vivaspin® centrifugation tubes with a MW cutoff of 30 kDa (Satorius Stedim, Göttingen, Germany). Prior to administration, animals were anaesthetized in an anesthesia chamber using isoflurane (5 %) and oxygen. Once the rat was completely anesthetized, the right knee was shaved. Animals were dosed IA with 50 µL of a HA-mAb formulation (1 %, 35.7 mg/mL) via injection through the patella into the knee joint. For injection, 26 G syringe needles were employed. A HA-free mAb solution served as reference. The study was performed during 48 hrs. At predefined time points (2 hrs, 4 hrs, 12 hrs, 24 hrs and 48 hrs) animals were sacrificed in an anaesthesia chamber using CO_2. Synovial fluid (SF) samples were obtained from each animal via synovial wash. Therefore, a small volume of PBS was injected into the joint cavity and subsequently removed. Moreover, blood samples were taken at each time point. Both, SF and blood samples were analyzed for mAb concentration via ELISA according to the Abbott standard protocol.

2.2.7 Lyophilization of mAb-alginate mixtures

Lyophilization of mAb-alginate mixtures was performed in 6 R glass vials (Schott, Mainz, Germany) on an Epsilon 2-6 D freeze-drier (Christ, Osterode, Germany). 2 mL per vial were frozen to -50 °C at 0.5 °C/min and held for 2 hrs. Primary drying was carried out at a shelf-temperature of -25 °C and 0.045 mbar within 30 hrs. Secondary drying was conducted at a shelf-temperature of 40 °C within 10 hrs at 0.045 mbar. Lyophilized vials were stoppered at 800 mbar under nitrogen atmosphere.

3 RESULTS AND DISCUSSION

3.1 Screening of HA materials and identification of suitable HA gel concentrations

For selection of the most suitable HA material, four HA qualities were evaluated. In order to provide a long residence time of the formulation at the site of application, the main focus was to develop a highly viscous gel. Besides viscosity, the injectability presents a basic requirement in formulation development also considering that thin needles are desired. Within this scope, the injection forces using 26 G needles were determined. Viscosity measurements were performed at 6 °C and 35 °C. The lower temperature was meant to resemble refrigerated product storage temperature, whereas the temperature of 35 °C presents the mean temperature in healthy knee joints [134]. HA gels were prepared and analyzed at 1 % and 1.5 %.

All gels showed a reversible shear thinning behavior as exemplarily illustrated in figure 3-2. The enormous decrease in viscosity with increasing shear rate presents a special property of HA. Various scientists studied this characteristic which can be explained by the ordering of the coiled HA molecules with the streamline of the flow [135-137]. This phenomenon is advantageous since it allows the injection through thin syringe needles, where high shear rates are applied. At the site of application, where the shear rates are small, it leads to the spontaneous formation of a viscous gel [138].

To be able to compare the results, the viscosity values at a shear rate of 1 s^{-1} were used (figure 3-3). By increasing the MW from 1.07 to 2.19 MDa the viscosity was raised by factor 4 to 5. This is consistent with literature where a non-linear relation between viscosity and MW of HA is described [139]. As expected, also the augmentation of the HA concentration induced a viscosity increase. This effect was shown to be non-proportional to the employed HA concentration. The 1 % HA gel with a MW of 2.19 MDa (TP0711-1) exhibited a viscosity of 53.2 Pa·s whereas at a concentration of 1.5 % the viscosity was elevated to 132 Pa·s. A similar trend was observed by Krause *et al.* [140] who analyzed HA gels (MW 1.6 MDa) at various concentrations. Comparing these results with the viscosity values of the present study, it becomes evident that at comparable concentrations, MW and shear rate the gels of the present study showed higher viscosity values. These differences can be explained by the fact that the source of HA has a great influence on the material properties which makes

direct comparison difficult [140]. Besides the influence of MW and concentration, the impact of the temperature on viscosity decrease was clearly visible (figure 3-3).

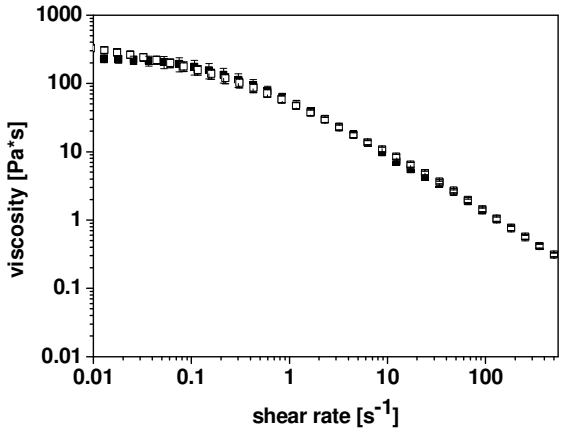

Figure 3-2 Viscogram of a HA gel 1 % (TP0711-1) at 20 °C with increasing (filled square) and decreasing (open square) shear rate.

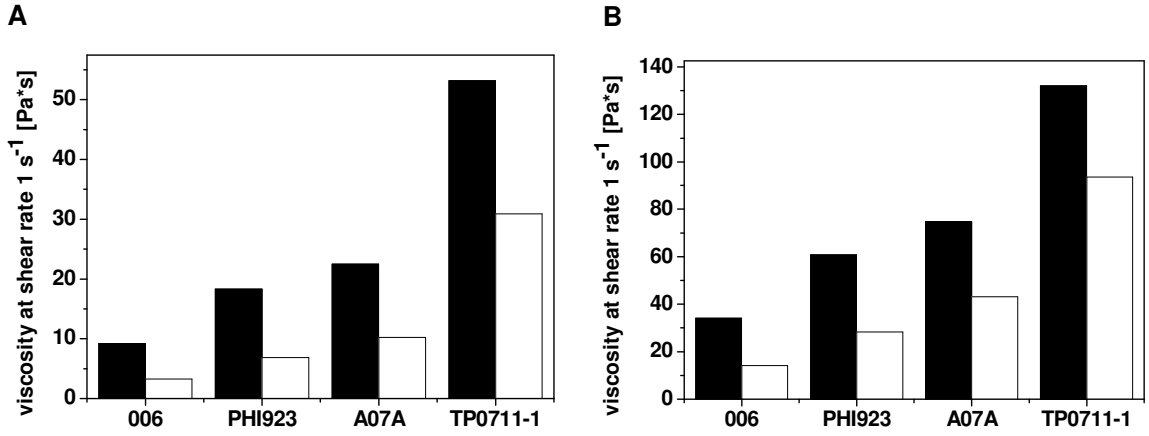

Figure 3-3 Viscosity at 1 s^{-1} of different HA gels (batch name as indicated) at a concentration of 1 % (A) and 1.5 % (B) at 6 °C (black) and 35 °C (white).

Injectability measurements were performed with the HA gels of batch TP0711-1 as this material provided the highest viscosity. Elevated injection forces were demonstrated for increasing HA content. However, a force of 4 N was not exceeded (HA gel 1 %: 1.9 ± 0.2 N, HA gel 1.5 %: 3.1 ± 0.5 N). In the following, the required injection force for higher concentrated HA gels was tested. The maximal injection force increased from 4 ± 0.4 N to 5.7 ± 0.7 N if the HA concentration changed from 2 % to 3 %, indicating that elevated HA concentrations could be used. In order to keep the injection forces as low as possible, HA material of batch TP0711-1 in a concentration of 1 % was chosen for following experiments.

3.2 Compatibility of mAb with HA

3.2.1 Impact of mAb on HA gel characteristics

One of the major requirements in formulation development is the compatibility of the carrier material with the incorporated drug. The compatibility of the chosen HA gel with the mAb solution was assessed by visual inspection and turbidity measurements. These analytical methods were used to identify any precipitation phenomena or changes in color or clarity indicating physical instabilities of both components. Additionally, viscosity and injectability measurements were intended to provide information concerning the impact of the protein on the gel characteristics.

3.2.1.1 Visual inspection and turbidity measurements of HA-mAb gel

Visual inspection over a storage period of one month at 2-8 °C revealed no evidence of visible particle formation due to precipitation or phase separation. Turbidity measurements did not show any significant difference between the sum of the individual gel components and the HA formulation containing the mAb (figure 3-4). These results underline the absence of pronounced interactions between mAb and HA leading to particle formation >100 µm.

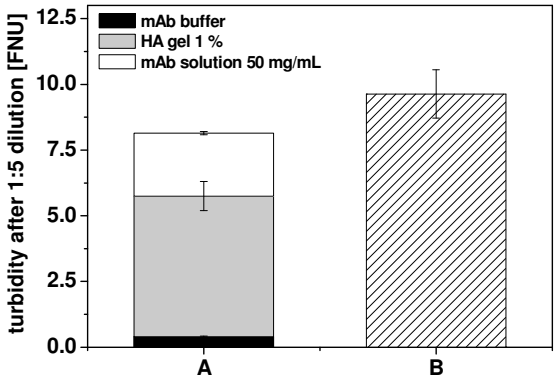

Figure 3-4 Turbidity contributions of the HA-mAb gel (1 %, 50 mg/mL) (A) and the sum of the individual components (B) after 1:5 dilution with mAb buffer.

3.2.1.2 Rheometry and injectability of HA-mAb gel

Rheometry did not reveal any significant differences between the viscosities of the placebo HA gel and the HA gel containing the mAb (HA gel 1 % 49.3 ± 7.3 Pa·s, HA-mAb gel 58.5 ± 1.6 Pa·s at a shear rate of 1 s^{-1}, figure 3-5). The impact of proteins on the viscosity of HA is controversially discussed in literature. More in general, Alfrey *et al.* argued that substances

that alter the solvent character may have any impact on the intrinsic viscosity of polymer solutions [141]. Balasz *et al.* reported about the absence of any impact of synovial proteins on the rheological properties of HA [135]. Contrary to that, the group of Fraser pointed out that proteins present in the SF are able to change the viscosity of HA [142]. Hence, the impact of proteins is hardly predictable and appears to be dependent on the HA characteristics (MW, concentration) as well as on the protein type and concentration.

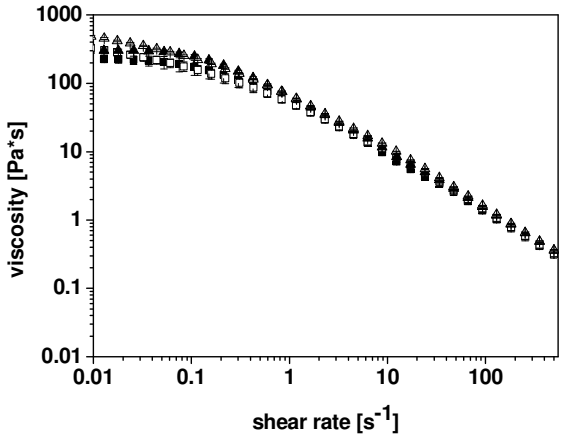

Figure 3-5 Viscosity of HA placebo gel (1 %, square) and HA-mAb gel (1 %, 50 mg/mL, triangle) with increasing (filled) and decreasing (open) shear rate at 20 °C.

Both HA placebo gel (1 %) and HA-mAb gel (1 %, 50 mg/mL) revealed excellent injectability through 23 G (Ø 0.6 mm) and 26 G (Ø 0.45 mm) syringe needles with maximal injection forces below 4 N (figure 3-6). The injection force slightly increased from 2.0 ± 0.2 N (HA placebo gel, 26 G) to 3.3 ± 0.1 N (HA-mAb gel, 26 G) in presence of mAb.

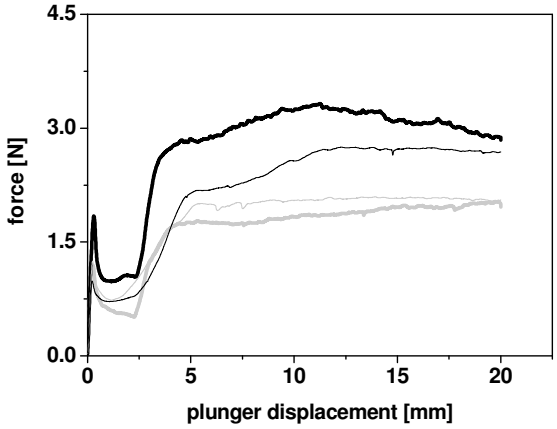

Figure 3-6 Injection force - plunger displacement diagram of injectability measurements of HA placebo gels (1 %, gray) and HA-mAb gels (1 %, 50 mg/mL, black) using 26 G (thick line) and 23 G (thin line).

It has been described in literature that formulations that require injection forces ranging up to 25 N *in vivo* are considered to be easy to inject [21]. As the experiment was performed by injection into air, a slight force increase *in vivo* is expected due to the limited physiological space and the higher resistance that needs to be overcome [21]. The use of a 23 G syringe needle aimed at an improvement of the injectability. This can be explained by the larger inner radius of the needle that influences the injectability according to the law of Hagen-Poiseuille with the power of 4. However, it has to be taken into consideration that the use of larger syringe needles is known to influence patient compliance due to injection pain [96]. With respect to potential *in vivo* animal studies, the use of thin needle sizes should always be aspired.

3.2.2 Impact of HA on mAb conformational stability

Besides the gel characteristics of the formulation, the maintenance of the mAb conformational stability is of major importance. The three-dimensional protein structure can be influenced by various factors such as formulation components, pH, ionic strength and/or the formulation preparation process [143]. In the following, the effect of HA on the mAb stability was assessed via DSC, second derivative UV and FTIR spectroscopy and HP-SEC.

T_m in presence and absence of HA was studied with the help of DSC analysis. The pure protein solution, used as reference, showed one irreversible endothermic event at 69.9 ± 0.1 °C. No difference in T_m value was identified after embedment into the HA gel, indicating that the thermal mAb stability remains untouched when adding HA. Matheus *et al.* [144] demonstrated with nano DSC measurements that an IgG1 mAb undergoes two endothermic events at ~73 °C and at ~80 °C. The first T_m value can be attributed to the unfolding of the Fab fragment whereas the second transition is related to the Fc fragment. In the present study, only one endothermic event was observed, due to the lower sensitivity of DSC measurements in crucibles compared to micro or nano DSC. Second derivative UV spectroscopy of the diluted HA-mAb gel revealed no peak shifts compared to the native mAb, indicating that the tertiary protein structure is not affected by the mAb embedment into the HA gel (figure 3-7 A). Analysis of the second derivative FTIR spectra demonstrated the absence of significant alterations in the characteristic IR bands between the wavenumbers of 1720 and 1560 cm^{-1} due to the combination of the mAb with HA (figure 3-7 B). Hence, also the secondary protein structure is maintained.

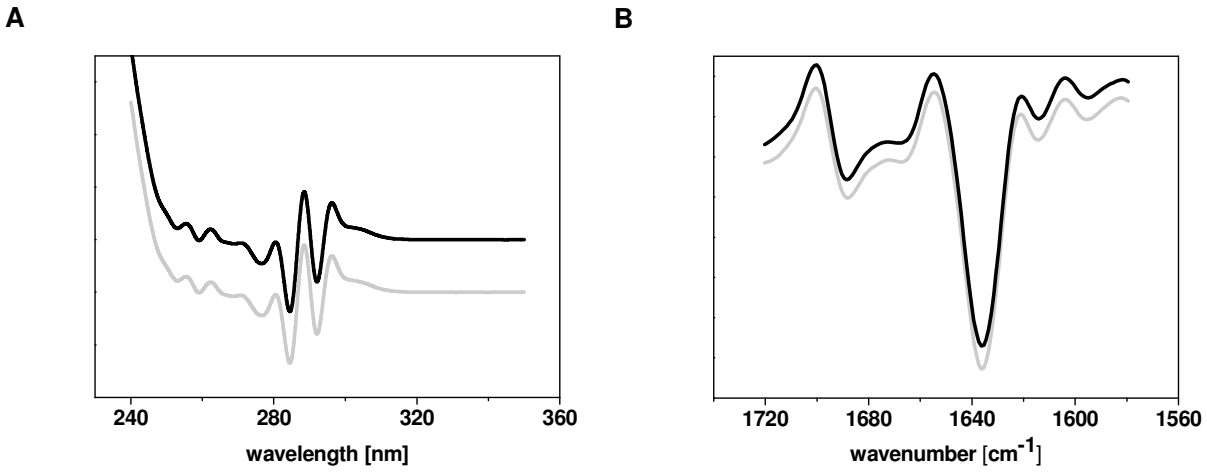

Figure 3-7 Second derivative UV (A) and area normalized FTIR spectra (B) of diluted HA-mAb gel (1 %, 50 mg/mL, black line) compared to native mAb solution (50 mg/mL, gray line). Artificial offset for clarity.

No additional aggregate or fragment formation was observed by HP-SEC analysis. The monomer recovery after addition of HA was preserved (mAb standard 99.7 ± 0.03 %, mAb in HA gel 99.8 ± 0.02 %). Conformational protein structure analysis was completed after the result had been reached that the mAb bioactivity after incorporation into the HA gel was fully maintained (102 ± 3.5 %).

3.3 Investigations on interactions between HA and mAb via surface plasmon resonance measurements

As described in the introduction, HA presents a linear polysaccharide with polyelectrolyte properties due to the repeating D-glucuronic acid monomers. With an estimated acid dissociation constant (pKa) of 3, attributed to the carboxylic groups [145, 146], the polymer is negatively charged under physiological conditions [147]. At physiological pH, proteins bear positively charged residues ascribed to basic side chains of the amino acids lysine (pKa 10.5), histidine (pKa 6.0) and arginine (pKa 12.5). The presence of these opposite charges enables electrostatic interactions between the polysaccharide and the protein. Interactions between HA and mAb could not be identified with the help of DSC, second derivative FTIR and UV measurements, analysis of turbidity, injectability, and viscosity as no alterations in either HA gel or mAb characteristics were detectable. These findings indicate that the potentially present interactions between HA and mAb are weak and for detection a highly sensitive method has to be used. Several studies have been reported which elucidate the non-specific interactions between HA and other macromolecules [137] and a few studies

investigated the occurrence of electrostatic complex formation between HA and e.g. BSA or lysozyme [148, 149]. In general, electrostatic interactions are dependent on the concentrations of the reaction partners, the ionic strength and pH of the surrounding medium, the charge density of the polyelectrolytes and the stereochemical accessibility of the charged moieties [147]. Macromolecular interactions can be identified by several methods. One approach uses the detection of precipitation phenomena by measuring the turbidity [147]. Another possibility is the application of chromatography where one of the complex partners is attached to a column resin and retention of the analyte is monitored [119]. Electrophoresis was successfully employed to elucidate the presence of electrostatic interactions as the mobility rate is affected if complex formation takes place [119]. Biomolecular interactions can be analyzed at high sensitivity using a quartz crystal microbalance. This method allows the detection of the mass increase per area upon binding of the analyte to the complex partner that is bonded on the chip surface. On account of the high sensitivity, the low required sample volumes and concentrations, surface plasmon resonance (SPR) was chosen as a method to gain insight into binding events between HA and mAb. This method was already successfully applied for analysis of interactions between heparin and complement proteins [150]. In brief, SPR allows the monitoring of weak interactions between two macromolecular components in real-time without labeling. The ligand is immobilized on a sensor chip and the binding partner is passed over the sensor surface by applying a continuous flow. Upon binding between ligand and partner, the refractive index on the sensor surface changes [150, 151].

Injection of the HA solution into the placebo cell led to a strong background signal of 80 RU induced by the refractive index difference between running buffer (10 mM phosphate, I=125 mM, pH 7.4) and HA solution (figure 3-8 A). In the sample cell with immobilized mAb, a signal response of 125 RU was detected (figure 3-8 B). Based on the resulting signal difference of 45 RU, a slight binding of HA to the mAb was concluded. The same signal response of 125 RU was identified by analysis of the immobilized human IgG upon injection of the HA solution (figure 3-8 C).

Lowering the ionic strength of the running buffer to <1 mM in order to reduce shielding effects [147] led to an increase of the response to 140 RU with immobilized mAb (figure 3-8 D). Again, this result was verified by analysis of the immobilized human IgG where the same signal intensity was obtained (figure 3-8 E).

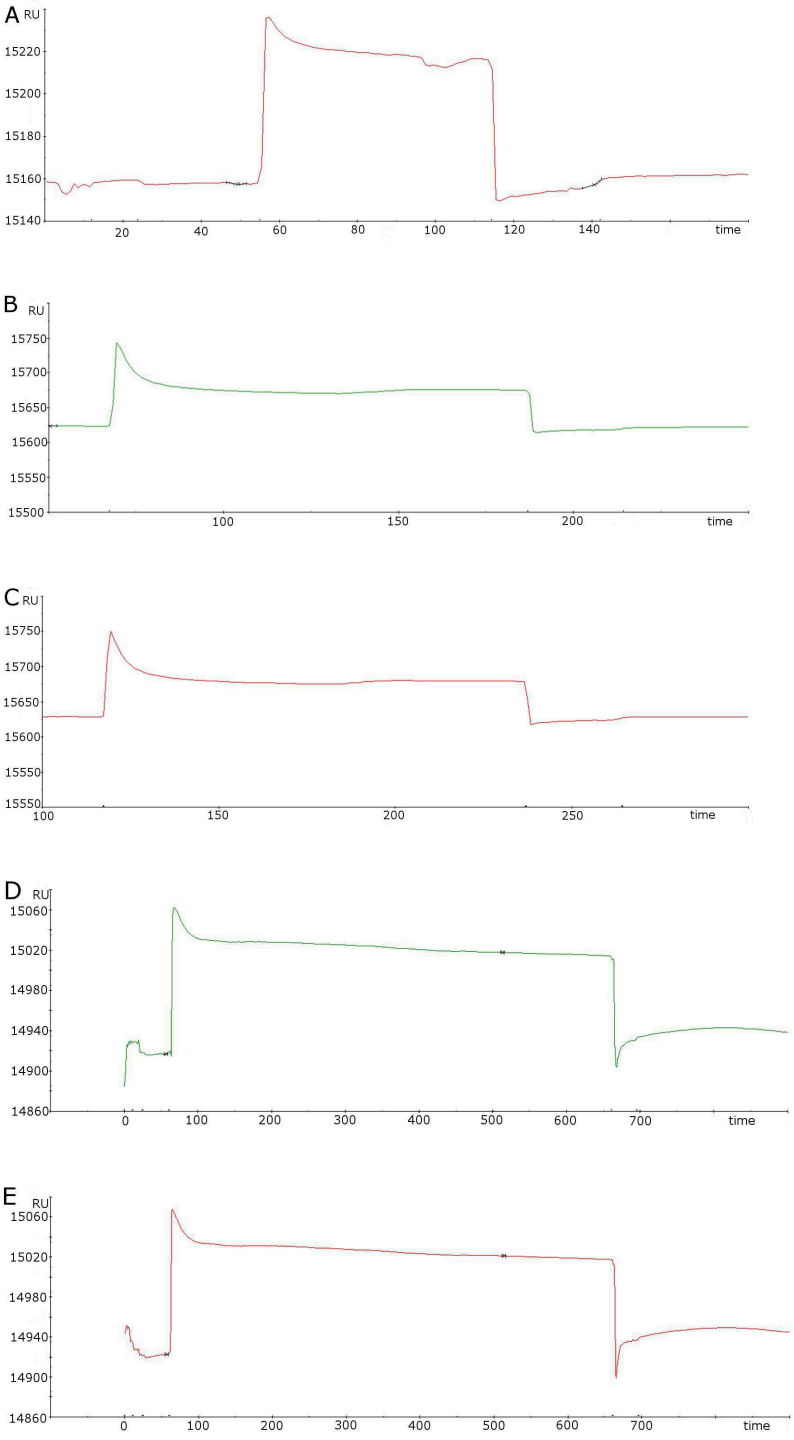

Figure 3-8 Sensorgrams upon injection of HA solutions (0.05 %) diluted with either 10 mM phosphate buffer (pH 7.4, I=125 mM) (A-C) or 15 mM histidine buffer (pH 7.4, I<1 mM) (D, E) into cells with (A) CM3® chip without ligand immobilization (placebo), (B, D) immobilized mAb and (C, E) immobilized human IgG.

These results indicate that the ionic strength has a substantial influence on the interaction between HA and mAb as the response difference between mAb and placebo cell increased from 45 RU to 60 RU when the ionic strength was reduced from 125 mM to <1 mM. The presence of electrostatic interactions was underlined by analysis of the human IgG that revealed the same binding intensity to HA. Hence, the interaction between mAb and HA presents a non-specific charge-induced binding event. Even though mAb and human IgG have a different pI value (mAb: pI=8.25 vs. human IgG: pI=7.2), the difference of the molecule net charge is not expected to have a significant impact on the binding intensity to HA. Mathes *et al.* determined the protein net charge of an IgG1 (pI=8.33) as a function of the pH. Between pH 7 and 8 the protein net charge did not change considerably [152]. Taking into account that some IgG antibodies are known to occure in isoforms at a pI range of up to 1.5 pH units [152], the overall net charge difference between mAb and human IgG is expected to be marginal. As shown by Yadav *et al.*, the charge distribution within the molecule plays an important role in electrostatic interactions of proteins [153] and the regions responsible for electrostatic binding might be similar in charge despite slightly different overall molecule net charge. Overall, the interactions were only slightly pronounced, which can be attributed to comparibly low charge density of both interaction partners. Comper *et al.* reviewed that at physiological pH, carboxylic groups of polysaccharides interact less intensively with positively charged molecules than e.g. sulfate groups. Besides the type, also the charge density affects the interaction strength. The number of negatively charged groups per disaccharide can vary from one (HA) up to four (heparan sulphate) [147]. In this context, Gelman *et al.* demonstrated a higher interaction strength of heparan sulfate with the the cationic polypeptide poly-L-lysine compared to HA [154]. These examples clearly indicate that the extent of polysaccharide-protein interactions is dependent on various factors.

3.4 *In vitro* release of mAb from HA gels

The *in vitro* mAb release was tested for one week using a diffusion flow-through cell. In order to slow down dissolution and dilution of the HA gel, simulating the release from the synovial cavity, a separating 0.2 µm pore size membrane was used. It is known from literature that the synovial half-life of HA ranges from 10 to 16 hrs depending on the MW [155, 156].

Similar to the results of Prisell [123], the mAb release was significantly reduced in presence of HA (figure 3-9). The control formulation revealed an intensive initial burst of 30 % within 4 hrs that was not seen in the HA formulation. After 7 days, only 75 % were released from

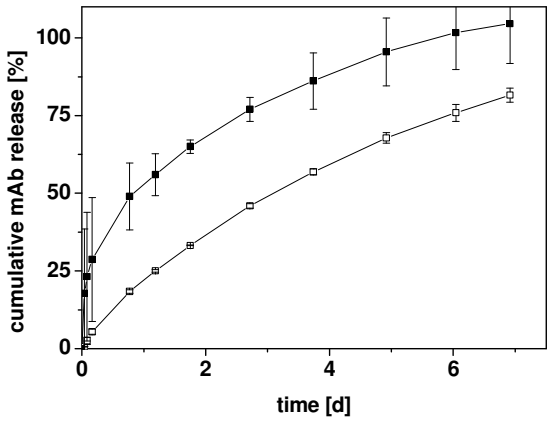

Figure 3-9 Cumulative *in vitro* release of mAb from HA-mAb gel (1 %, 50 mg/mL, open square) compared to a HA-free control formulation (mAb solution 50 mg/mL, filled square).

the HA formulation. However, the shape of both release curves showed high similarity. This leads to the presumption that the overall slower mAb release from the HA gel can be attributed to initial retardation of the mAb diffusion out of the gel induced by the dense gel structure. After day one, the initial retardation effect was diminished as the slope of the curve resembles that of the control formulation. This can be ascribed to dilution and dissolution effects of the gel induced by the continuous flow of the release medium that is pumped through the cell. Obviously, the interactions between HA and mAb, detected with the help of SPR measurements, have no impact on the mAb release from the gel. The dissolution of HA during the first day followed by adjustment of the mAb release rate to the reference agrees with the synovial half-life of HA known from literature. Assuming that mAb retention is related to the presence of HA, enhanced mAb release is expected upon dilution of the HA gel and clearance from the donor compartment. The detected initial retardation phenomenon, also known as macromolecular sieving or dynamic filtration effect, is described in literature as a typical property of polysaccharide gels [135, 137, 157, 158]. The mobility of molecules entrapped in a three-dimensional gel network built by overlapping HA chains is strongly reduced as soon as a certain concentration is exceeded. De Smedt *et al.* investigated the diffusion behavior of fluorescein isothiocyanate (FITC)-dextran in HA solutions of different concentrations via fluorescence recovery after photobleaching (FRAP). It was demonstrated that the diffusion coefficients were decreased with increasing HA concentration. Based on these results, they were able to calculate the average mesh size of the three-dimensional HA network [157]. From these findings, it can be concluded that the detected retardation effect is expected to be even more pronounced if a higher HA concentration would be used. This would lead to a higher density of the gel network. Taking into account that the present

formulation revealed an excellent injectability, as presented in section 3.2.1.2, a further increase in HA concentration appears feasible. The increase of the HA concentration up to 3 % was shown to provide adequate injection force using 26 G syringe needles and could therefore be used for prolongation of the mAb release.

3.5 *In vivo* mAb release from HA gels after IA application

In order to gain some insight into the pharmacokinetic profile of the HA-mAb formulation and the physiological impact on the mAb release, an *in vivo* study with healthy rats was performed. Serum mAb concentrations in animals that were dosed with the HA-free mAb solution increased during the first 12 hrs until a maximum level was reached (figure 3-10 A). This level sustained up to 48 hrs. In contrast, HA-mAb gels initially revealed significantly lower serum levels at 2 and 4 hrs. After 12 hrs, a serum level similar to the HA-free formulation was reached that declined again after 48 hrs. Thus, overall lower serum levels were achieved with the HA gel. The increase in serum mAb concentration during the first 12 hrs was accompanied by a decrease in SF mAb concentration (figure 3-10 B). Initially, high SF levels were detected in both sample and reference that decreased over time. Only after 4 hrs a significant difference in SF level between buffer and HA gel was detectable. After 48 hrs, the remaining mAb amount in SF was only 1.7 % of the initial concentration. The use of the SF / serum concentration ratio (SF / S ratio) of a drug is known to be a valuable tool to compare e.g. the permeability of the synovial membrane for proteins [159]. In the present study, this ratio was used as an indicator for the retention of the administered protein at the site of application: a high SF / S ratio reflects high mAb retention in the joint cavity. It can be concluded from the results that HA affects the mAb retention at the site of application at the beginning of the study only (figure 3-10 C). After 12 hrs, no difference between HA gel and HA-free formulation can be seen as the SF / S ratio of both formulations reaches the same level of approximately 3. These findings indicate that the mAb retention at the site of application due to the HA gel is only marginal. The study reflects well the findings of the *in vitro* study where significant slower mAb release rates were observed during the first 12 hrs.

Based on the results from the *in vitro* release study, a poor *in vitro – in vivo* correlation can be seen with respect to the duration of mAb release. While a continuous mAb release over 7 days was observed *in vitro*, rapid mAb release from the gel during 48 hrs was identified *in vivo*. This could be attributed to the mechanical conditions present in the knee joint that were

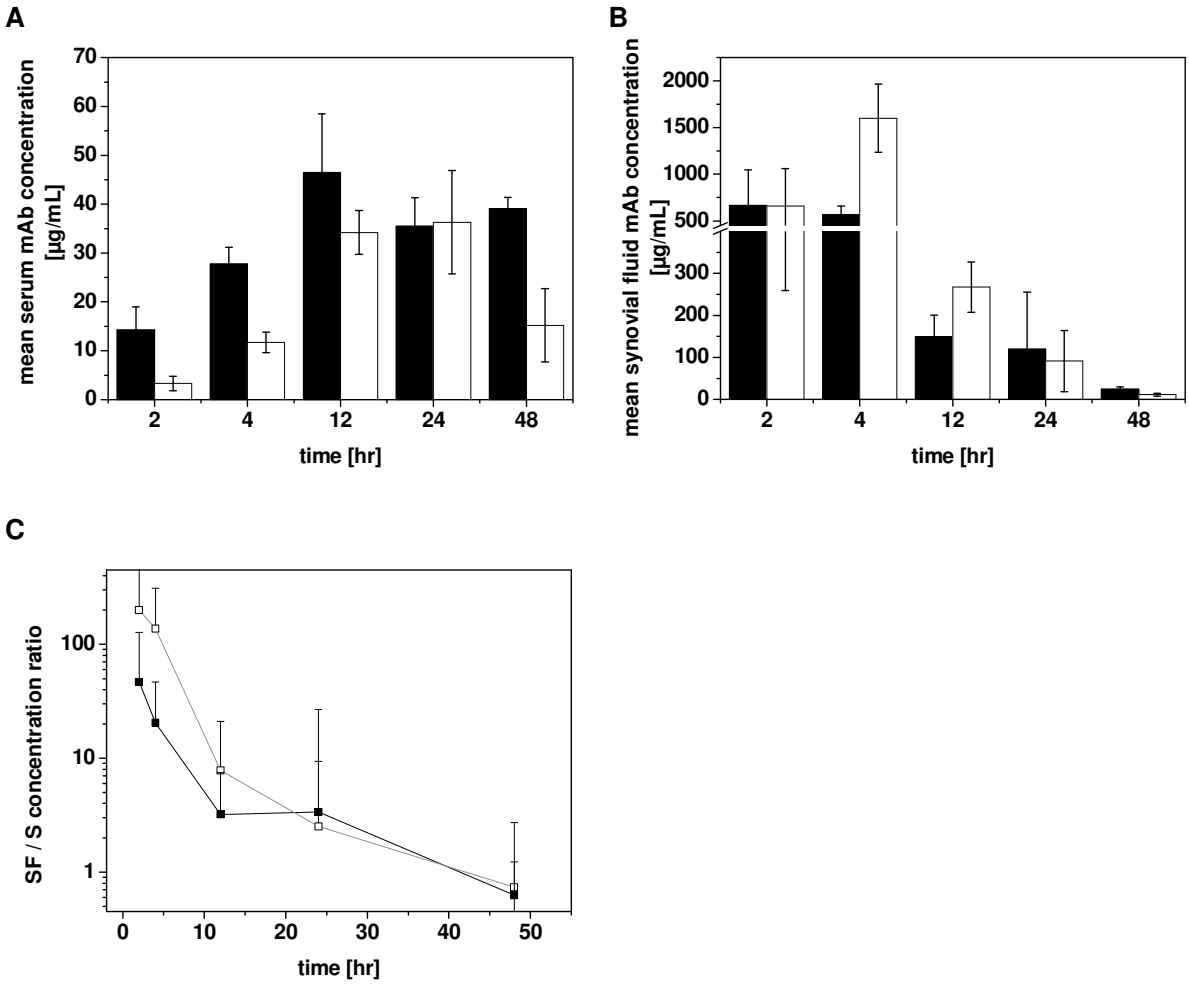

Figure 3-10 Mean serum mAb concentrations (A), mean synovial fluid mAb concentrations (B) and ratio of SF and serum mAb concentration (SF / S) (C) at various time points in Lewis rats after IA administration of 50 µL of a HA-mAb formulation (1 %, 35.7 mg/mL, white) or a mAb solution (35.7 mg/mL, black).

not simulated in the *in vitro* release model. As the animals were moving physiologically few minutes after injection, the formulations were presumably squeezed between the upper and lower knee compartment within the joint cavity. These mechanical conditions could have a tremendous impact on the release profile induced by an increase of the contact area between gel and surrounding SF. As animals can hardly be immobilized over a longer period of time, the exact impact of the mechanical conditions on mAb release is difficult to determine. Besides the mechanical influence, the synovial turnover of HA has to be taken into account. Brown *et al.* [155] reported that the synovial half-life of HA with a MW of >6.0 MDa in rabbits is only 13.2 hrs. Lower MW species with a MW of 90 Da revealed a similar half-life of approximately 10.2 hrs. Lindholm *et al.* studied the half-life of HA of different MW upon IA injection in carpal joints of horses. They reported about a half-life of

12.5 and 16 hrs for high and low MW, respectively [156]. Thus, the clearance of HA from the synovial space is only slightly influenced by the MW of the used HA species and is rather short [155]. However, Larsen *et al.* demonstrated that cross-linking of HA causes a significant prolongation of the residence time of IA administered HA. The mean half-life of cross-linked HA was prolonged to 8.8 ± 0.9 days [160]. The rapid clearance from the synovial space in general can be explained by the anatomical, fenestrated structure of the synovial membrane offering a trans-synovial diffusion in and out of the joint cavity [161]. This flux, however, is reported to be size-dependent. Molecules with a radius less than 250 nm were shown to exhibit a rapid diffusion in and out of the joint cavity. HA is described to have a radius of gyration of 28 – 260 nm, depending on the MW [139]. Also mAb with a radius of ~5 nm is consequently rapidly cleared from the synovial space which was distinctly seen in the present *in vivo* study. Based on these facts it can be concluded that the molecular size of injected molecules plays a pivotal role in the synovial residence time. Consequently, the limited mAb retention at the site of application in the present *in vivo* study can be ascribed to both the mechanical conditions and the rapid clearance of the used HA type from the joint. In order to prolong the residence time of mAb upon IA injection, the use of a high MW cross-linked HA species presents a promising approach as synovial clearance is expected to be reduced.

3.6 Investigations on the interactions between sodium alginate and mAb

Numerous polysaccharides such as HA, chondroitin sulphate and alginate possess negatively charged groups at a broad pH range. Depending on the type and number of these functional groups, the polyelectrolyte character is differently pronounced. HA with only one carboxylic group per disaccharide exhibits a lower negative charge density than alginate that possesses two carboxylic groups per disaccharide. As described in section 3.3, slight interactions between HA and mAb were identified with the help of SPR measurements. With increasing charge density of the polysaccharide the tendency to form complexes with positively charged proteins is reported to be enhanced [131]. As the interactions between HA and mAb did not affect the mAb release at an adequate level, the interactions between sodium alginate and mAb had to be studied. Alginate in solution can be cross-linked in presence of bivalent cations such as calcium, which results in gelation. The formation of insoluble complexes between alginate and proteins is described in literature [132]. Reversible mAb precipitation within the joint cavity presents a promising approach to prolong the residence time at the site of application due to reduced synovial clearance. As

precipitation phenomena in general occur as soon as the solubility is exceeded, dissolved and precipitated mAb exist in equilibrium. Upon injection into the joint cavity, dissolved mAb is expected to be continuously cleared which causes redissolution of precipitated mAb and thus generation of a sustained release system. In order to identify potentially relevant parameters and conditions at which insoluble mAb-alginate complexation occurs, mixtures of mAb with two different sodium alginate qualities ($\eta_{(1\ \%,\ 25\ °C)}$ 4-12 mPa·s (low MW), $\eta_{(1\ \%,\ 20\ °C)}$ 350-550 mPa·s (high MW)), ratios (mAb:alginate ratio 5, 1 and 0.5 / 0.3 (high MW / low MW)), and calcium concentrations (0, 10, 50 and 150 mM) were prepared. It was known from preliminary experiments that mAb precipitates in presence of alginate when spray-dried powder is reconstituted with water. In order to generate dry particles in a high throughput setup, lyophilization was used instead of spray drying. Reconstitution of the dry cakes was performed with 10 mM histidine buffer at ionic strength of 10 mM at pH 5.5 and 7.4.

3.6.1 Impact of mAb-alginate ratio on the precipitation efficiency prior to lyophilization

After adding alginate to the mAb solution, samples immediately turned turbid (figure 3-11 A). Both low and high MW alginate samples revealed high turbidity values next to the detection limit of the instrument (3.5 AU). In order to quantify the dissolved mAb amount, samples were centrifuged for 30 min at 25,000 x g and the supernatant was analyzed. Overall high precipitation efficiencies above 70 % were observed. With increasing mAb-alginate ratio, the precipitation efficiency increased (figure 3-11 B).

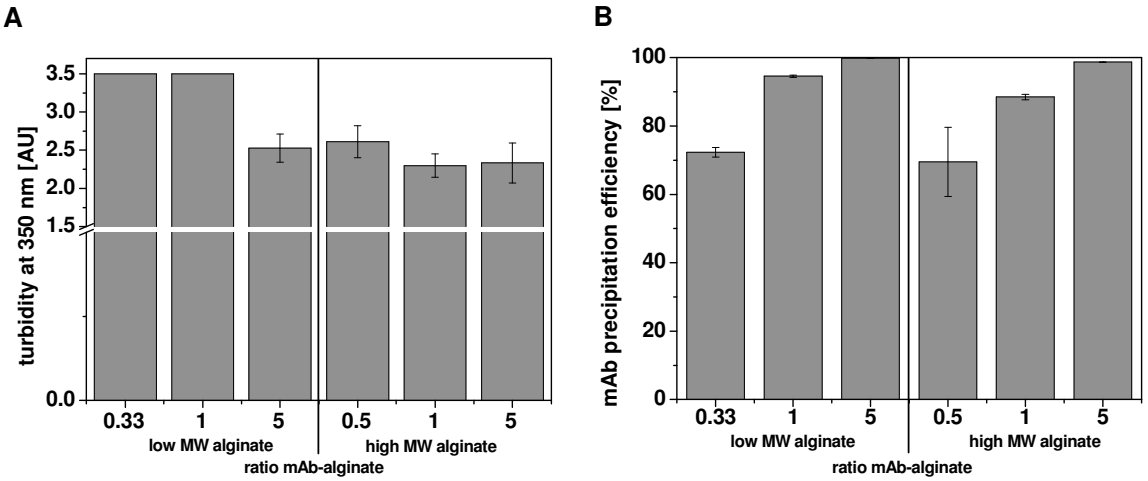

Figure 3-11 Results of turbidity measurements (A) and determination of the mAb precipitation efficiency (B) of mAb-alginate mixtures prior to addition of calcium and lyophilization.

In order to study the reversibility of mAb precipitation and the impact on mAb conformational stability, the insoluble pellet of the sample with a mAb-alginate ratio of 1 after centrifugation was resuspended in either 500 µL histidine buffer (I=150 mM, pH 5.5) or water. It became apparent that the addition of histidine buffer induces a drastic reduction of the turbidity. This indicates that the precipitate partially redissolved (figure 3-12). However, the turbidity level of the placebo sample was not reached which underlines the fact that either a slight fraction of precipitated mAb remained or mAb partially irreversibly unfolded. The redissolved fraction was analyzed by HP-SEC. It was shown that the monomer content was preserved (mAb-high MW alginate 99.7 ± 0.03 %, mAb-low MW alginate 99.8 ± 0.01 %, mAb standard 99.7 %). These results demonstrate that mAb redissolution is not accompanied by formation of additional soluble aggregates of fragments. As the resuspension in water did not lead to any reduction in turbidity, it can be concluded that the ionic strength and/or the pH contribute to the effect of mAb precipitation in presence of alginate.

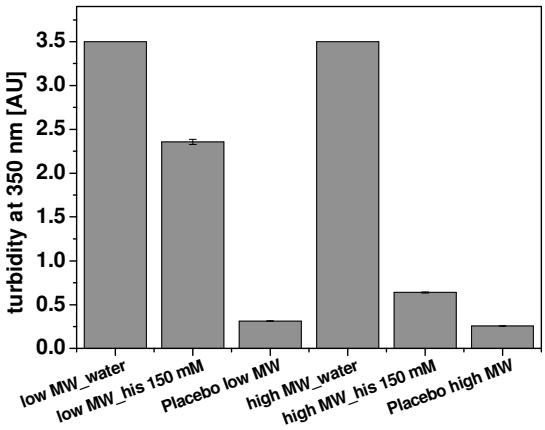

Figure 3-12 Turbidity measurements of mAb mixtures with low and high MW alginate after mixing, separation of the precipitate via centrifugation and resuspension in either histidine buffer (I=150 mM, pH 5.5) or water.

Analysis of the second derivative FTIR spectra after resuspension in water revealed that the strong band at 1640 cm^{-1} was shifted to lower wavenumbers (figure 3-13). This signifies the presence of perturbations in the secondary protein structure. In contrast, upon resuspension in histidine buffer (I=150 mM, pH 5.5) no peak shifts were noticable and a high similarity to the control spectrum was seen. Based on these results it was concluded that mAb precipitation in presence of alginate is accompanied by conformational changes in the secondary protein structure. Due to the reversibility of these changes, mixtures of mAb and sodium alginate could be an interesting formulation approach.

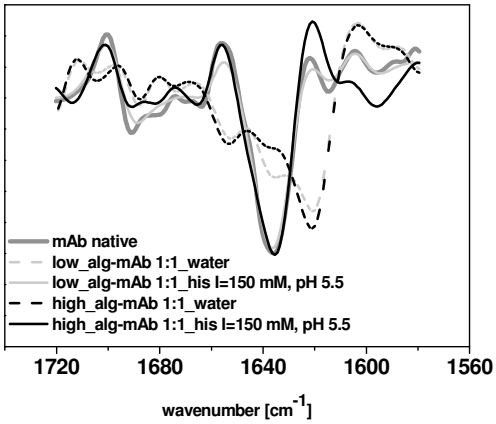

Figure 3-13 Second derivative FTIR spectra of alginate-mAb pellets resuspended in either histidine buffer (I=150 mM, pH 5.5) or water. As reference, a native mAb solution was used.

3.6.2 Impact of mAb-alginate ratio, MW of alginate, calcium concentration and pH of the reconstitution buffer on efficiency of mAb precipitation by alginate after lyophilization

The conditions at which insoluble mAb-alginate complexes are formed were within the scope of the present study. After lyophilization and reconstitution of the samples with histidine buffer (10 mM, I=10 mM) at a pH of either 5.5 or 7.4, all samples turned turbid. In absence of calcium ions, complete mAb precipitation was observed. With increasing calcium concentration, the turbidity and precipitation efficiency of the samples decreased (figure 3-14 and 3-15). The addition of calcium ions also induced gelation of alginate which can be ascribed to cross-linkage of the polysaccharide induced by ionic interactions. The gelation intensity was shown to correlate with the used calcium concentration. Based on these results it was concluded that mAb is replaced by the calcium ions from the charge-complex. As the calcium-alginate complex seems to have a higher solubility than the mAb-alginate complex, a turbidity decrease was observed. The protein-alginate interaction in the presence of calcium was also investigated by Zhao *et al.* [120]. They analyzed BSA-alginate complexes in conjunction with calcium ions. It was demonstrated that BSA can be replaced by calcium ions from the alginate complex due to a higher binding strength.

Besides the calcium concentration, also the mAb-alginate ratio was identified to affect the mAb precipitation efficiency. This effect was clearly pronounced at low concentrations (10 mM) or in the absence of calcium. At these conditions, increased precipitation efficiency was observed when the mAb-alginate ratio was raised from 0.3/0.5 to 5. The effect can be

explained by presuming that charge-induced precipitation phenomena are favoured close to complete charge neutralization of the complex. At a low mAb-alginate ratio, the negative charges of the alginate molecules are not saturated. Induced by the unsaturated negative charges of the alginate molecules, the formation of insoluble mAb-alginate complexes is incomplete. With increasing mAb-alginate ratio, the number of mAb molecules per alginate molecule is raised. This causes saturation of the negative charges and therefore higher precipitation efficiency. Hence, in order to achieve complete complex precipitation, a molar excess of mAb needs to be provided. At higher calcium concentrations (>10 mM) the impact of the mAb-alginate ratio on mAb precipitation efficiency was not apparent.

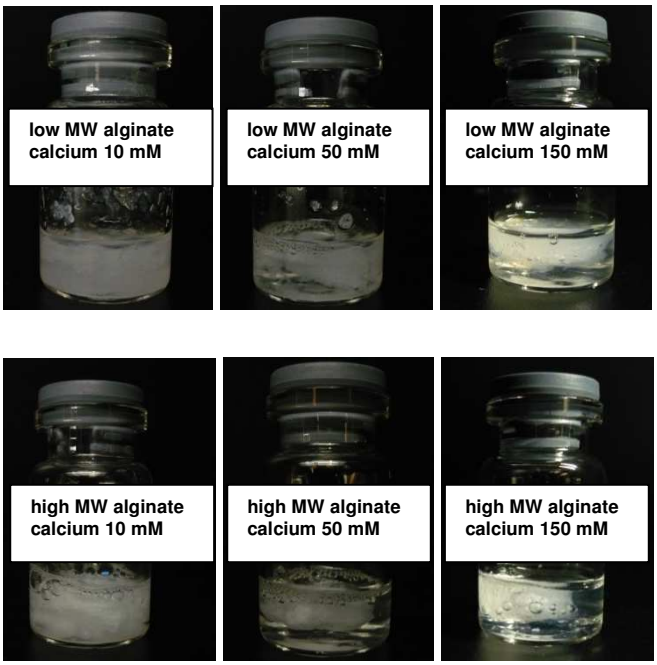

Figure 3-14 Exemplary pictures of samples 24 hrs after reconstitution with histidine buffer (I=10 mM) at pH 5.5 with a mAb-alginate ratio of 5 and calcium concentrations ranging from 10 to 150 mM.

Overall slightly higher precipitation efficiencies were achieved at pH 5.5 compared to 7.4. At pH 5.5 and 7.4, sodium alginate (pKa_1 3.4, pKa_2 3.6) is calculated to be nearly completely dissociated with 99.0% and 99.9 % respectively. Similar to that, the degree of dissociation of the positively charged amino acids arginine (pKa 12.5) and lysine (pka 10.5) is estimated to be 99.9 % at both pH values. Histidine (pKa 6.0) is nearly completely undissociated (3.8 %) at pH 7.4 while exhibiting a degree of dissociation of 76 % at pH 5.5. Therefore, the observed higher precipitation efficiencies at pH 5.5 can be attributed to enhanced electrostatic interactions between mAb and alginate caused by a slightly higher positive net charge at pH 5.5 compared to pH 7.4.

The MW of alginate had no significant influence on the mAb precipitation efficiency. Besides the impact of calcium concentration, pH and mAb-alginate ratio, also the ionic strength is reported to affect protein-alginate interaction. De Kruif *et al.* [131] reported about the dissociating effect of salts on the polyelectrolyte complex formation. With increasing salt concentration, the charges were shielded by the salt ions leading to reduction of electrostatic interactions. As shielding effects could contribute to the detected reduction of the precipitation efficiency at increasing calcium concentrations, the predominant mechanism of the mAb-alginate complex dissociation in the presence of calcium ions was to be investigated by replacing calcium chloride with sodium chloride.

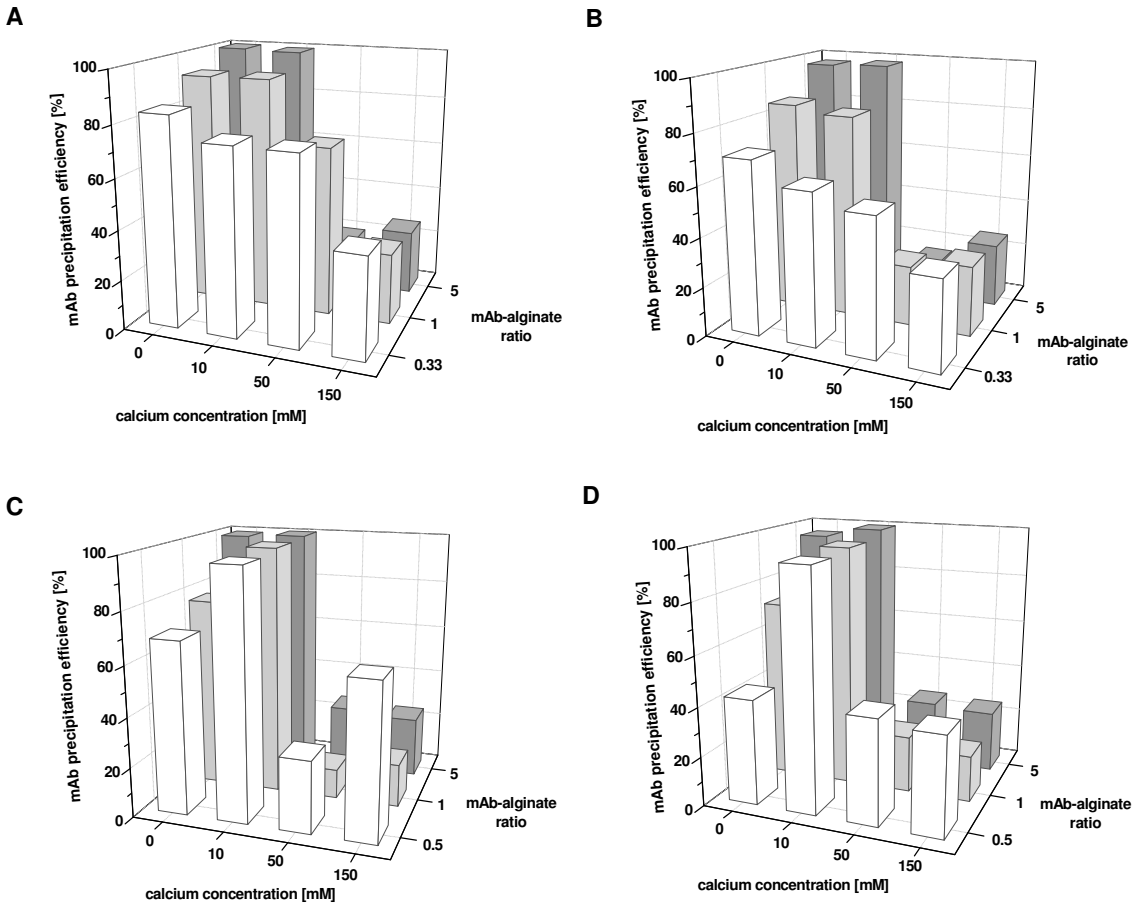

Figure 3-15 MAb precipitation efficiency in dependence of the calcium concentration and the mAb-alginate ratio for low (A, B) and high MW alginate (C, D). Samples were lyophilized and reconstituted with 10 mM histidine buffer, pH of 5.5 (A, C) or 7.4 (B, D).

3.6.3 Impact of the salt concentration and type on the efficiency of mAb precipitation by alginate

The influence of the salt concentration and type on the mAb precipitation efficiency in the presence of alginate was studied with the help of the replacement of calcium chloride with sodium chloride. Ionically cross-linkage of alginate is not described for sodium ions [162]. Thus, replacement of mAb from the alginate complex caused by binding competition with sodium ions is not expected. However, the impact of shielding effects on the mAb-alginate interaction should be detectable. For this purpose, mAb-alginate mixtures at a ratio of 5 and with low MW alginate were prepared.

With increasing salt concentration the turbidity decreased significantly (figure 3-16). A slight turbidity at 150 mM NaCl persisted. As expected, no gelation of alginate was observed upon addition of NaCl. In absence of salt and in presence of 10 mM calcium chloride and sodium chloride the mAb was precipitated completely (figure 3-17). In the presence of 50 mM and 150 mM NaCl the precipitation efficiency was strongly reduced to about 80 % and 10 % respectively. Thus under physiological conditions the mAb precipitation appears to be highly reversible. In the presence of calcium, the precipitation efficiency was reduced to 20 % already at 50 mM. The different impact of NaCl and $CaCl_2$ concentration on mAb precipitation efficiency at 50 mM and 150 mM can be explained by the 3 times higher ionic strength in $CaCl_2$ compared to NaCl at same molar concentration Consequently, 50 mM $CaCl_2$ and 150 mM NaCl, rendering the same ionic strength of 150 mM, show comparable precipitation efficiency. The slightly increased precipitation efficiency at 150 mM $CaCl_2$ may be an artifact due to mAb entrapment in the stronger calcium alginate gel network prohibiting recovery in

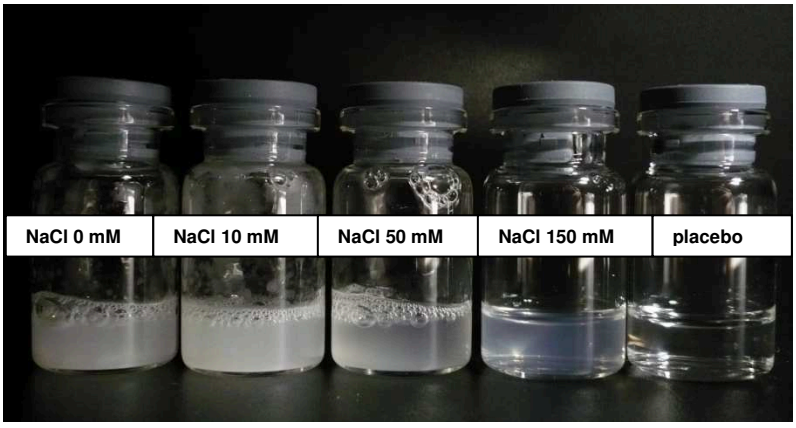

Figure 3-16 Visual appearance of samples containing mAb-low MW alginate mixtures in a ratio of 5 after addition of 10, 50 or 150 mM NaCl.

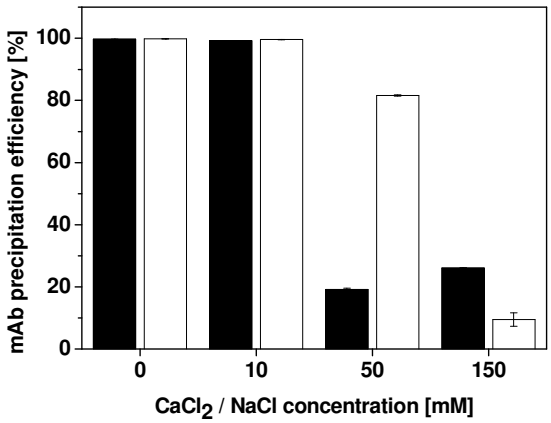

Figure 3-17 MAb precipitation efficiency [%] from mAb-low MW alginate mixtures (ratio of 5) after addition of different molar concentrations of $CaCl_2$ (black) or NaCl (white).

the supernatant. However, as the overall precipitation efficiency drastically decreased with increasing salt concentration, it can be concluded that this phenomenon is attributed to shielding effects instead of competitive effects between mAb and Ca^{2+} ions with alginate binding.

3.6.4 Determination of the precipitation efficiency of mAb-alginate mixtures at physiological conditions

The previous experiments had revealed that the mAb precipitation efficiency strongly depends on the ionic strength of the surrounding medium. In terms of an application *in vivo*, the impact of physiological conditions on the mAb precipitation is of major importance. Therefore, lyophilized mAb-alginate mixtures were reconstituted with physiological phosphate buffer (PBS 10 mM phosphate, 145 mM sodium chloride, pH 7.4). Besides the visual appearance and the turbidity 24 hrs after reconstitution, the mAb precipitation efficiency was determined.

All samples almost completely dissolved independent of the mAb-alginate ratio with only a slight turbidity remaining compared to placebo samples (figure 3-18 A). Quantification of mAb in the supernatant after centrifugation revealed that more than 95 % of the mAb-alginate complexes redissociated (see figure 3-18 B). Thus, the stronger precipitation phenomena of mAb with alginate compared to HA that could potentially enhance the residence time of the mAb at the site of application, are expected to be less pronounced *in vivo*. Little information concerning the synovial half-life of sodium or calcium alginate can be found in literature.

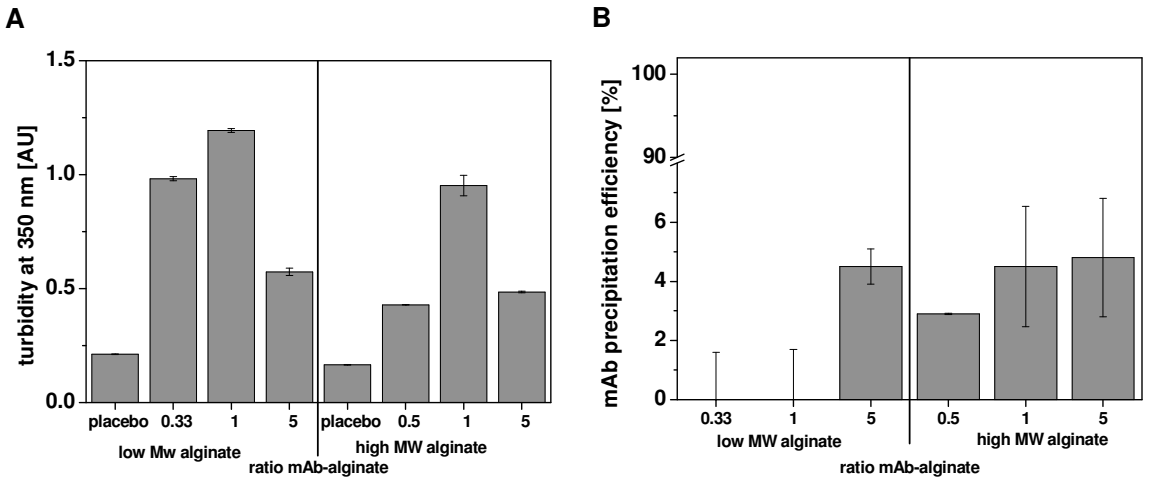

Figure 3-18 Turbidity (A) and mAb precipitation efficiency (B) after reconstitution of mAb-low and high MW alginate mixtures of varying ratios in PBS.

However, the synovial clearance of the high MW alginate might be reduced compared to the used HA caused by the higher estimated average MW of alginate. The application of insoluble mAb-alginate complexes could be beneficial when incorporated into a solidifying or gel forming matrix based on e.g. PLGA, thermo-reversible polymer systems or thermally induced gelling systems. On account of the solid or semi-solid matrix, the influx of the surrounding medium is expected to be decelerated and therefore alginate-mAb complex dissociation and mAb release should be retarded. Besides this approach, mAb retention at the site of application could moreover be achieved by steric entrapment of the drug into an alginate gel cross-linked with calcium ions. Drug release from this system is reported to be governed by diffusion and polymer erosion [163]. Due to a slow disintegration of the gel network induced by loss of calcium ions, mAb release over a prolonged period of time can be achieved. As alginate solutions start gelation immediately after contact with calcium, the injectability of mAb containing calcium alginate systems is limited. Hence, a simultaneous injection of mAb-alginate solution and calcium chloride solution using a double barrel syringe could be applied, leading to *in situ* gelation of the alginate and entrapment of mAb [164].

4 SUMMARY AND CONCLUSION

In this study the suitability of HA as carrier for local IA delivery of a therapeutic mAb was investigated. The focus was on the development of a HA-mAb formulation with high protein concentration, high gel viscosity but adequate injectability through thin syringe needles. Based on viscosity and injectability measurements, the HA material with a MW of 2 MDa at a concentration of 1 % revealed the most suitable gel characteristics. After incorporation of the mAb at a concentration of 50 mg/mL into the gel, no significant impact of mAb on the HA gel characteristics could be identified. The compatibility of HA with the incorporated mAb was assessed via various analytical methods. It was demonstrated that the secondary and tertiary protein structure as well as the protein unfolding temperature remained unchanged upon HA-mAb formulation preparation. Moreover, the mAb monomer content and the bioactivity of the protein were shown to be preserved. Based on these promising results, the presence of HA-mAb interactions that could contribute to mAb retention in the gel was analyzed with the help of SPR. The existence of weak interactions between HA and mAb was demonstrated employing a 10 mM phosphate buffer pH 7.4 with an ionic strength of 125 mM. The result was underlined by making use of a running buffer with reduced ionic strength where potential shielding effects induced by the buffer components were reduced. The binding signal increased with decreasing ionic strength, hence it was concluded that the observed HA-mAb binding is based on charge-charge interactions. *In vitro* release experiments revealed an overall significantly slower mAb release compared to a HA-free control formulation caused by restricted mobility and reduced diffusion rate of the molecules entrapped in the dense gel network. This effect occurred at the beginning of the experiment where dissolution of the gel by the release medium was less pronounced. Already after 24 hrs, the mAb release rates from buffer and HA gel became identical. Similar results were obtained upon IA administration of the HA-mAb formulation in rats. There, slightly lower mAb serum levels were achieved for the gel system compared to the HA-free mAb solution during the first 12 hrs. Afterwards, no significant difference in mAb release from HA gels or buffer was identified which indicates that dilution and dissolution of the HA gel followed by synovial clearance of HA molecules strongly reduces mAb retention at the site of application. Based on the fact that the density of the gel network has been described to be dependent on the HA concentration, the mAb release could be further prolonged by increasing the HA concentration.

As the charge interactions between HA and mAb were apparently too weak to affect mAb release from the HA gel, combinations of sodium alginate that exhibits a higher charge density than HA, and mAb were studied. It was shown that alginate strongly interacts with mAb leading to complete mAb precipitation. The conditions at which mAb precipitation occurs were demonstrated as being slightly dependent on pH and mAb-alginate ratio. The presence of increasing concentrations of calcium ions induced gelation of alginate but simultaneously caused mAb redissolution. Increased ionic strength was shown to reduce the alginate-mAb precipitation considerably. At physiological conditions 96 % of mAb were dissolved. Hence, enhanced mAb retention at the site of application due to formation of alginate induced mAb precipitates is expected to be less effective.

CHAPTER 4

DEVELOPMENT OF A PHOSPHOLIPID-BASED FORMULATION FOR THE INTRA-ARTICULAR DELIVERY OF A THERAPEUTIC ANTIBODY

1 INTRODUCTION

For many years, the use of lipid-based systems for the delivery of proteins or peptides has been in the focus of numerous research groups. In addition to the development of solid lipid implants [70] or solid lipid nanoparticles [71], the use of lipid-based vesicular drug delivery systems for proteins or peptides offers a promising approach for generating prolonged therapeutic responses [165]. Such lipidic drug delivery systems are advantageous if drugs with short half-lives are administered or local drug retention at the injection site is desired. Vesicular drug delivery systems, such as liposomal formulations, have been intensively characterized with respect to vesicle size [166] and lamellarity [167], drug encapsulation efficiency [168] or stability during storage and upon administration *in vivo* [169]. Numerous studies have described experiments where liposomal formulations were applied to achieve the sustained release of proteins. The encapsulation of interleukine-2 into liposomes was shown to effectively prolong the half-life in comparison to free drug after intraveneous (IV) injection [170]. As reported by Stevenson *et al.*, the encapsulation of insulin in phospholipid vesicles revealed prolonged plasma levels after subcutaneous (SC) administration in diabetic dogs, compared to free insulin [171]. Furthermore, drastically increased residence time of liposomal encapsulated ^{111}indium-labeled desferrioxamine at the site of application was observed after SC administration which was not seen for the free molecule [172]. The enhanced retention effect at the SC injection site in general is reported to be highly pronounced for large vesicles and can be explained by a slower clearance via the lymphatic capillaries with increasing size [173]. Despite successful studies found in literature, the encapsulation of proteins into liposomes in general is challenging as oftentimes preparation methods are applied that might induce protein denaturation, comprising the use of organic

solvents or liposomal treatment by sonication, freeze-thaw stress, elevated heat or pressure [174]. As an alternative approach, Tian *et al.* proposed the entrapment of proteins into vesicular phospholipid gels [225]. These highly concentrated vesicular phospholipid dispersions are prepared by forced hydration of the phospholipids using a dual asymmetric centrifuge. This preparation method was shown to provide high protein stability and sustained release of the entrapped drug from the formulation [68]. As demonstrated by Brandl *et al.*, vesicular phospholipid gels allow high drug encapsulation and present therefore an attractive alternative to liposomes where commonly low drug encapsulation efficiencies are obtained [175]. Another approach for vesicle preparation without the use of harsh processing methods was introduced by Nuernberg *et al.* who reported about the spontaneous formation of vesicles upon infusion of oil-bath preparations containing fatty oil, lipophilic detergent, active substance and phospholipids [176]. The size of the phospholipid vesicles in general can be mainly tailored by the preparation process: formulation preparation by e.g. dual asymmetric centrifuge or high pressure homogenization leads to small sized vesicles in the nm-range with narrow vesicle size distribution and low lamellarity [177, 178]. In comparison, spontaneously formed vesicles prepared by e.g. thin film hydration show high vesicle size distribution in the lower µm-range [179].

Due to the potential to prolong the drug residence time at the site of application and thus to reduce systemic exposure [180], lipid-based vesicular drug delivery systems present an attractive vehicle for the intra-articular (IA) administration of therapeutic drugs in the treatment of inflammatory joint diseases. This method was first introduced by Shaw *et al.* in 1976 [33] who described the beneficial therapeutic effect of liposomally encapsulated corticosteroids. Bonanomi *et al.* studied the pharmacokinetic profile of dexamethasone palmitate-loaded liposomes after IA administration in rabbits and compared the synovial drug concentrations with that of microcrystalline triamcinolone acetonide, administered in non-liposomal form. It turned out that after 6 hrs 36 % of the liposomal formulation was still present in the joint while 98 % of non-encapsulated drug had been cleared [35]. Similar results were obtained upon IA administration of liposomal lidocain in rabbits [37]. Also the residence time of liposomal iohexol was shown to be drastically prolonged after IA administration in sheep; while the liposomal drug revealed a synovial elimination half-life of 138 hrs, non-encapsulated iohexol was completely cleared from the joint already 3 hrs after injection [39]. The extent of synovial retention was shown to increase with vesicle size [39]. Similarly, enlargement of the vesicle size from 160 nm to 750 nm led to an increased synovial retention of dexamethasone palmitate by a factor of 2.6 [35]. Williams *et al.* demonstrated that methotrexate-loaded liposomes with a size of 1.2 µm revealed higher

therapeutic efficacy than small-sized 100 nm variants [36]. Despite various successful studies that have shown the beneficial effect of the IA administration of liposomal drugs, only one liposomal formulation for IA administration, Lipotalon® containing dexamethasone-21-palmitate for the treatment of rheumatic disorders, can be found on the German market [180].

The aim of the study outlined in this chapter was the development of a phospholipid (PL)-based drug delivery system for the IA administration of a therapeutic monoclonal antibody (mAb). Due to the limitations of IA injection with respect to frequency and volume, the formulation had to provide a high drug load. Moreover, both the formulation components and the formulation preparation process were to be highly protein-compatible. The scope of the study was limited to two different formulations. Firstly, a PL-mAb formulation, consisting of spray-dried mAb particles suspended within a non-aqueous PL solution was to be developed, which spontaneously transfers into a vesicular formulation upon contact with synovial fluid. This should lead to dissolution of the incorporated mAb particles and mAb entrapment in the vesicles. Alternatively, the spontaneous formation of the vesicles can be performed *ex vivo* by simply mixing a non-aqueous PL solution with a highly-concentrated mAb solution. After being administered into the joint cavity, both formulations were expected to provide prolonged residence time and thus sustained synovial mAb concentration with improved therapeutic effects. Both formulation approaches were based on knowledge from previous studies where the formation of large vesicles was demonstrated when they were spontaneously formed [179], and a high drug load and excellent protein stability was reported when using highly viscous phospholipid-based formulations [68, 175]. Besides the detailed characterization of the PL formulations, the compatibility with the mAb employed was to be assessed via a bundle of analytical methods. Additionally, the pharmacokinetic profile after IA administration was to be addressed with an *in vivo* study.

2 MATERIALS AND METHODS

2.1 Materials

2.1.1 Monoclonal antibody (mAb)

The mAb (IgG1) used for preparation of the vesicular phospholipid formulation was formulated at 70 mg/mL, pH 5.2 with sodium chloride (105.5 mM), monobasic sodium phosphate dihydrate (5.5 mM), dibasic sodium phosphate dihydrate (8.6 mM), sodium citrate (1.16 mM), citric acid monohydrate (6.19 mM), mannitol (65.9 mM) and polysorbate 80 (0.1 %) and had a molecular weight (MW) of 148 kDa. MAb solution used for spray drying was formulated at a concentration of 100 mg/mL in trehalose (201.6 mM), histidine (15 mM) and polysorbate 80 (0.01 %) at pH 5.4. The bulk solutions were stored at -80 °C until use. Prior to use, protein solutions were filtered through an Acrodisc® 0.2 µm PVDF syringe filter (Pall, Dreieich, Germany). For an *in vivo* experiment, instead of the human mAb, the murine variant was used, which was formulated in histidine buffer (15 mM) at pH 6.0 and a concentration of 24.5 mg/mL.

2.1.2 Phospholipids

Table 4-1 lists all phospholipid (PL) components used throughout this chapter.

Table 4-1 List of PL used in this work.

Product name	Composition	Source
1,2-dipalmitoyl-*sn*-glycero-3-phosphate, sodium salt		Lipoid, Ludwigshafen, Germany
1,2-dipalmitoyl-*sn*-glycero-3-phospho-*rac*-glycerol, sodium salt		Lipoid, Ludwigshafen, Germany
Phosal®50PG	phosphatidylcholine 52.3 % lysophosphatidylcholine 0.9 % dissolved in propylene glycol	PHOSPHOLIPID, Köln, Germany
Phospholipon®90G	phosphatidylcholine 97.3 % lysophosphatidylcholine 1.5 %	PHOSPHOLIPID, Köln, Germany

2.1.3 Excipients, reagents and chemicals

Table 4-2 lists the excipients, reagents and chemicals used throughout this chapter. All substances were of analytical grade. Ultrapure water for all buffers was used from a PureLab UV/UF system (Elga LabWater, Celle, Germany).

Table 4-2 List of excipients, reagents and chemicals used in this chapter.

Excipients, reagents, chemicals	Source
Alexa®Fluor488	Life Technologies, Darmstadt, Germany
Citric acid monohydrate	Carl Roth, Karlsruhe, Germany
Cholesterol	Synopharm, Barsbuettel, Germany
Dibasic potassium phosphate	AnalR Normapur, VWR international, Leuven, Belgium
Dibasic sodium phosphate dihydrate	Merck, Darmstadt, Germany
Dimethyl sulfoxide (DMSO)	Merck, Darmstadt, Germany
Ethanolamine	Sigma-Aldrich Laborchemikalien, Seelze, Germany
Ethylenediaminetetraacetic acid	Sigma-Aldrich Laborchemikalien, Seelze, Germany
Fetal calf serum	Biochrom, Berlin, Germany
Glycine	Sigma-Aldrich Laborchemikalien, Seelze, Germany
L-histidine	Merck, Darmstadt, Germany
N-2-hydroxyethylpiperazine-*N*-2-ethansulfonic acid	Merck, Darmstadt, Germany
N-methyl pyrrolidone (NMP)	Fluka Chemie, Buchs, Switzerland
Mannitol	Riedel-de Haen, Seelze, Germany
Monobasic sodium phosphate dihydrate	Merck, Darmstadt, Germany
N-ethyl-*N*9-(dimethylaminopropyl) Carbodiimide	Sigma-Aldrich Laborchemikalien, Seelze, Germany
N-hydroxy succinimide	Sigma-Aldrich Laborchemikalien, Seelze, Germany
Nile red	Sigma-Aldrich Laborchemikalien, Seelze, Germany
Octyl glycoside	Carl Roth, Karlsruhe, Germany
ortho-phosphoric acid	Zentrale Versorgung LMU München, Germany
Polyethylene glycol 300 (PEG 300)	Sasol, Marl, Germany

Polysorbate 20	Merck, Darmstadt, Germany
Polysorbate 80	Merck, Darmstadt, Germany
Potassium chloride	Caelo, Hilden, Germany
Propylene glycol	BASF, Ludwigshafen, Germany
Sodium citrate	Caelo, Hilden, Germany
Sodium chloride	AnalR Normapur, VWR international, Leuven, Belgium
Sodium hydroxide, 1M	Merck, Darmstadt, Germany
Trehalose	Merck, Darmstadt, Germany
XenoLight™ CF680	Caliper Life Sciences, Hopkinton, USA

2.2 Methods

2.2.1 Spray drying with the Mini Spray Dryer B-290

Spray drying experiments were performed on a Mini Spray Dryer B-290 (Büchi Labortechnik, Flawil, Switzerland). This instrument comprised a heating system with inlet temperature (T_{in}) sensor for the drying air, a spray nozzle, a drying chamber with outlet temperature (T_{out}) sensor, a high efficiency cyclone for separation of the dried powder, a collection vessel and an aspirator with particle filter. For atomization of the spray drying solution, a two fluid nozzle (tip Ø 0.7 mm, cap Ø 1.5 mm) was used with compressed air from an in-house supply. The use of a LT Mini dehumidifier (Deltatherm, Much, Germany) ensured a constant low residual moisture within the system. Cooling water was circulated through a jacket around the nozzle. The T_{in}/T_{out} was 130 °C/64 °C, the aspirator flow rate was 38 m^3/hr or 100 % and the atomizing air flow rate was 667 L/hr. The mAb spray drying solution was pumped with a liquid feed rate of 3 mL/min by means of an internal pump. All liquid samples were filtered through Acrodisc® 0.2 µm PVDF syringe filter prior to spray drying. After the process, the resulting powder was collected in glass vials, closed and stored in a desiccator at ambient atmosphere. The yield was calculated from the amount of powder recovered in the collection vessel in relation to the solid content of the used spray drying solution.

2.2.2 Karl-Fischer analysis

The residual moisture (RM) content of the spray-dried (sd) powder was determined by coulometric Karl-Fischer titration using an Aqua 40,00 titrator with headspace module (Analytik Jena, Jena, Germany). Therefore, 10-20 mg of the respective powder were accurately weighed into a 2 R glass vial, sealed with rubber stopper and heated up to 100 °C. For determination of the RM content, the evaporated water was transferred into the titration solution. As reference, a standard with defined RM was used (apura® water standard oven 1 %, Merck, Darmstadt, Germany).

2.2.3 Formulation preparation

2.2.3.1 Non-aqueous PL-mAb suspension

This non-aqueous formulation was prepared by dispersing sd mAb powder, providing a final concentration of 50 mg/g mAb, in a 2:1 (w/w) mixture of Phosal®50PG and propylene glycol or a 60 % (w/w) Phospholipon®90G in PEG 300 solution (Phospholipon®90G was dissolved in PEG 300 at 80 °C), using a dual-syringe system consisting of two Luer-Lock syringes (VWR International, Ismaning, Germany) connected by a syringe adapter (Braun, Melsungen, Germany).

2.2.3.2 Vesicular PL-mAb formulation

Formulations were all prepared by emulsifying Phosal®50PG with mAb solution of 70 mg/mL (if not stated otherwise) (active) or mAb formulation buffer (placebo) by means of a dual-syringe system, leading to a mAb content of 50 mg/g. The respective amounts of both components were filled into Luer-Lock syringes, the two syringes were connected by a syringe adapter and the content was carefully mixed by moving the syringe plungers.

In a study to optimize the encapsulation efficiency the vesicular PL-mAb formulations were subjected to either:

- 3 to 5 freeze-thaw cycles by repetitive sample freezing for 30 s in liquid nitrogen and subsequently thawing at 30 °C in a water bath for 4 min
- treatment with a T 10 Ultra-Turrax® equipped with a S10N-5G dispersing tool (IKA®-Werke, Staufen, Germany) for 15 s, 30 s or 45 s at 8000 rpm. All samples were kept on ice during mixing.

Alternatively, formulation preparation was carried out in a Speed-Mixer™ DAC 150 FVZ (Hauschild, Hamm, Germany) according to the method described by Tian *et al.* [68]. Formulation components were weighed into a 30 g polypropylene container and centrifuged at 3500 rpm and room temperature (RT) for 30 min or 60 min with steps of 1.5 min centrifugation followed by cooling on ice.

2.2.4 Buffer exchange and up-concentration of mAb solutions

In order to obtain mAb concentrations >70 mg/mL, mAb solution at a concentration of 100 mg/mL, formulated in trehalose (201.6 mM), histidine (15 mM) and polysorbate 80 (0.01 %) at pH 5.4, was buffer exchanged against sodium chloride (105.5 mM), monobasic sodium phosphate dihydrate (5.5 mM), dibasic sodium phosphate dihydrate (8.6 mM), sodium citrate (1.16 mM), citric acid monohydrate (6.19 mM) and mannitol (65.9 mM). Therefore, a Vivaflow®50 tangential flow filtration cassette at a MW cutoff of 30 kDa (Satorius stedim, Göttingen, Germany) was used.

2.2.5 Injectability

The maximal injection force, required for injection of 0.4 mL of the formulation into air, was determined by means of a TA.XTplus texture analyzer (Stable Micro Systems, Surrey, UK) at RT. This value was defined as the highest force measured before the plunger reached the end of the syringe after having overcome the plunger-stopper breakloose force. Therefore, 1 mL Luer-Lock syringes connected to 26 G syringe needles (Terumo Europe, Leuven, Belgium) were clamped in a tripod underneath the punching tool of the instrument. The crosshead velocity was set to 1 mm/s, a representative velocity for the manual syringe delivery [96]. After 20 s, the measurement stopped automatically.

2.2.6 Rheometry

The rheological properties of the formulations were studied on a plate-cone rheometer (Physica MCR 100, Anton Paar, Ostfildern, Germany) with in- and decreasing shear rate (10-100 s^{-1}, 100-10 s^{-1}) at a gap position of 0.042 mm using a cone with a diameter of 50 mm and an angle of 1 °. Analysis was performed at 25 °C using 600 mg of the respective formulation.

2.2.7 Dynamic light scattering (DLS)

DLS measurements were performed on a Zetasizer Nano ZS (Malvern, Herrenberg, Germany) at 25 °C using 0.5 mL cuvettes (Brand, Wertheim, Germany). Formulations were diluted with PBS by factor 100 and analyzed in triplicate.

2.2.8 Cryo-transmission electron microscopy (Cryo-TEM)

Cryo-TEM analysis was performed on a LEO 912 OMEGA electron microscope (Zeiss, Oberkochen, Germany). Prior to analysis, samples were diluted with PBS to a lipid concentration of 5-10 mM. Approximately 7 µL were plotted on a copper grid (Quantifoil S7/2 100 x 400 mesh, Quantifoil Micro Tools, Jena, Germany). Excess sample volume was removed from the copper grid by means of a filter paper. The sample-loaded grid was immediately shock-frozen by immersing it into liquid ethane using a CryoBox (Carl Zeiss, Oberkochen, Germany) cooled with liquid nitrogen. The sample grid was transferred into the TEM by means of a pre-cooled cryogenic sample holder (626-DH, Gatan, Warrendale, USA). Images were recorded in vacuum atmosphere at -175 °C and 120 kV with a 6,300-12,500-fold magnification in underfocus mode and processed with the iTEM software (Olympus, Muenster, Germany).

2.2.9 UV spectroscopy (OD 280, second derivative, absorbance at 350 nm)

Protein concentrations were determined photometrically on an Agilent 8453 UV-Vis spectrometer (Agilent Technologies Deutschland, Böblingen, Germany) equipped with a Peltier temperature controller (Agilent Technologies Deutschland, Böblingen, Germany) at λ=280 nm and 25 °C in quartz UV cuvettes with a path length of 1 cm. An extinction coefficient of either 1.39 $mL \cdot mg^{-1} \cdot cm^{-1}$ (mAb) or 1.40 $mL \cdot mg^{-1} \cdot cm^{-1}$ (murine mAb) was applied. Samples were diluted to a concentration ranging from 0.1 to 0.7 mg/mL prior to analysis. Corresponding blank spectra were subtracted from the protein spectra. Second derivative protein spectra were calculated between 240 and 350 nm by means of the ChemStation software. Determination of turbidity of protein or vesicle containing samples was performed with a UV plate reader (FLUOstar Omega, BMG LABTECH, Ortenberg, Germany) in 96-well plates (Nunc®, Sigma-Aldrich Laborchemikalien, Seelze, Germany) and a filling volume of 300 µL.

2.2.10 Fourier transform infrared spectroscopy (FTIR)

FTIR spectra were recorded with the Tensor 27 FTIR spectrometer (Bruker Optics, Ettlingen, Germany) using a Bio-ATR unit (attenuated total reflection) connected to a thermostat at 20 °C (DC30-K20, Thermo Haake, Dreieich, Germany). Corresponding blank spectra were subtracted from the protein spectra. After a 120-scan measurement, the second derivative

spectrum was generated with the help of the spectrometer software (OPUS, Bruker Optics, Ettlingen, Germany). For investigation of changes in secondary protein structure, the vector normalized second derivative spectra between the wavenumbers of 1720 and 1580 cm^{-1} were compared with the spectra of the native, untreated protein.

2.2.11 High performance size exclusion chromatography (HP-SEC)

Size exclusion chromatography was used for quantification of soluble aggregates, monomer and fragments of the mAb. The measurement was performed on a HPLC 1100 chromatograph (Agilent Technologies Deutschland, Böblingen, Germany) using a Superose® 6 10/300 GL column (GE Healthcare, Uppsala, Sweden) with UV detection at 214 and 280 nm. The mobile phase consisted of 0.15 M sodium chloride in 0.02 M sodium phosphate, adjusted to pH 7.5 with *ortho*-phosphoric acid. The flow rate was 0.5 mL/min. Samples were diluted with mobile phase to a target concentration of 1 mg/mL and centrifuged for 10 min at 12,000 rpm (Sigma 1-15, Sigma Laborzentrifugen, Osterode am Harz, Germany) in order to remove insoluble aggregates. Chromatograms were integrated manually by means of the ChemStation software Rev. B.02.01 (Agilent Technologies Deutschland, Böblingen, Germany). For quantification, the area under the curve was used. Protein concentrations were calculated based on a calibration curve.

2.2.12 Fluorimetry

Protein concentrations below 0.1 mg/mL were determined with a Varian Carry Eclipse fluorimeter (Varian, Darmstadt, Germany). Solutions were measured at 20 °C in 0.5 mL cuvettes (Brand, Wertheim, Germany). Excitation occurred at a wavelength of 280 nm with an excitation slit of 5 nm. The emission spectrum was recorded from 280 nm to 600 nm. For protein quantification a calibration curve, ranging from 0.002 to 0.1 mg/mL at the emission maximum at 334 nm, was used.

2.2.13 MAb extraction from PL formulations

2.2.13.1 Extraction by using a detergent

For further analysis, mAb was extracted from the lipid matrices by solubilization of the lipids in 100 mM octyl glycoside (OG) solution. The volume ratio of matrix to detergent solution was adapted to provide a clear micellar solution.

2.2.13.2 Extraction by centrifugation

MAb extraction without use of detergents was performed by centrifugation of the vesicular PL-mAb formulations for 1 hr at 186,000 x g (Optima™ TLX Ultracentrifuge, Beckman Coulter, Krefeld, Germany) at 20 °C. For mAb analysis the clear lower aqueous phase was used.

2.2.14 MAb bioassay

The biological activity of mAb after extraction from the vesicular PL formulation was assessed by a cell based bioassay performed at Abbott, Ludwigshafen, Germany according to the Abbott standard protocol. This assay is based on the determination of cell viability upon neutralization of cytotoxic recombinant human TNF (rhTNF) by mAb. Mouse L-929 cells were incubated with defined amounts of rhTNF and various concentrations of mAb. After incubation for 48 hrs at 37 °C the survived cells were stained with crystal violet and their color intensity was determined photometrically at 620 nm. The bioactivity [%] was then calculated in comparison to a reference. MAb samples, extracted by centrifugation from vesicular PL formulations, were diluted to a mAb concentration of 1 mg/mL with formulation buffer. As reference, a mAb solution at same concentration was used.

2.2.15 Determination of the encapsulation efficiency (EE)

For determination of the EE, vesicular PL-mAb samples were diluted with PBS to a mAb concentration of 1 mg/mL (c_0) and 850 µL of the diluted samples were centrifuged for 40 min at 2739 x g and 20 °C (Sigma 4K15, Sigma Laborzentrifugen, Osterode am Harz, Germany) using Vivaspin®2 centrifugation tubes (Satorius stedim, Göttingen, Germany) with a MW cutoff of 1 MDa. As reference, a non-encapsulated active sample with same mAb concentration was used and treated equally. MAb concentrations in the first elution fraction of

PL-mAb formulation (c_{active}) and reference ($c_{reference}$) were determined by UV spectroscopy. The EE [%] was calculated based on equation (1):

$$(1) \qquad EE\,[\%] = 100\,\% - \left(\frac{100\,\% \cdot c_{active}}{c_{reference}} \right)$$

For quantification of the liposomally encapsulated mAb, samples were centrifuged as described before. After centrifugation, the eluted volume was replaced by PBS and this centrifugation/washing procedure was performed another 5 times. The absence of mAb in the elution fraction was confirmed fluorimetrically (see section 2.2.12). Thereafter, the purified vesicles were admixed with OG solution (100 mM) in a 1.37:1 ratio in order to solubilize the lipids and to release encapsulated mAb. MAb was quantified by fluorimetry. The EE [%] was calculated based on equation (2):

$$(2) \qquad EE\,[\%] = \frac{100\,\% \cdot c_{liposomal}}{c_0}$$

2.2.16 Separation of non-encapsulated mAb from loaded vesicles

For purification of mAb loaded PL vesicles from non-encapsulated mAb, vesicular PL-mAb formulations were diluted with PBS to a mAb concentration of 1 mg/mL and subsequently transferred into Vivaspin®2 centrifugation tubes with a MW cutoff of 1 MDa. Samples were centrifuged for 40 min at 2739 x g and 20 °C (Sigma 4K15, Sigma Laborzentrifugen, Osterode am Harz, Germany) and the eluted volume was replaced by PBS. The washing procedure was repeated until the complete absence of mAb in the elution fraction was achieved. The elution fraction was checked for presence of mAb by determination of the intrinsic fluorescence (see section 2.2.12).

2.2.17 Labeling of mAb with AlexaFluor®488

MAb bulk solution (70 mg/mL) was dialyzed against 10 mM PBS using Vivaspin®6 centrifugation tubes (Satorius stedim, Goettingen, Germany) with a MW cutoff of 30,000 Da. After dialysis, the protein concentration was adjusted with PBS to 2 mg/mL. For covalent binding of the fluorescent dye to the protein, 1 mL of the mAb solution was admixed with 0.1 mL bicarbonate solution (1 M). To the protein solution, 4 µL of AlexaFluor®488, formulated in DMSO at a concentration of 10 mg/mL, were added. The sample was incubated for 1 hr at room temperature on a horizontal shaker at 350 rpm (Titramax 101,

Heidolph, Schwabach, Germany) under exclusion from light. After incubation, the sample was transferred into a Vivaspin® centrifugation tube with a MW cutoff of 30,000 Da and washed with at least the 10-fold volume of PBS for separation of the free fluorescent dye. The elution fractions were checked for absence of free dye via UV spectroscopy at 494 nm. The molar protein concentration [IgG] and the degree of labeling after purification were determined according to equations (3) and (4) [181]:

(3) $$[IgG] = \frac{[A_{280} - (A_{494} \cdot 0.11)] \cdot dilution\ factor}{203{,}000}$$

(4) $$Degree\ of\ labeling = \frac{A_{494} \cdot dilution\ factor}{71{,}000 \cdot [IgG]}$$

2.2.18 Labeling of mAb with XenoLight™ CF680

MAb bulk solution (70 mg/mL) was dialyzed against 10 mM PBS using Vivaspin®6 centrifugation tubes with a MW cutoff of 30,000 Da. After dialysis, the protein concentration was diluted with PBS to 1 mg/mL. For pH adjustment of the protein solution, 1 mL of the mAb solution was admixed with 0.1 mL bicarbonate solution (1 M). Preparation of the near-infrared dye stock solution was performed by dissolution of 0.1 µmole XenoLight™ CF680 in 25 µL anhydrous DMSO. For covalent binding of the dye to the protein, 12 µL dye stock solution were added to the mAb solution and the mixture was incubated for 1 hr at room temperature under exclusion of light on a horizontal shaker. Unconjugated dye was removed by ultrafiltration using NanoSep membrane filtration vials provided by the supplier and using PBS. Labeled protein concentration after separation of the free dye [IgG] [mg/mL] and degree of labeling were determined according to equations (5) and (6) [182]:

(5) $$[IgG] = \frac{[A_{280} - (A_{681} \cdot 0.09)] \cdot dilution\ factor}{1.39}$$

(6) $$Degree\ of\ labeling = \frac{A_{681} \cdot 148{,}000 \cdot dilution\ factor}{210{,}000 \cdot [IgG]}$$

2.2.19 Staining of PL vesicles with nile red

PL vesicles were stained with nile red for fluorescence microscopy. Therefore, 1 µL of a 1 mg/mL nile red solution in acetone was spiked to the PL vesicles prior to microscopy analysis.

2.2.20 Fluorescence microscopy

Visualization of stained PL vesicles loaded with fluorescence-labeled mAb (F-mAb) was carried out on a Biozero BZ-8100E fluorescence microscope (Keyence Deutschland, Frankfurt, Germany) combined with the BZ-Analyzer software (Keyence Deutschland, Frankfurt, Germany).

2.2.21 Surface plasmon resonance (SPR) measurements

SPR measurements were performed in order to investigate the impact of the labeling procedure on mAb binding affinity to its target. The study was carried out at the Abbott Bioresearch Center, USA using a BICORE T100 instrument (GE Healthcare, Uppsala, Sweden) in combination with Biaevaluation® Software. Goat anti-huIgG-FC antibody was immobilized on a carboxy methylated (CM5®) research chip following the standard immobilization procedures described by Biacore Life Science. The sensor chip surfaces of sample and reference cells were first activated by a 6-min injection of a solution containing 0.4 M *N*-ethyl-*N*9-(dimethylaminopropyl) carbodiimide and 0.1 M *N*-hydroxy-succinimide. After goat anti-huIgG-FC antibody immobilization in the sample cell via amine linkage of lysine residues, residual activated carboxymethyl groups of both sample and reference cell were deactivated with ethanolamine. The running buffer contained 0.01 M HEPES, 0.15 M sodium chloride, 0.003 M EDTA and 0.05 % Polysorbate 20 at pH 7.4. F-mAb samples were diluted with running buffer to a concentration of 0.2 µg/mL. Capturing by the immobilized anti-huIgG-FC antibody occurred at a flow rate of 5 µL/min within 30 s. Afterwards, TNFα-solutions in a concentration range of 25-0.39 nM were carried through the cell at a flow rate of 50 µL/min. As reference, non-labeled mAb was used at same concentrations. Surface regeneration was performed with 50 µL of 0.01 M glycine solution at pH 1.5 with a flow rate of 100 µL/min. Samples were measured in duplicate. Determination of the dissociation constant K_D was carried out with the help of the instrument software.

2.2.22 *In vivo* experiments

In vivo studies were performed at the Abbott Bioresearch Center in Worcester, USA in order to assess the pharmacokinetic profile of PL-mAb formulations upon IA injection. The studies were carried out with healthy male Lewis rats weighing approximately 275 – 300 g at the start of the study.

In a first study, the vesicular PL-mAb formulation was analyzed. Instead of the human mAb, the murine variant was used. As the murine mAb was formulated in histidine buffer (15 mM) at a concentration of 24.5 mg/mL, the solution was buffer exchanged against mAb formulation buffer and up-concentrated to 50 mg/mL using Vivaspin® centrifugation tubes with a MW cutoff of 30 kDa (Satorius stedim, Göttingen, Germany). Prior to injection, animals were anaesthetized in an anesthesia chamber using isoflurane (5 %) and oxygen. Once the rat was completely anesthetized, the right knee was shaved. Animals were dosed IA with 50 µL of the formulation (mAb content 35.7 mg/g) via injection through the patella into the knee joint using a 26 G needle. As reference a murine mAb solution at same concentration was used. The study was performed during 48 hrs. At predefined time points (2 hrs, 4 hrs, 12 hrs, 24 hrs and 48 hrs) animals were sacrificed in an anaesthesia chamber using CO_2. Synovial fluid (SF) samples were obtained from each animal via synovial wash. Therefore, a small volume of PBS was injected into the joint cavity and subsequently removed. Moreover, blood samples were taken at each time point. Both, SF and blood samples were analyzed in regard to mAb concentration via ELISA according to the Abbott standard protocol.

In a second study, the pharmacokinetic profile of mAb-loaded PL vesicles separated from non-encapsulated mAb was investigated. This study was carried out with the human mAb. The mAb concentration in the PL vesicles was 1 mg/mL. As reference, empty PL vesicles with spiked mAb as well as a mAb solution at same concentration were analyzed. The study was performed during 10 d. At predefined time points (1 hr, 4 hrs, 1 d, 3 d, 7 d, 10 d) blood samples were collected from the tail nick of the animals and stored at -80 °C until analysis. At day 10, animals were sacrificed in an anesthesia chamber using CO_2 and SF was removed by synovial wash. Blood and SF samples were analyzed in regard to mAb concentration.

In order to study the fate of the mAb-loaded vesicles after IA administration, the encapsulated mAb was labeled with a near-infrared dye according to 2.2.18 prior to mAb encapsulation and separation of non-encapsulated protein. The study was carried out with the human mAb at a mAb concentration in the PL vesicles of 1 mg/mL. Three days after injection of 50 µL of the formulation into the right hind leg, the animals (n=2) were sacrificed

and the full animal body prior to and after laparotomy were examined using a Fluobeam™ 700 fluorescence imaging system (excitation wavelength 680 nm, emission wavelength >700 nm, Fluoptics, Cambridge, USA).

3 RESULTS AND DISCUSSION

3.1 Non-aqueous PL-mAb suspension

3.1.1 Pre-screening experiments

3.1.1.1 MAb stability in Phosal®50PG-mAb formulation and propylene glycol

After preparation of the non-aqueous PL-mAb suspension based on Phosal®50PG (phosphatidylcholine 52.3 %, lysophosphatidylcholine 0.9 %, dissolved in propylene glycol) and a mAb content of 50 mg/g added as sd powder, the analysis of the protein conformation was in the focus of the study. *In situ* vesicle formation upon contact with SF was simulated by injection of the formulation into PBS at a 1:2 (w/w) ratio using a 26 G needle. After dissolution of the sd mAb and entrapment into the vesicles, mAb was intended to be extracted for analytical purpose via centrifugation for 1 hr at 186,000 x g. In contrast to the placebo sample, it was not possible to separate the lipid structures from the aqueous phase. Alternatively 100 mM OG solution was added to the samples for solubilization of the lipid phase. Compared to the placebo sample, addition of the detergent did not render a clear solution but a white precipitate remained. The precipitated sample was characterized by second derivative FTIR spectroscopy. Furthermore, the supernatant after centrifugation was subjected to second derivative UV spectroscopy and mAb quantification in order to determine the extend of mAb precipitation.

Compared to the spectrum of the native mAb solution, drastical changes in the amide I spectral region of the second derivative FTIR spectrum and thus in the secondary protein structure were seen for the precipitate (figure 4-1 A). The native mAb spectrum showed the characteristic predominant bands at 1638 cm^{-1} and 1688 cm^{-1} and a weak band at 1612 cm^{-1} which can be attributed to intramolecular β-sheet structures [183, 184]. The spectrum of the precipitated mAb exhibited a band intensity increase at 1615 cm^{-1}. The strong band at 1638 cm^{-1} was shifted to 1625 cm^{-1} with a decrease in intensity which can be assigned to the formation of intermolecular β-sheet elements and thus protein aggregation [185]. An additional band at 1650 cm^{-1} was found which is indicative for the presence of non-ordered structures. The peak at 1680 cm^{-1} as well as the slight shift from 1688 cm^{-1} to higher wavenumbers can be ascribed to the formation of turns [144, 184]. Determination of the mAb concentration in the supernatant liquid revealed that most of the protein had been

precipitated as only 8.2 % of the mAb was recovered. Alterations in band position were also found in the second derivative UV spectrum compared to the native mAb reference (figure 4-1 B): a slight shift to lower wavelength was observed for the bands at 284 nm and 275 nm. These changes in the tertiary protein structure can be ascribed to alterations in the microenvironment of the aromatic amino acids tyrosine and tryptophane [102, 103] causing an enhanced propensity to aggregation.

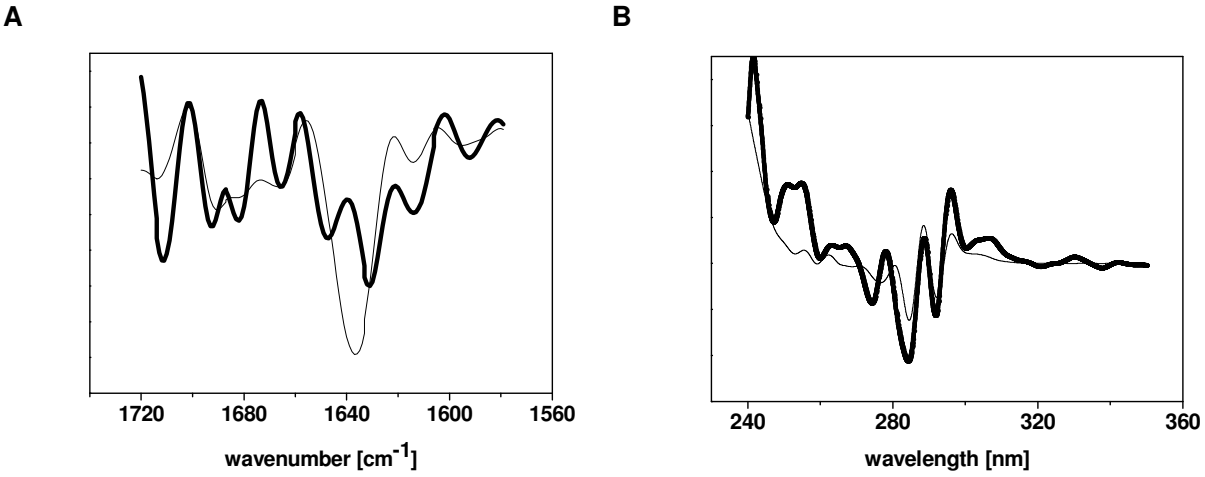

Figure 4-1 Second derivative FTIR (A) and UV (B) spectra of mAb from PL-mAb suspension after vesicle formation in PBS and addition of OG solution (thick line) compared to native mAb solution (thin line).

This observed protein instability might be attributed to the destabilizing effect of the employed organic solvent propylene glycol or to incompatibilities with the phospholipid component used for formulation preparation and the lamellar structure formation. From previous studies, the denaturing impact of various organic solvents on proteins in aqueous solution is well-known [186, 187]. Water-miscible organic solvents mainly destabilize proteins by direct binding via hydrophobic interactions or indirectly via perturbation of the hydration shell which causes aggregation. The extent of destabilization depends on the degree of protein hydration and concentration of the organic solvent [188] but also on the fact whether the protein is in dissolved or dried state. Griebenow *et al*. demonstrated that the secondary structure of lysozyme was maintained when the protein was suspended in pure organic solvent but changed when dissolved in organic solvent-water mixtures. This behavior was explained by the fact that the protein conformation is restricted in anhydrous environment. In presence of only low amounts of water, the protein mobility increases which may cause aggregation [189]. Additionally, the formation of hydrophilic-hydrophobic interfaces, as observed when e.g. using poorly water-miscible organic solvents or lipidic components, might also contribute to protein instabilities in aqueous solutions. As surface-active

molecules, proteins tend to aggregate on such interfaces. In a study of Morlock *et al.* it was demonstrated that erythropoietin mainly formed aggregates during the first emulsification step of encapsulation into PLGA microparticles using a double-emulsion technique [84]. In another study, the stability of lysozyme in aqueous solution upon emulsification with methylene chloride was investigated and it was shown that 20 to 35 % of the protein non-covalently aggregated at the water-organic solvent interface [190]. In conclusion, the type and the concentration of the organic solvent employed, as well as whether the protein is in dissolved or in a dried state influence protein stability in general.

In order to investigate the potential role of propylene glycol in mAb denaturation, sd mAb particles were suspended at 50 mg/g in propylene glycol and admixed with PBS in a ratio of 1:2 (w/w). Directly after mixing a strong turbidity occurred. Similar to foregoing experiments, FTIR measurements revealed alterations in the second derivative spectrum (figure 4-2 A). The predominant band at 1638 cm^{-1} was shifted to lower wavenumbers with shoulder formation at 1640 cm^{-1} and decrease in intensity which is indicative for the presence of intermolecular β-sheet structures. A slight band shift at 1688 cm^{-1} to higher wavenumbers was found which can be assigned to the formation of turns. More than 99 % of the initial protein content was precipitated as determined via UV analysis of the supernatant liquid after centrifugation. HP-SEC analysis of the supernatant revealed a decline in monomer recovery from 99.5 % to 96 % with drastical increase in soluble aggregate formation in comparison to the native mAb. No structural changes in the second derivative UV spectrum of the remaining mAb in solution were identified (figure 4-2 B).

These results underpin the suspicion that propylene glycol induces mAb aggregation in aqueous environment. As it is known from literature that solvent-induced protein instabilities might be dependent on the concentration of the organic solvent [188], the impact of the propylene glycol concentration on the mAb stability was examined in a further step. To this end differently concentrated propylene glycol/water mixtures were added in equal volumes to a 50 mg/mL mAb solution, leading to a mAb concentration of 25 mg/mL and propylene glycol concentrations of 20 to 50 % in the sample. MAb stability was assessed via second derivative FTIR and UV spectroscopy and HP-SEC.

After the addition of the propylene glycol/water mixtures to the mAb solution, all samples remained clear without evidence of visible particle formation. No alterantions in the second derivative FTIR and UV spectra were identified in comparison to the native mAb spectrum (figure 4-3 A and B). HP-SEC analysis did not show additional aggregates or fragments.

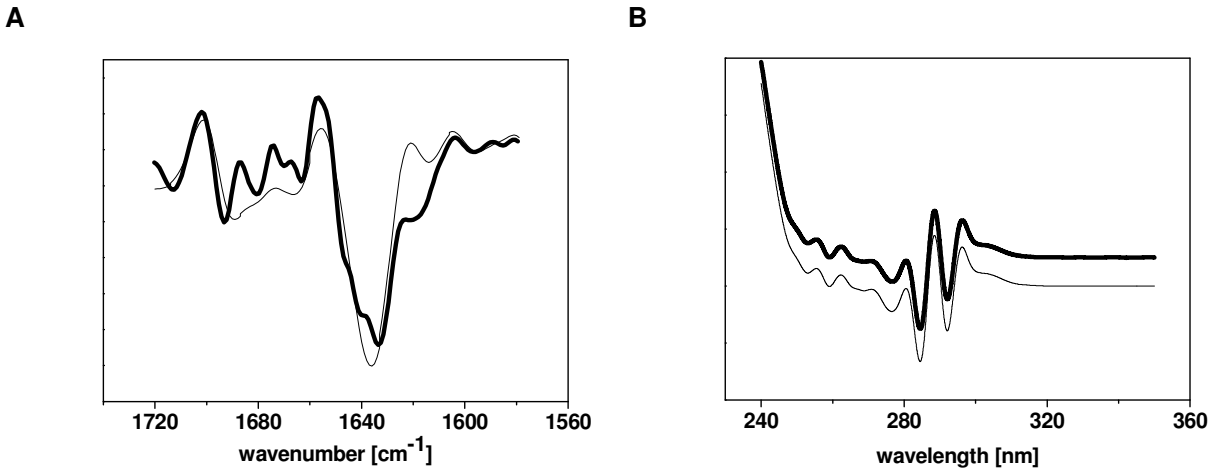

Figure 4-2 Second derivative FTIR (A) and UV spectra (B, concentration normalized, artificial offset for clarity) of mAb suspension in propylene glycol at 50 mg/g mixed with PBS in a 1:2 ratio (w/w) (thick line) compared to native mAb solution (thin line).

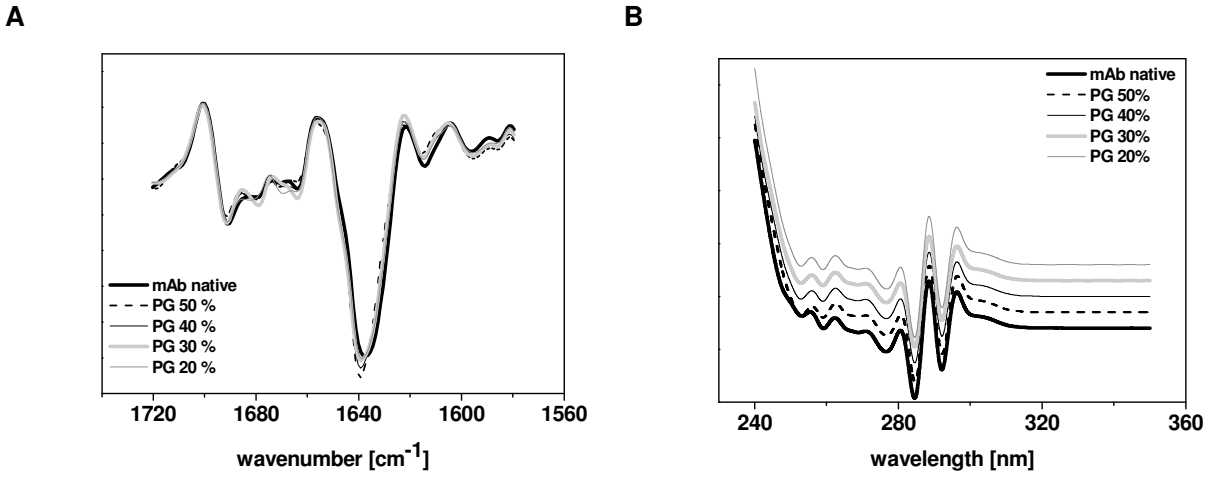

Figure 4-3 Second derivative FTIR (A) and UV spectra (B, artificial offset for clarity) of mAb in different propylene glycol (PG)/water mixtures in comparison to the spectrum of the native mAb solution.

Thus propylene glycol up to 50 % does not result in mAb instability. In contrast, during dissolution of the sd mAb particles suspended in propylene glycol or Phosal®50PG, the mAb initially faces high propylene glycol concentrations which lead to mAb aggregation.

3.1.1.2 Screening of mAb-compatible organic solvents for PL

As a consequence of the destabilizing effect of propylene glycol and thus Phosal®50PG on mAb, the non-aqueous PL solution for preparation of the PL-mAb suspension had to be modified. Therefore, different organic solvents were tested with respect to mAb

conformational stability and suitability as solvent for the PL component. Based on Strickley [99], who reviewed organic solvents commonly used for parenteral formulations, PEG 300, DMSO, and NMP were selected. Spray-dried mAb was dispersed in the solvents at 50 mg/mg and subsequently admixed with PBS for redissolution.

After mixing the suspensions with PBS in a 1:2 (w/w) ratio only PEG 300 rendered a clear solution, whereas the use of DMSO and NMP induced strong mAb precipitation. FTIR and UV spectroscopy confirmed a high compatibility of mAb with PEG 300 as no changes in tertiary and secondary protein structure were detected (figure 4-4). Furthermore, Phospholipon®90G, the PL component of Phosal®50PG, showed a maximal solubility of 60 % (w/w) in PEG 300. Hence, this solution was used for further experiments.

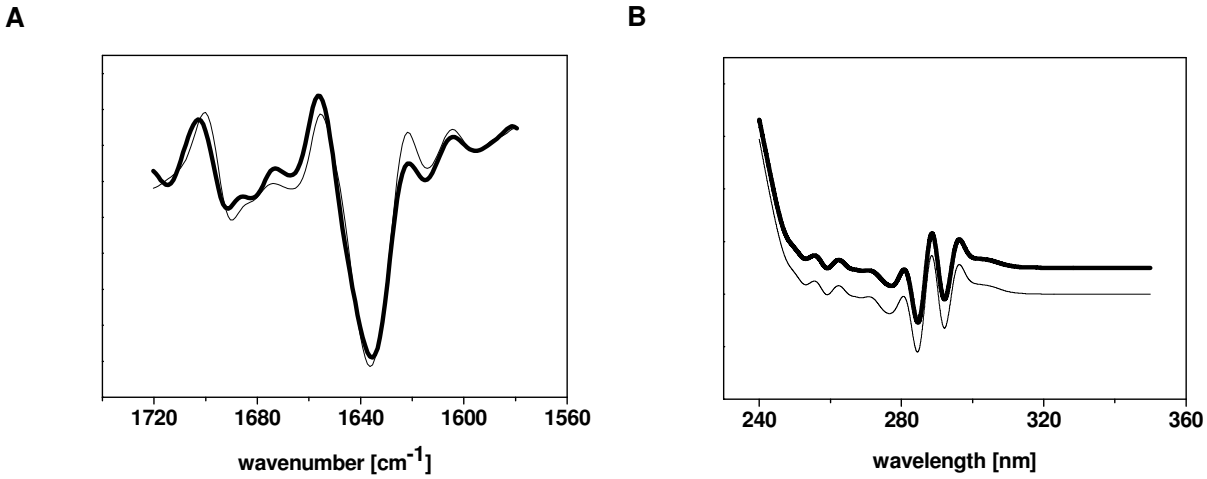

Figure 4-4 Second derivative FTIR (A) and UV spectra (B, artificial offset for clarity) of mAb suspension in PEG 300 mixed with PBS (thick line) compared to the spectrum of native mAb solution (thin line).

3.1.1.3 MAb stability in Phospholipon®90G-PEG 300 formulation

The stability of sd mAb suspended at a concentration of 50 mg/g in the 60 % Phospholipon®90G / 40 % PEG 300 solution was studied after injection into PBS in a 1:2 (w/w) ratio and vesicle formation. Similar to the placebo formulation it was possible to separate the lipidic from the aqueous phase by centrifugation for 1 hr at 186,000 x g. No changes in tertiary and secondary structure of the protein in the aqueous phase were identified by second derivative FTIR and UV spectroscopy (figure 4-5). HP-SEC analysis revealed a monomer recovery of 99.2 ± 0.04 %. Based on these results, it was concluded that the Phospholipon®90G-PEG 300 solution can be used for preparation of the PL-mAb suspension.

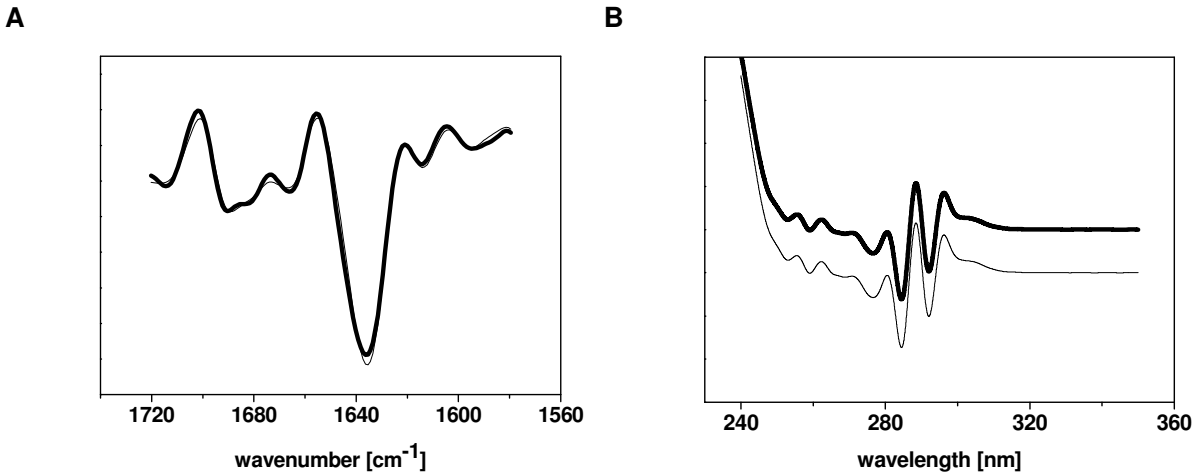

Figure 4-5 Second derivative FTIR (A) and UV spectra (B, artificial offset for clarity) of sd mAb suspended in the 60 % Phospholipon®90G / 40 % PEG 300 solution after injection into PBS for vesicle formation, mAb dissolution and centrifugation for 1 hr at 186,000 x g (thick line). Comparison with the spectrum of native mAb solution (thin line).

3.1.2 Cryo-TEM analysis of PL-mAb suspension after vesicle formation in PBS

Cryo-TEM analysis of the vesicular structures formed after injection of the PL-mAb formulation (sd mAb suspended at 50 mg/g in a solution of 60 % Phospholipon®90G in PEG 300) into PBS in a 1:2 (w/w) ratio and carefully manual shaking revealed a broad vesicle size distribution ranging from ~100 to 1000 nm with presence of multilamellar (MLVs), bilamellar (BLVs) and unilamellar vesicles (ULVs) of round or oval shape (figure 4-6).

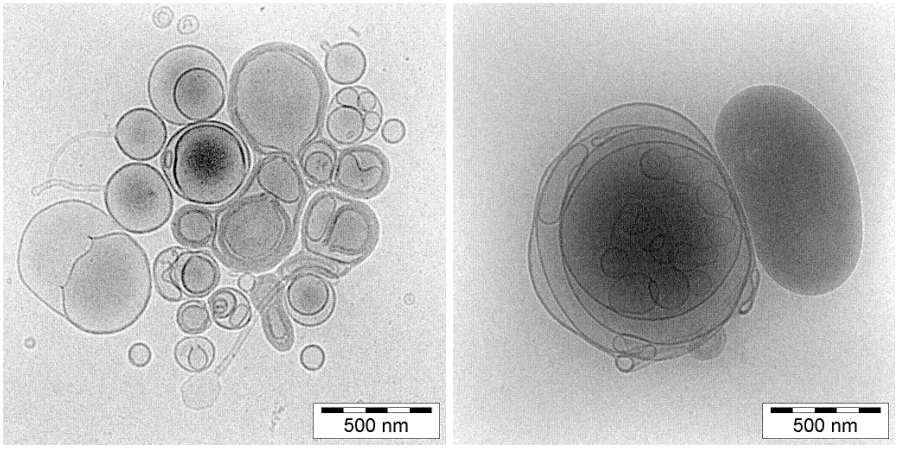

Figure 4-6 Cryo-TEM images of PL-mAb suspension composed of sd mAb (50 mg/g) in a 60 % Phospholipon 90G / 40 % PEG 300 solution after vesicle formation in PBS. For microscopy analysis, vesicular samples were further diluted in a 1:25 ratio.

Brandl *et al.* also demonstrated that semi-solid PL dispersions which were manually shaken upon dilution yielded both large MLVs and small ULVs [191]. With respect to IA retention, the formation of large MLVs is of advantage, since clearance from the synovial cavity is known to be reduced for large vesicles. In a study with healthy rabbits Bonanomi *et al.* showed that increasing the vesicle diameter from 160 nm to 750 nm led to a prolongation of IA vesicle retention by a factor of 2.6 [35]. Besides the increase in IA retention, the amount of encapsulated drug is described to be elevated with increasing vesicle diameter [191].

3.1.3 Determination of the mAb EE after vesicle formation of the PL-mAb suspension

For determination of the EE, the PL-mAb suspension composed of 50 mg/g sd mAb suspended in a solution of 60 % Phospholipon®90G in PEG 300 was injected into PBS in a 1:2 (w/w) ratio in order to allow mAb dissolution and vesicle formation. No significant encapsulation was detected as at the end of the washing procedure mAb was eluted with a recovery of 102.5 ± 7.3 % (figure 4-7). This result was underlined by fluorescence measurements after the addition of OG to the purified vesicles rendering an EE of 2.5 ± 0.5 %.

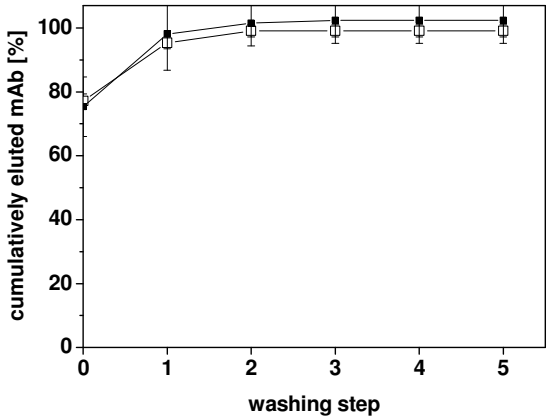

Figure 4-7 Elution profile of mAb after injection of the PL-mAb suspension (50 mg/g sd mAb in a solution of 60 % Phospholipon®90G in PEG 300) into PBS in a 1:2 ratio for vesicle formation and further dilution to a mAb concentration of 1 mg/mL (filled square) in comparison to empty vesicles with spiked, extravesicular mAb at same concentration (opened square).

Marrink *et al.* simulated the association of dipalmitoylphosphatidylcholine into vesicles [192]. They reported that vesicle formation takes place within nanoseconds with formation of intermediate structures such as bicelles and cup-like vesicles. In contrast, dissolution of the sd mAb particles in water was determined to occur within 3.2 ± 0.1 min. Hence, the low

observed EE can be explained by the time differences between vesicle formation and dissolution of sd particles. Since non-encapsulated drug is rapidly cleared from the synovial space, a high EE is mandatory for achieving prolonged drug retention. Thus, the use of mAb suspended in a PL concentrate was not further pursued.

3.2 Vesicular PL-mAb formulation

The application of preformed mAb containing vesicles using a highly-concentrated mAb solution presents an attractive alternative. The development and characterization of such a formulation was the focus of the following part of this work.

3.2.1 MAb stability in vesicular PL-mAb formulation

As shown in preliminary experiments (section 3.1.1.1), propylene glycol up to 50 % has no destabilizing effect on mAb. In the following section, the suitability of Phosal®50PG (phosphatidylcholine 52.3 %, lysophosphatidylcholine 0.9 %, dissolved in propylene glycol) for the preparation of a vesicular PL-mAb formulation using a highly-concentrated mAb solution was investigated. Therefore, Phosal®50PG was admixed with a 70 mg/mL mAb solution and emulsified using a dual-syringe system leading to a vesicular PL-mAb formulation with a mAb content of 50 mg/g. MAb extraction from the formulation was performed both via centrifugation for 1 hr at 186,000 x g as well as by the addition of an OG solution for solubilization of the lipid matrix. Similar to the placebo sample, phase separation was achieved for the PL-mAb formulation by centrifugation. The addition of OG led to a clear micellar solution without evidence of visible particle formation or signs of turbidity. The mAb-containing aqueous phase obtained by centrifugation was analyzed by second derivative FTIR and UV spectroscopy, HP-SEC and determination of the mAb bioactivity.

Second derivative FTIR and UV spectroscopy did not show structural changes compared to the native mAb (figure 4-8). HP-SEC analysis revealed that the monomer content was preserved (99.7 ± 0.03 %) and the extracted mAb did not show a change in bioactivity (104 ± 17.1 % vs. 112 % mAb standard). The high mAb compatibility of Phosal®50PG can be explained by the low total propylene glycol concentration of 11.8 % in the sample after addition of the mAb solution, as shown in section 3.1.1.1. Additionally, it was concluded that the presence of vesicular interfaces, formed by the phospholipid component, does not lead to any instability of the surface-active protein molecules.

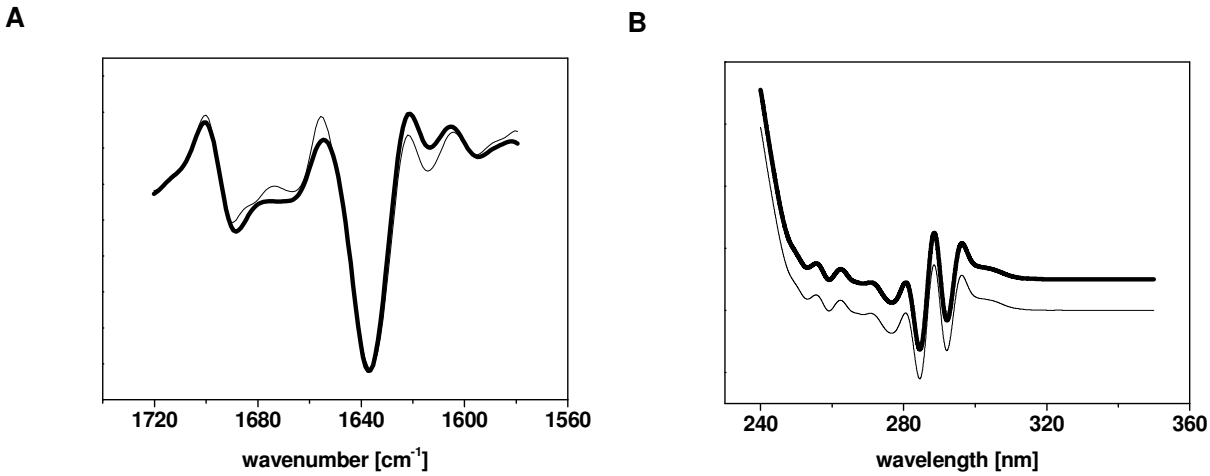

Figure 4-8 Second derivative FTIR (A) and UV spectra (B, artificial offset for clarity) of mAb after extraction from the vesicular PL-mAb formulation (Phosal®50PG and mAb solution (70 mg/mL) emulsified using a dual-syringe system leading to a mAb concentration of 50 mg/g) by centrifugation for 1 hr at 186,000 x g (thick line) compared to the spectrum of native mAb solution (thin line).

3.2.2 Characterization of vesicular PL-mAb formulation

3.2.2.1 Rheometry and injectability

Rheometry of the vesicular PL-mAb formulation (Phosal®50PG and mAb solution (70 mg/mL) emulsified using a dual-syringe system leading to a mAb concentration of 50 mg/g) did not reveal any significant differences between placebo and mAb-containing vesicular PL formulation (0.48 ± 0.02 Pa·s (active) vs. 0.39 ± 0.03 Pa·s (placebo) at 10 s^{-1}) (figure 4-9), indicating that the viscosity is not affected by the addition of mAb or any PL-mAb interactions. Both formulations showed a pronounced shear thinning behavior and should enable easy injectability.

Determination of the maximal injection force revealed that the vesicular PL-mAb formulation can in fact easily be handled. Low maximal injection forces were required (3.2 ± 1.2 N) that did not differ significantly from injection force values determined for the placebo formulation. Hence it was concluded that the presence of mAb had no impact on injectability.

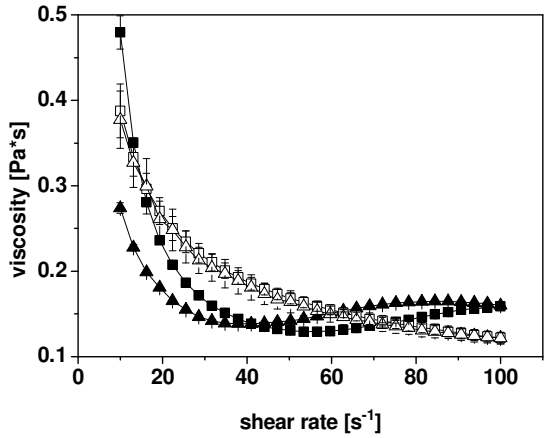

Figure 4-9 Viscosity of vesicular PL-mAb formulation (Phosal®50PG and mAb solution (70 mg/mL) emulsified using a dual-syringe system leading to a mAb concentration of 50 mg/g, filled symbol) and vesicular PL-placebo formulation (opened symbol) with increasing (square) and decreasing (triangle) shear rate.

3.2.2.2 Cryo-TEM and DLS analysis

Cryo-TEM analysis of the vesicular PL-mAb formulation revealed a broad size distribution ranging from ~100 nm to 800 nm with the presence of MLVs, BLVs and ULVs (figure 4-10). These results are comparable to the vesicular structure resulting from PL-mAb suspensions (section 3.1.2).

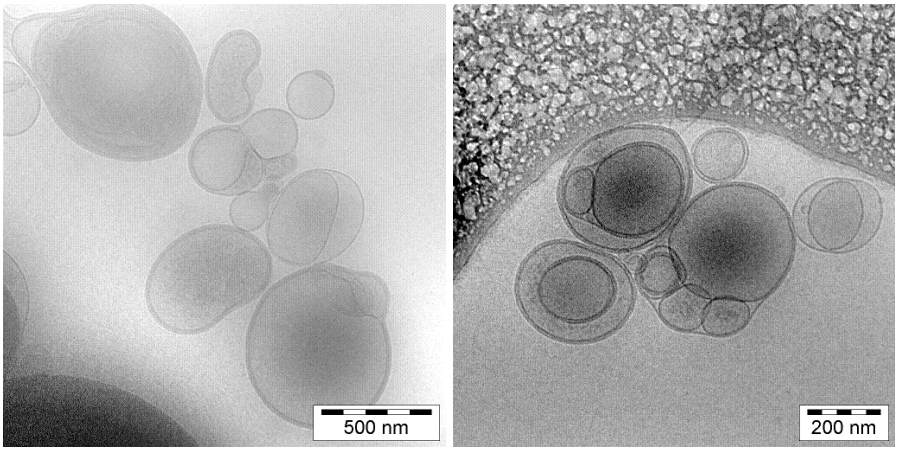

Figure 4-10 Cryo-TEM images of vesicular PL-mAb formulation (Phosal®50PG and mAb solution (70 mg/mL) emulsified using a dual-syringe system leading to a mAb concentration of 50 mg/g) after 1:20 dilution with PBS (lipid concentration 10 mM).

The broad vesicle size distribution was underpinned by a high polydispersity index of 0.4 ± 0.1 (placebo) and 0.5 ± 0.04 (active) in DLS measurements. Placebo and mAb containing vesicles showed comparable average vesicle size (411.2 ± 57.3 nm (placebo) and

520.4 ± 28.6 nm (active)). Hence, due to the presence of large vesicles it might be possible to encapsulate higher amounts of protein and a reduced clearance from the synovial cavity is expected compared to small sized vesicles.

3.2.2.3 Determination of mAb EE

Determination of the EE in the first elution fraction after Vivaspin® centrifugation, as described in section 2.2.15, revealed that 15.9 ± 1.0 % of the mAb were encapsulated. This result was confirmed by quantification of encapsulated mAb after vesicle purification and solubilization of the lipids rendering an EE of 14.2 ± 2.0 %.

Many publications describe the encapsulation of proteins or peptides in liposomes. Apart from the drug to be encapsulated, the method of preparing the liposomes determines the vesicle size and thereby the EE value. Colletier *et al.* encapsulated acetylcholinesterase in 200 nm sized liposomes using the film hydration method and achieved an EE of less than 10 %. With increasing number of additional freeze-thaw cycles, the EE was elevated to ~25 % under preservation of the enzyme activity [193]. Zhao *et al.* incorporated recombinant human growth hormone into preformed placebo phosphatidylcholine/cholesterol liposomes using a freeze-thaw technique. Depending on the number of freeze-thaw cycles and the incubation time after each freeze-thaw cycle, EE values ranging from 40-80 % were achieved. Liposomes had a mean size of 1.7-2.5 µm. Even though this preparation technique was considered as mild, no information concerning the protein stability after liposome preparation are provided and thus protein instabilities that might contribute to the determination of a high EE value should be taken into account [194]. Xu *et al.* analyzed the EE of the enzyme superoxide dismutase in ULVs with a size between 150 and 180 nm. Depending on the number of applied freeze-thaw cycles, an EE between 34 % and 50 % was achieved while maintaining of the enzyme activity [195]. Taking into consideration that the vesicular PL-mAb formulation was prepared under avoidance of harsh volatile organic solvents or critical freeze-thaw cylces by using a simple emulsification technique, an EE of 15 % can be regarded as an adequate value.

3.2.3 *In vivo* experiments with the vesicular PL-mAb formulation

In order to study the pharmacokinetic profile of the vesicular PL-mAb formulation (Phosal®50PG and mAb solution emulsified using a dual-syringe system) upon IA administration *in vivo*, an animal study was performed at the Abbott Bioresearch Center. This study was carried out with the murine mAb variant and the mAb concentration in the PL

formulation was reduced to 35.7 mg/g. Compared to the PL-free reference group (murine mAb solution), a slightly lower mAb absorption rate into the systemic circulation was seen upon application of the vesicular PL-mAb formulation (figure 4-11). This difference was most pronounced after 4 and 12 hrs. Thereafter, no or only slight differences between both formulations were observed. The increase in mAb serum concentration occurred concomitantly to a decrease in the SF mAb concentration. However, only at the 4 hr time point did a significant difference between PL-mAb formulation and mAb solution become apparent in SF.

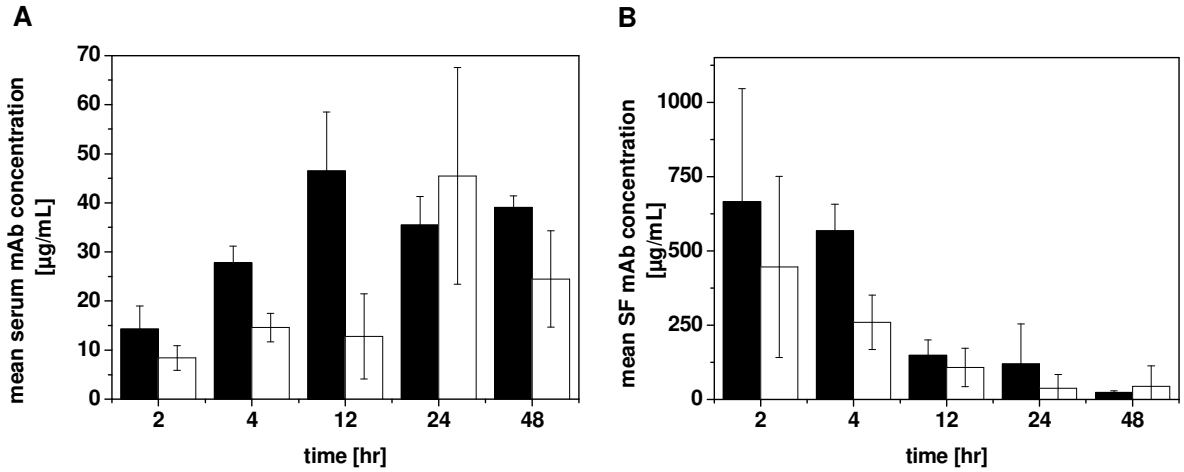

Figure 4-11 Mean serum mAb concentrations (A) and mean SF mAb concentrations (B) in Lewis rats after IA administration of the vesicular PL-mAb formulation (Phosal®50PG and murine mAb solution (50 mg/mL) emulsified using a dual-syringe system leading to a murine mAb concentration of 35.7 mg/g, white) or a murine mAb solution (35.7 mg/mL, black).

Various studies can be found in literature demonstrating the prolonged residence time of drug-loaded PL vesicles within the joint cavity [38, 39, 41]. However, these studies were performed with drug-loaded vesicles after separation of non-encapsulated drug. This makes direct comparison with the results of the present study difficult, as the vesicular PL-mAb formulation tested contained both encapsulated and non-encapsulated drug. Obviously, retention of non-encapsulated mAb due to a potential steric entrapment within the PL matrix was not achieved. One reason for the observed low drug retention within the joint cavity could be the EE value of 15 % which might be too low for detection of a retardation effect in comparison to the PL-free mAb solution, as non-encapsulated mAb is rapidly cleared from the synovial cavity. After the observation period of 48 hrs, the effect of the vesicularly encapsulated mAb could not become evident. In order to increase the percentage of drug retained at the site of application, an increase in EE and/or separation of non-encapsulated

mAb would be beneficial. Furthermore, insufficient SF stability of mAb-loaded vesicles could be another reason for the low synovial retention. In this case, mAb release from the vesicles would be facilitated causing rapid clearance from the joint cavity. Alternatively, vesicular binding to e.g. the joint cartilage or migration into the surrounding tissue under preservation of the vesicular structure could also be hypothesized. This would initially lead to a lack of mAb recovery in both serum and SF. Therefore, knowledge about the fate of the mAb-loaded vesicles presents an important aspect.

3.2.4 Approaches to increase the EE of the vesicular PL-mAb formulation

A major drawback of vesicular PL-based delivery systems is the limited EE [191]. The various attempts towards increasing the EE can be classified into two overall groups: formulation- and preparation-related approaches [195]. Formulation-related approaches comprise the increase of the lipid content [191, 195], the addition of cholesterol [168, 195] and the change of the lipid composition [195]. The increase of the lipid content is reported to improve the EE of drugs due to the enlargement of the membrane area, leading to an augmentation of the vesicle number per unit volume. Thus, the encapsulation volume and amount of encapsulated drug is enhanced [191]. Xu *et al.* found out that the EE of the enzyme superoxide dismutase changed from 26.5 % to 51.9 % when the lipid content was raised by a factor of three [195]. The addition of cholesterol is known to increase the packing density of lipid vesicles causing a reduction of the membrane permeability [168, 169]. Cagdas *et al.* demonstrated that the hydrophilic protein cytochrome C could only be encapsulated when cholesterol was present in the membrane [168]. The change of the lipid composition, for instance by the addition of anionic lipids might lead to an increase of the EE of positively charged drugs induced by electrostatic interactions. Preparation-related approaches include the application of a freezing step after vesicle formation followed by thawing [195] as well as the use of homogenization methods such as ultra-turrax® treatment [196] or DAC [177]. The positive effect of vesicle freezing and thawing can be mainly explained by the reversible physical disruption of the vesicle membrane due to ice crystal formation, and the presence of an osmotic gradient between vesicle exterior and interior, leading to augmentation of intravesicular drug concentration. The required number of freeze-thaw cycles to reach a concentration equilibrium mainly depends on the lamellarity of the vesicle and on the diffusion coefficient of the drug to be encapsulated [195]. Laloy *et al.* introduced a simple liposome preparation method where dispersions of lipids in aqueous bovine hemoglobin solution were emulsified by means of an ultra-turrax®. The high shear

forces during mixing induce the reordering of the vesicle membrane. In this study, liposomes with an EE of 24 % were generated. However, no information concerning the protein stability were provided [196]. Liposome preparation using a DAC was reported to yield small sized liposomes with high EE values due to the efficient homogenization based on oppositely vectored rotating movements. Massing *et al.* employed this method to prepare calcein containing vesicular phosphospholipid gels showing EE values up to 56 % upon dilution [177]. The suitability of the aforementioned approaches in generating high mAb entrapment was subsequently investigated and is described in the following section.

3.2.4.1 Increase of lipid content

In a first effort to improve the EE, formulations with lipid contents ranging from 152 mg/g to 355 mg/g were prepared with the dual-syringe system. To keep the total mAb concentration in the formulation at a constant 50 mg/g, the lipid content was increased by using mAb solutions at concentrations ranging from 70 mg/mL (PL content 152 mg/g) to 150 mg/mL (PL content 355 mg/g) (table 4-3). A further increase of the lipid content was not possible as the viscosity of the formulation drastically increased and homogeneous mixing could not be achieved. By changing the PL content from 152 mg/g to 236 mg/g, the EE was raised by a factor of 2 from 15.9 ± 1.0 % to 31.5 ± 4.4 % (figure 4-12 A). A further increase of the lipid content did not further augment the EE. Vesicle size and size distribution decreased with increasing PL content from 520 ± 28 nm (PdI 0.5 ± 0.02) at 152 mg/g to 210 ± 6 nm (PdI 0.2 ± 0.02) at 355 mg/g (figure 4-12 B).

Table 4-3 Formulation compositions used for improvement of the EE by increasing the lipid content.

Mixing ratio Phosal®50PG:mAb solution (w/w)	Concentration mAb solution [mg/mL]	Resulting PL content [mg/g]
1:2.5	70	152
1:1.25	90	236
1:0.63	130	327
1:0.5	150	355

The limited increase of the EE with plateau formation was also reported by Xu *et al.* [195]. Similar observations were made by Shew *et al.* who investigated the EE of both alkaline phosphatase and hemoglobin at various lipid contents. They explained the limited increase of the EE by presuming that with raising lipid content mainly MLVs instead of ULVs are formed

which leads to plateau formation with respect to the captured volume [197]. The DLS measurements (figure 4-12 B) revealed that with increasing lipid content, vesicle size and size distribution were reduced. However, from these data it is not possible to draw conclusions concerning lamellarity of the vesicles. Since with increasing lipid content the number of vesicles is supposed to be raised, a direct correlation between results of EE determination and DLS measurements cannot be found. The decline in vesicle size with increasing lipid content can be explained by the viscosity increase of the formulation leading to vesicle deformation and smaller sizes during formulation preparation. With respect to IA administration it should be noticed that a high vesicle size is preferred as clearance from the synovial space is reportedly thereby reduced. Therefore, for several reasons, the use of PL contents above 236 mg/g offers no advantage. Due to the possibility to raise the EE by the factor of 2 when increasing the lipid content from 152 mg/g to 236 mg/g, this approach is highly beneficial with regards to the reduction of the free drug amount.

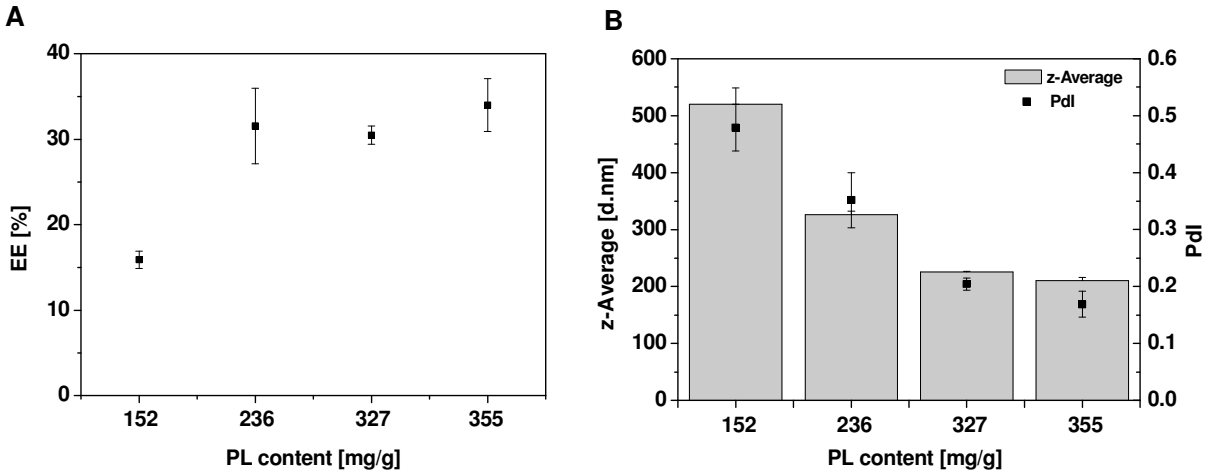

Figure 4-12 EE (A) and DLS results (B) of PL-mAb formulations composed of Phosal®50PG and mAb solutions at concentrations ranging from 70 mg/mL to 150 mg/mL, prepared with the dual-syringe system, leading to PL contents ranging from 152 mg/g to 355 mg/g and a mAb content of 50 mg/g.

3.2.4.2 Addition of cholesterol

In a second approach, cholesterol was dissolved in Phosal®50PG at 40 °C at molar cholesterol:PL concentrations of 1:9, 2:8 and 2.5:7.5 (corresponding cholesterol concentration in Phosal®50PG: 3 %, 6.5 % and 8.4 %) prior to formulation preparation. Higher amounts of cholesterol could not be added as solubility was exceeded. All formulations were prepared with a PL content of 236 mg/g. Therefore, the mAb solution at a concentration of 90 mg/mL was employed. The addition of small amounts of cholesterol (ratio

1:9) significantly elevated the EE from 31.5 ± 4.4 % to 43.4 ± 2.2 % (figure 4-13 A). A further increase of the cholesterol content (ratio 2.5:7.5) induced a reduction of the EE to 23.4 ± 1.1 %. The vesicles were slightly smaller compared to a cholesterol-free formulation with the same lipid content (figure 4-13 B) and the size distribution was not affected by addition of cholesterol.

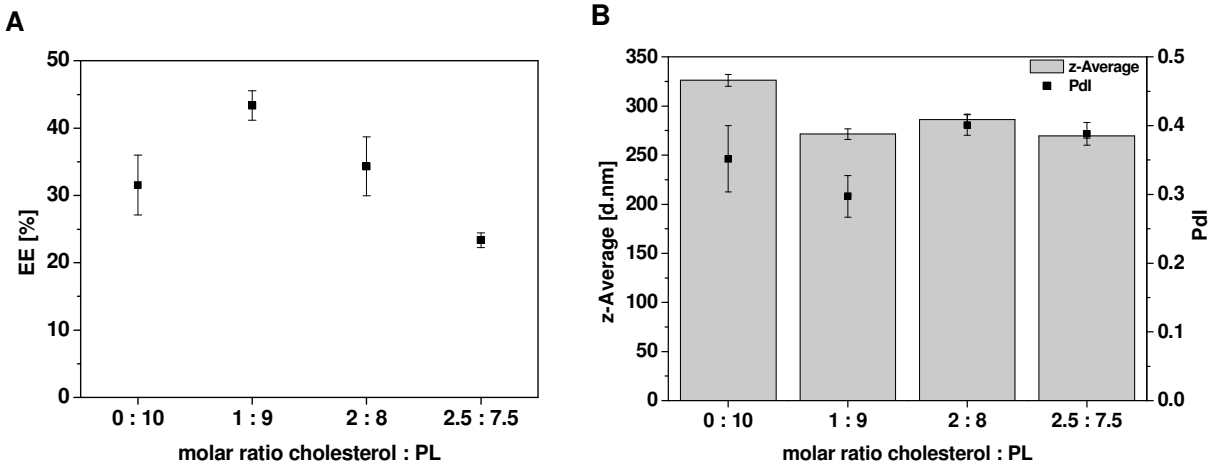

Figure 4-13 EE (A) and DLS results (B) of PL-cholesterol-mAb formulations, composed of cholesterol dissolved in Phosal®50PG, emulsified with mAb solution (90 mg/mL) by using a dual-syringe system, leading to a mAb concentration of 50 mg/g and a PL content of 236 mg/g.

In general, cholesterol is incorporated into the PL bilayer via interactions between the 3β-OH group and the hydrophilic part of the PL molecules as well as between the sterol backbone and the PL fatty acid chains [198]. Cholesterol incorporation into the bilayer leads to enhanced liposomal membrane rigidity, higher physical stability of the vesicles and reduced membrane permeability due to a higher packing density of the membrane forming molecules [168, 199]. The observed EE increase upon addition of small amounts of cholesterol is in good accordance with published research [200]. The concentration dependent increase and decrease of the EE was also seen by Shimizu *et al.* [201]. They found that the addition of small amounts of cholesterol led to a noticeable increase of the EE of an antibody into egg lecithin/cholesterol liposomes, but a further increase of cholesterol reduced the efficiency drastically. However, while Shimizu *et al.* observed a reduction of EE at a molar cholesterol:lipid ratio of 1:2, these changes were already observed at a cholesterol:PL ratio of 2:8 in the present study. Ramana *et al.* demonstrated that the EE of nevirapine increased significantly at a cholesterol:PL ratio of 1:9. A further increase in cholesterol led to a slight reduction of the EE [202]. Similar results were also found by Deniz *et al.* who reported that the entrapment of the hydrophobic drug celecoxib in liposomes decreased with increasing

cholesterol content. This was explained by the competition between the drug molecule and cholesterol for incorporation in the PL membrane [203], a phenomenon which should not play a role for mAb loading of vesicles. On the other hand, as the hydrophobicity of the bilayer is expected to be elevated at increased cholesterol concentrations, it is likely that potential protein-PL interactions are reduced, leading to the observed decline in EE. Taking into account that the increase of the EE with the addition of small amounts of cholesterol was accompanied by a decrease of the vesicle size, the addition of cholesterol is not expected to provide a benefit compared to the cholesterol-free formulation with respect to prolongation of the IA residence time of the vesicles.

3.2.4.3 Addition of negatively-charged lipids

Another potential approach to increase the EE is the addition of negatively-charged lipids. Such lipids are commonly used for the preparation of liposomes as they can result in higher zetapotential, thus reduce aggregation and fusion tendencies and can provide better liposome stability during storage. Moreover, the uptake of negatively-charged liposomes by mononuclear phagocytes is reported to be enhanced [204], which is an advantage when passive targeting is envisaged. Commonly used lipids are phosphatidylglycerol, phosphatidic acid and phosphatidylserin that are negatively charged at physiological pH. The addition of negatively-charged lipids moreover offers the possibility to increase the EE of positively charged drugs via electrostatic interactions. As the present mAb has a positive net charge at physiological pH, a charge-induced increase of the EE could be hypothesized. Therefore, phosphatidylglycerol and phosphatic acid were intended to be dissolved in Phosal®50PG. However, as these lipids proved to be insoluble in the PL solution, even at elevated temperature, this approach was not further investigated.

3.2.4.4 Freeze-thaw treatment

The application of freeze-thaw cycles to vesicular drug-containing formulations is a common preparation step to achieve high drug encapsulation and can be explained by different theories. As demonstrated by Mayer *et al.*, reduced solute concentrations were found inside the vesicle core upon dispersion of egg phosphatidylcholine in aqueous buffer causing an osmotic gradient between vesicle exterior and interior. The application of repetitive freezing and thawing balance out the solute gradient leading to increased EE [205]. Another explanation is that during freezing, ice crystals form across the liposome and this water removal from the hydrated bilayer via phase separation causes breakage of the membrane [206]. On thawing, ice crystals are transformed into water channels that allow drug diffusion

along the concentration gradient from the surrounding medium into the vesicular core before the vesicles are reformed [195, 207]. Freezing is commonly performed by sample immersion into liquid nitrogen (ca. -200 °C) [207] until complete solidification is achieved. This freezing technique results in the formation of heterogeneous small ice crystals by directional solidification as a consequence of a low degree of supercooling and thus fast freezing rate [208]. The beneficial effect of this technique on the drug EE, however, might be accompanied by protein instabilities as repetitive freezing and thawing may induce protein denaturation induced by the formation of a large liquid-ice interface or the concentration increase upon ice formation [208, 209]. Several studies can be found in literature in which protein-loaded liposomes were subjected to repetitive freeze-thaw cycles for improvement of the EE under maintenance of protein stability. It was shown that e.g. the enzyme activity of superoxide dismutase encapsulated in lipid vesicles was preserved after two freeze-thaw cycles [195]. Encapsulation of rhG-CSF by application of 5 freeze-thaw cycles did not lead to changes in protein structure [69]. At first, to study the impact of repetitive freeze-thaw cycles on mAb stability, a 2 mg/mL mAb solution, containing sodium chloride (105.5 mM), monobasic sodium phosphate dihydrate (5.5 mM), dibasic sodium phosphate dihydrate (8.6 mM), sodium citrate (1.16 mM), citric acid monohydrate (6.19 mM) and mannitol (65.9 mM), was subjected to 2, 4, 6 and 8 freeze-thaw cycles by immersion into liquid nitrogen and subsequent thawing at 30 °C in a water bath. Samples were analyzed by HP-SEC and turbidity measurement at 350 nm.

The application of up to 6 freeze-thaw cycles had no impact on the HP-SEC monomer recovery. Additional aggregates (0.2 %) were detectable after 8 freeze-thaw cycles (figure 4-14 A). No increase in turbidity which could indicate formation of larger protein aggregates compared to the native mAb solution was identified (figure 4-14 B) and also visual appearance did not change.

In order to investigate the impact of repetitive freeze-thaw cycles on the mAb EE, the vesicular PL-mAb formulation at PL content of 236 mg/g (Phosal®50PG and mAb solution (90 mg/mL) emulsified by using a dual-syringe system, leading to a mAb concentration of 50 mg/g) was subjected to 3 and 5 freeze-thaw cycles. As illustrated in figure 4-15 A, the encapsulated amount of mAb was not increased by the freeze-thaw cycles. Furthermore, neither vesicle size nor vesicle size distribution was affected by the freeze-thaw treatment (figure 4-15 B).

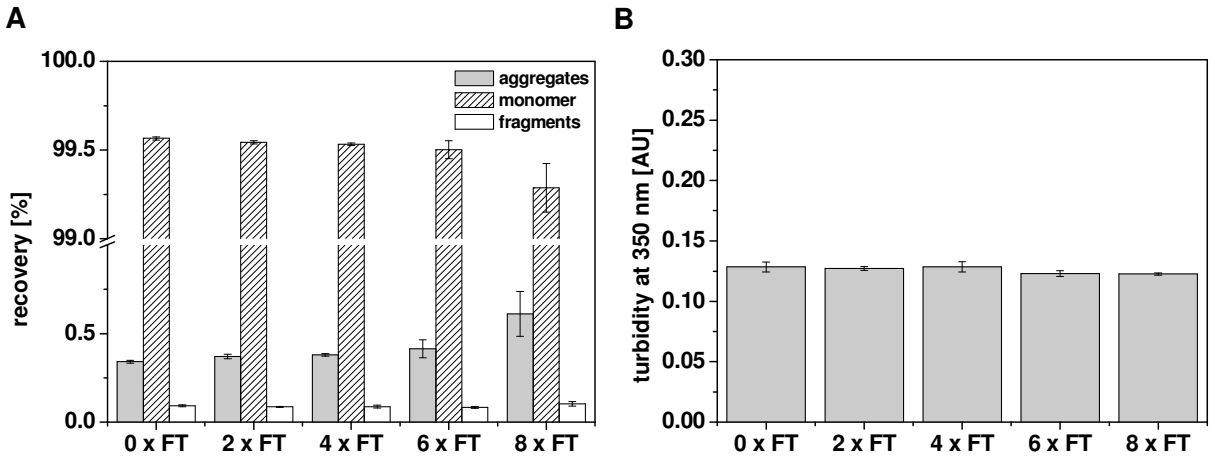

Figure 4-14 Impact of repetitive freeze-thaw (FT) cycles on HP-SEC recovery (A) and turbidity at 350 nm (B) of a 2 mg/mL mAb solution.

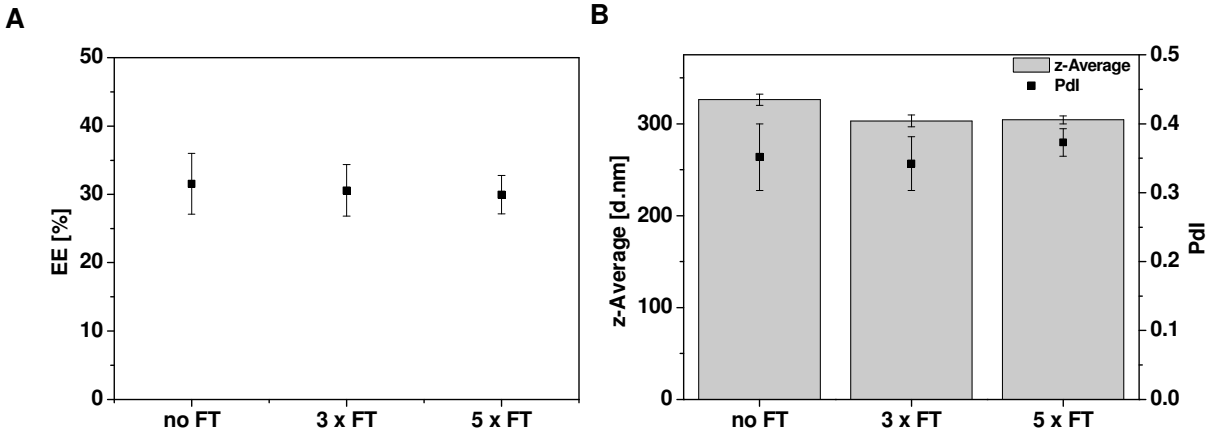

Figure 4-15 EE (A) and DLS results (B) of PL-mAb formulation (Phosal®50PG and mAb solution (90 mg/mL) emulsified by using a dual-syringe system, leading to a mAb concentration of 50 mg/g) after 0, 3 or 5 freeze-thaw (FT) cycles.

Ice crystal formation during freezing, which causes disruption of the PL bilayer, is described to be influenced by various factors such as cooling rate and type of excipients employed [210]. A fast cooling rate of >20 °C/min is reported to induce complete intra-liposomal ice formation leading to expansion of the intra-vesicular aqueous phase and thus to membrane disruption [207]. The presence of cryoprotectants such as trehalose or surcrose prevents the PL bilayer from ice crystal damage via water replacement and thus contributes to liposome stabilization during freezing [211]. In addition, these excipients build a vitrified matrix in which the liposomes are embedded on freezing [212]. The use of organic solvents such as ethylene glycol, propylene glycol and glycerol was reported to improve the liposomal retention of calcein upon freeze-drying and subsequent rehydration in the presence of cycloinulohexaose. This phenomenon was explained by the ability of the additives to interact

with the lipid molecules via hydrogen bonding. These interactions lead to membrane stabilization and maintenance of a certain distance of the vesicles which prevents fusion and aggregation [213]. The present vesicular PL-mAb formulation contains propylene glycol as PL solvent in Phosal®50PG. Based on the aforementioned study the presence of propylene glycol could be one reason for the missing increase of the EE following the repetitive freeze-thaw cycles. Mannitol, contained in the mAb solution used for formulation preparation, is a common bulking agent in freeze-drying due to its ability to form a crystalline matrix. However, depending on the applied cooling rate, amorphous mannitol can also be found. Cavatur *et al.* analyzed the morphology of mannitol in relation to the cooling rate via X-ray diffractometry. They were able to show that a rapid cooling rate inhibited mannitol crystallization whereas slow cooling rates led to crystalline matrices [214]. As the sample immersion into liquid nitrogen is leading to a rapid cooling rate [208], the initial formation of amorphous mannitol could be speculated that leads to membrane stabilization via water replacement and embedment of the vesicles into the vitrified matrix. However, the mannitol concentration in the sample was only 1 % and thus the impact of amorphous mannitol on the vesicle stabilization might be of minor importance. The presence of extravesicular mAb could also contribute to vesicle stabilization by embedment into the amorphous protein matrix formed upon freezing. As the concentration of free mAb in the sample was 3.5 %, the non-encapsulated mAb could be hypothesized as predominant reason for to the missing increase of the mAb EE. Based on these considerations, the application of freeze-thaw cycles for improvement of the EE has limited applicability for the present formulation. However, from the present results it can be also concluded that the vesicular PL-mAb formulation offers the possibility to freeze the formulation for storage or shipping purpose without loss of mAb EE or mAb stability.

3.2.4.5 Ultra-turrax® treatment

The impact of ultra-turrax® emulsification on the EE of mAb was studied with the vesicular PL-mAb formulation at a PL content of 236 mg/g, prepared by emulsification of Phosal®50PG with mAb solution (90 mg/mL) by means of a dual-syringe system. As it is known that shear stress may induce protein aggregation [215], the impact of different mixing times on mAb stability was assessed first. A 2 mg/mL mAb solution was subjected to ultra-turrax® homogenization for 15, 30 or 45 s at 8000 rpm and analyzed via HP-SEC and turbidity measurement at 350 nm.

Ultra-turrax® treatment of up to 45 s had no impact on HP-SEC monomer recovery but an increase in turbidity was observed (figure 4-16). On account of the unchanged HP-SEC data, the slight increase in turbidity could be ascribed to the presence of insoluble aggregates formed. However, the general impact of this additional preparation step on the mAb EE was studied by ultra-turrax® treatment of the PL-mAb formulation for 45 s. The EE of the PL-mAb formulation (30.7 ± 4.4 % ultra-turrax® vs. 31.5 ± 4.4 % untreated) as well as its vesicle size and size distribution (330.0 ± 14.3 nm, 0.4 ± 0.01 (ultra-turrax®) vs. 326.5 ± 6.1 nm, 0.4 ± 0.05 (untreated)) were unchanged. Based on these results it was concluded that the shear forces induced by the instrument were insufficient to induce opening and reformation of the vesicles which might contribute to an increase of EE. Moreover, it was demonstrated that the present formulation provides a high mechanical stability which is of advantage if samples are intended to be shipped.

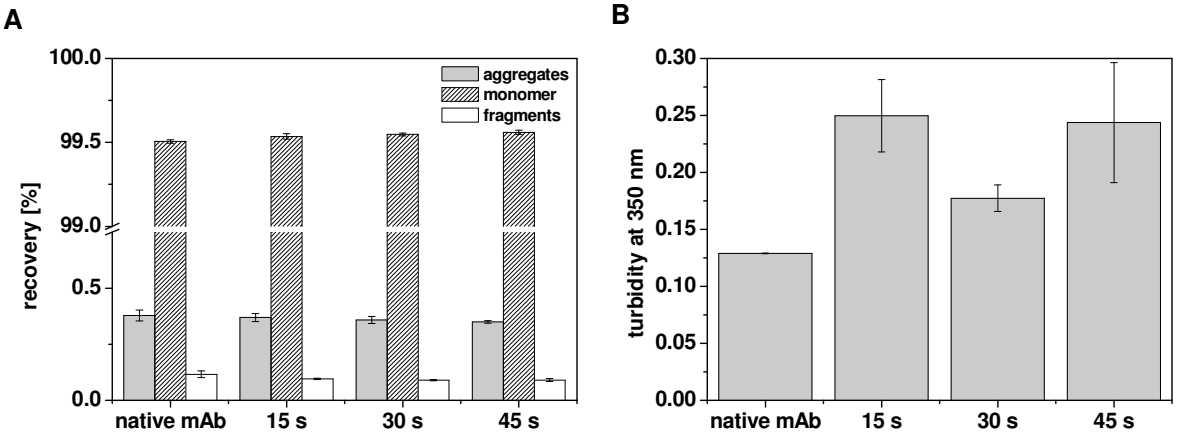

Figure 4-16 Impact of ultra-turrax® emulsification at 8000 rpm for 15, 30 and 45 s on HP-SEC recovery (A) and turbidity at 350 nm (B) of a 2 mg/mL mAb solution.

3.2.4.6 Formulation preparation using the dual asymmetric centrifuge

The DAC as alternative preparation method was evaluated with respect to increasing the EE of the PL-mAb formulation with lipid contents of 236 mg/g and 355 mg/g. Compared to the preparation by dual-syringe system, the use of the DAC for 30 min did not lead to a significant increase in EE (figure 4-17 A). Similar to previous results (section 3.2.4.1) an increase of the lipid content from 236 mg/g to 355 mg/g had no impact on the EE. The change in total centrifugation time induced an increase in EE from 38.7 ± 5.6 % (30 min) to 53.3 ± 5.4 % (60 min). The formation of small sized vesicles with narrow size distribution was observed in samples prepared via DAC (figure 4-17 B). At a higher lipid content, the polydispersity index was further reduced, which corroborates results from literature [177].

The results demonstrate that increased EE values are obtained by extended centrifugation time which can be explained by the enhanced homogenization of the formulation and thus increased exposure of the vesicles to shear forces. Since the prolonged centrifugation time had no impact on the vesicle size, it can be concluded that the elevated entrapment efficiency is induced by continuous reformation of the vesicles under maintenance of the size. Apparently, the shear forces in the DAC are much higher than upon mixing within the dual-syringe system as the vesicle size and size distribution of formulations prepared by syringe-mixing were significantly higher compared to the DAC method. At higher lipid content, size distribution was further reduced using the DAC.

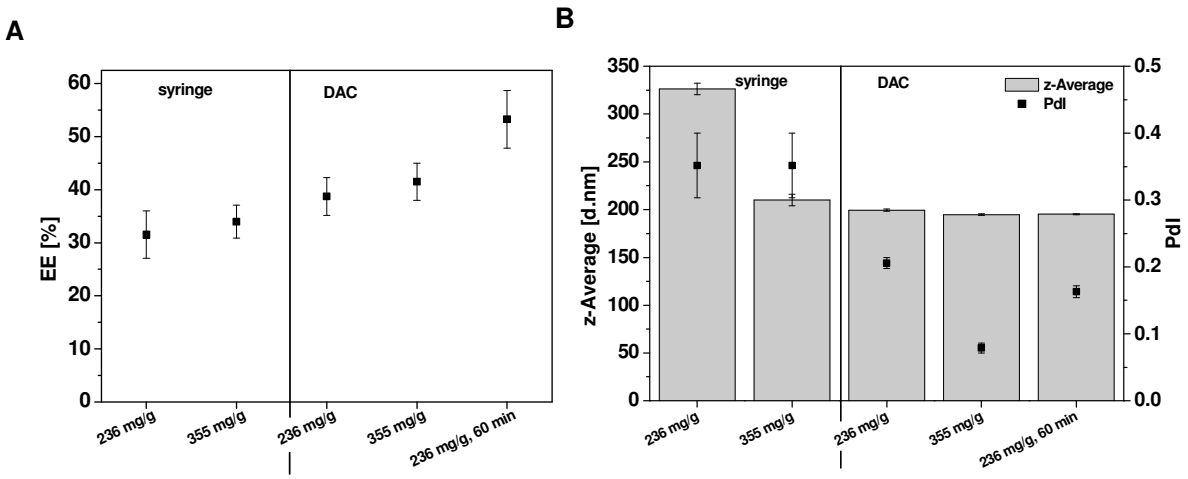

Figure 4-17 EE (A) and DLS results (B) of PL-mAb formulations at lipid contents of 236 or 355 mg/g (Phosal®50PG emulsified with mAb solution at 90 mg/mL or 150 mg/mL) after formulation preparation with the DAC in comparison to the dual-syringe system. If not stated otherwise, a total centrifugation time of 30 min was applied.

Above results showed that the EE of mAb can be increased by raising the lipid content, by application of freeze-thaw cycles and by use of homogenization methods such as ultra-turrax® and DAC. The overall increase achieved was only up to a maximum of approximately 30 %. In contrast to this, EE values of up to 40 % were achieved after the addition of small amounts of cholesterol to the formulation. The application of a DAC centrifugation time of 60 min led to the highest EE value of 53.3 ± 5.4 %. Most of these approaches resulted in vesicle sizes smaller than 300 µm. Bearing in mind that small vesicles are rapidly cleared from the synovial space, the increase in EE might not lead to prolonged drug retention at the site of application. Furthermore, even with an EE of 53 %, the percentage of free mAb is still high, which makes the assessment of pharmacokinetic differences to IA injected liposomal-free mAb difficult. Therefore, despite of the achievements in EE, the separation of non-

encapsulated mAb from mAb containing vesicles presents an attractive approach in order to study the pharmacokinetic profile of the present formulation *in vivo*.

3.2.5 Short time stability study of PL-mAb vesicles after separation of non-encapsulated mAb in PBS

Leakage of encapsulated drugs out of PL vesicles presents a frequently observed phenomenon. The extent of leakage is described to be dependent on the lamellarity of the vesicle, the molecular size of the entrapped molecule [191] and the membrane composition [216]. The physical stability of the mAb-containing vesicles was studied using a PL-mAb formulation with PL content of 236 mg/g prepared with the dual-syringe system. Non-encapsulated mAb was separated from the vesicles using Vivaspin®2 centrifugation tubes. The purified PL-mAb vesicles were stored for 7 d at 2-8 °C and subsequently again centrifuged for 40 min at 2739 x g and 20 °C in Vivaspin®2 centrifugation tubes. The elution fractions were fluorimetrically analyzed with regards to the released mAb. As reference the elution fractions of the last purification step prior to storage were employed. After storage for one week, the fluorescence intensity of the elution fractions was insignificantly higher than before storage (figure 4-18). Based on these results it was concluded that mAb is retained by the vesicle membrane and is not released under the given conditions. This is in good accordance with literature, where it was reported that the PL membrane permeability is very low when high MW drugs are encapsulated [169].

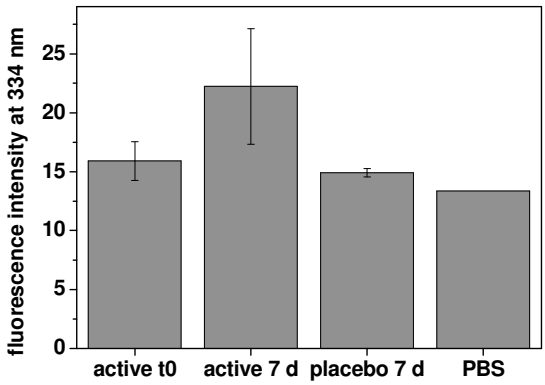

Figure 4-18 Intrinsic fluorescence intensity of elution fractions before and after storage of purified mAb containing PL vesicles in PBS (2-8 °C, 7 d) in comparison to placebo and PBS.

Additionally, the mAb stability in the purified vesicles was studied. Therefore, samples stored for 1 d, 7 d and 14 d at 2-8 °C were subjected to one freeze-thaw cycle in order to release encapsulated mAb. The application of detergents for release of encapsulated mAb was not

applied as the HP-SEC analysis of mAb in presence of lipid-containing micelles was intended to be avoided. Vesicles were separated from released mAb by centrifugation for 1 hr at 186,000 x g and 20 °C. The supernatant was subjected to HP-SEC analysis. The monomer recovery slightly decreased during the observation period from 98.7 ± 0.03 at day 1 to 97.1 ± 0.9 % at day 14 (figure 4-19) which might be ascribed to the exposure of the encapsulated mAb to the lipid membrane of the vesicles.

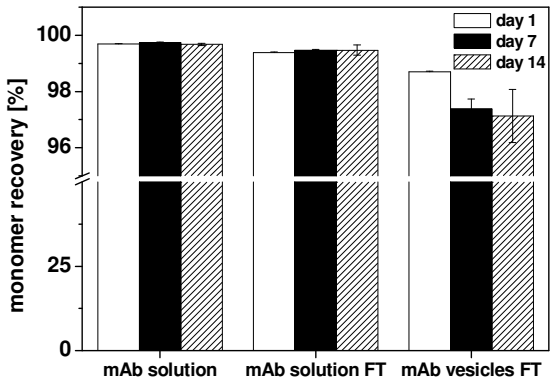

Figure 4-19 HP-SEC monomer recovery of mAb upon encapsulation into PL vesicles, vesicle separation from non-encapsulated mAb, storage at 2-8 °C and mAb release induced by one freeze-thaw (FT) cycle in comparison to a PL vesicle-free mAb solution with and without FT treatment.

3.2.6 Fluorescence microscopy of fluorescence-labeled PL-mAb vesicles

In order to visualize the encapsulation of mAb into the PL vesicles, both mAb and PL vesicles were labeled with a fluorescent dye and analyzed by using a fluorescence microscope. After labeling of mAb with AlexaFluor®488, HP-SEC analysis confirmed that the labeling process did not induce mAb aggregation (mAb standard 99.3 % vs. F-mAb 98.8 %). SPR measurements confirmed that the labeling procedure did not affect the binding affinity of mAb to its antigen as reflected by an unchanged dissociation constant K_D (mAb standard $7.7 \times 10^{-11} \pm 6.4 \times 10^{-12}$ mol/L vs. F-mAb $6.7 \times 10^{-11} \pm 4.8 \times 10^{-12}$ mol/L). For the PL-mAb formulation preparation at PL content of 236 mg/g a 1:10 F-mAb to non-labeled mAb mixture, up-concentrated to 90 mg/mL, was used. Fluorescence microscopy analysis was performed after dilution to a mAb concentration of 1 mg/mL. Observation under bright-field mode revealed the vesicles varying in size (figure 4-20 A). Due to the limited resolution of the microscope, only vesicles of the upper size range were detectable. Observation upon excitation at 480 nm for visualization of F-mAb showed bright shining spots of green color

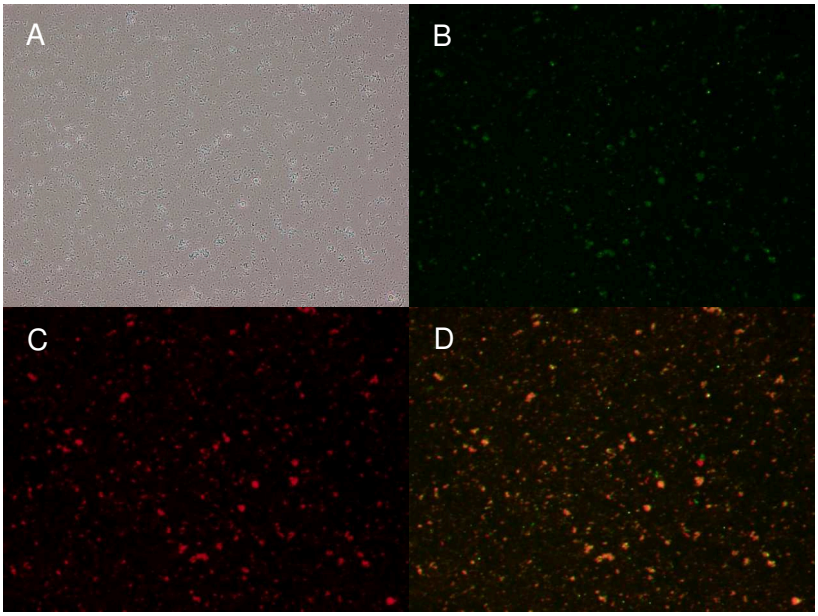

Figure 4-20 Fluorescence microscopy images of F-mAb-loaded PL vesicles, stained with nile red. (A) bright-field mode for visualization of PL vesicles (exposure time 1/70 s) (B) excitation at 480 nm for F-mAb visualization (exposure time 1.8 s), (C) excitation at 560 nm for visualization of PL vesicles (exposure time 1/13 s), (D) overlay of (B) and (C).

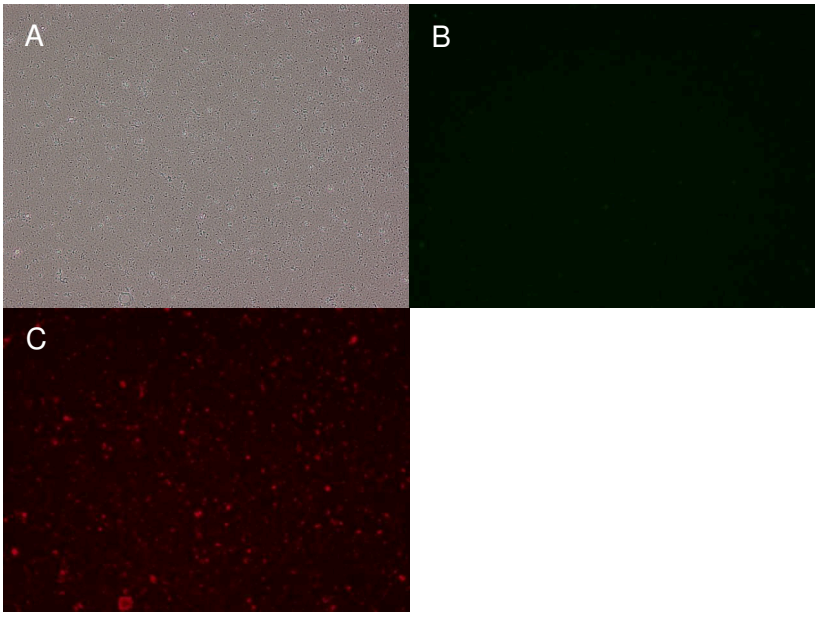

Figure 4-21 Fluorescence microscopy images of empty PL vesicles, stained with nile red and spiked F-mAb. (A) bright-field mode (exposure time 1/70 s), (B) excitation at 480 nm (exposure time 1.8 s), (C) excitation at 560 nm (exposure time 1/13 s).

(figure 4-20 B) indicating vesicularly entrapped protein. Extravesicular F-mAb was not detectable. On excitation at 560 nm, nile red-stained PL vesicles were identified by red

fluorescence (figure 4-20 C). Overlay of the images of green and red fluorescence observation mode proved that the F-mAb was associated with the PL vesicles (figure 4-20 D).

In order to investigate whether the green fluorescence is ascribed to F-mAb adsorption on the outer PL membrane or encapsulation in the inner PL vesicle core, empty vesicles were prepared, spiked with a F-mAb/mAb solution at 1 mg/mL and incubated for 1 day at 2-8 °C. Fluorescence microscopy revealed that only the nile red-stained PL vesicles were detectable. Observation in green fluorescence mode revealed a dark background (figure 4-21). Overlay of 4-21 B and C led to a dark image and is therefore not depicted. Hence, the green spots detected in figure 4-20 B are ascribed to F-mAb encapsulated in PL vesicles.

3.2.7 Short time stability study of PL-mAb vesicles in serum

Not only stability of the vesicles *ex vivo* is critical, but also increased permeability of drug-loaded PL vesicles in the presence of serum has been widely reported in literature. Allen *et al.* demonstrated that the *in vitro* efflux of calcein from small ULVs was raised with increasing serum concentrations present in the incubation medium [217]. Scherphof *et al.* postulated that the enhanced permeability of ^{125}I-labeled albumin from liposomes in the presence of plasma can be ascribed to a transfer of phosphatidylcholine to high-density lipoproteins which leads to disintegration of the vesicles [218]. Another study reported that the complement system plays an important role in the destabilization of liposomes [219]. Investigations of the impact of BSA on the stability of methotrexate-loaded liposomes revealed enhanced leakage with increasing BSA concentrations present in the surrounding medium [220]. Also upon incubation of drug-loaded liposomes in SF, obtained from patients suffering from rheumatoid arthritis, a remarkable release of entrapped ^{125}I-lactoferrin from PL vesicles was identified [38]. These studies demonstrate that vesicle stability in body fluids presents an important parameter for the prediction of the drug delivery upon *in vivo* application. For stability analysis of PL-mAb vesicles in body fluids, the PL-mAb formulation at a lipid content of 236 mg/g was prepared using a 1:10 F-mAb/mAb solution. After dilution of the formulation to a mAb concentration of 1 mg/mL, non-encapsulated F-mAb/mAb was separated from the F-mAb/mAb-loaded vesicles. Purified vesicles were incubated in fetal calf serum (FCS) and stored at 37 °C for 4 days.

Fluorescence microscopy images of F-mAb/mAb-loaded vesicles incubated in PBS showed no changes during the observation period. In contrast, incubation in FCS led to strong

agglomeration of the vesicles that did not change upon incubation for 4 days (figure 4-22). As the detected agglomerates showed strong fluorescence intensity, it was hypothesized that at least a majority of the mAb content was retained inside the vesicular structures. Analysis of

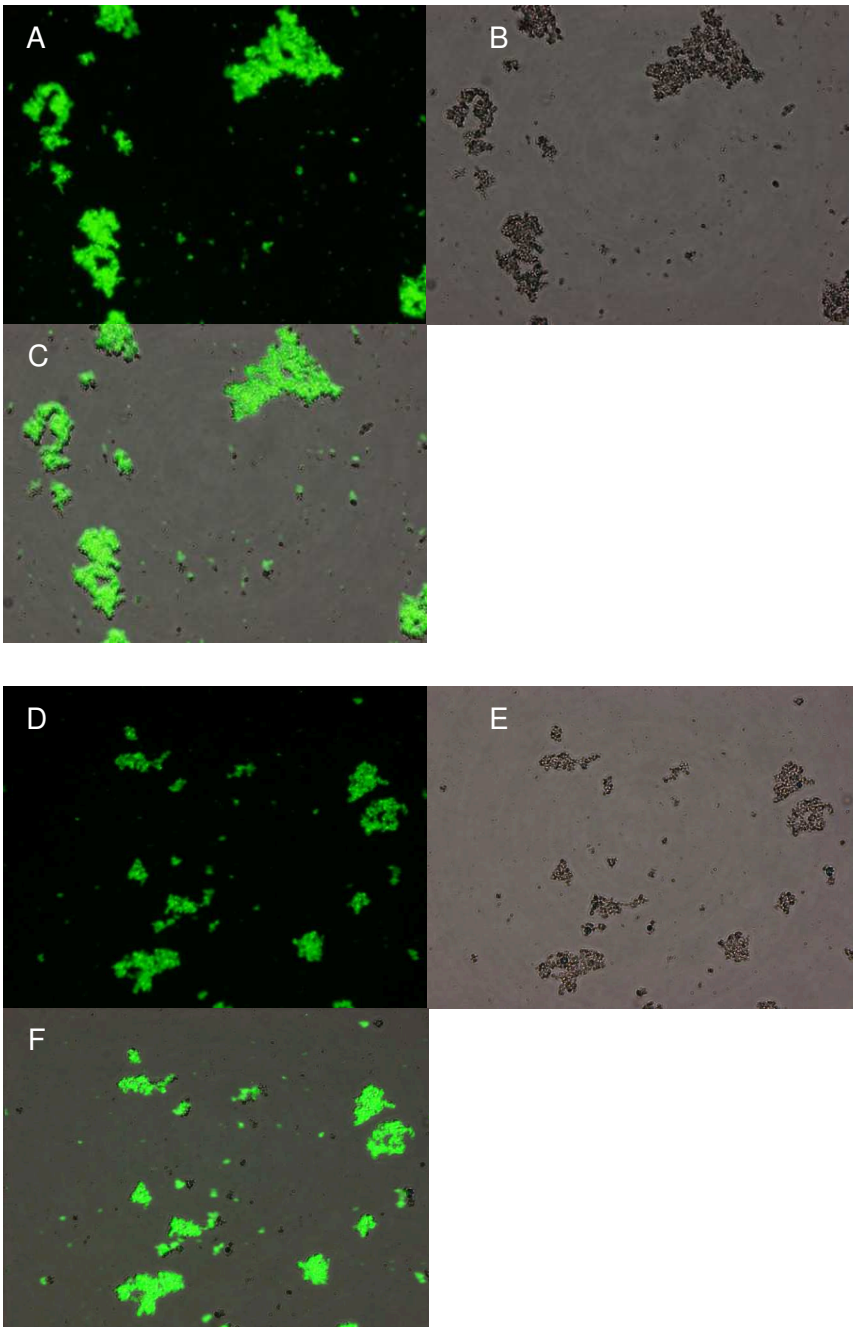

Figure 4-22 Fluorescence microscopy images of PL-F-mAb/mAb-vesicles directly after incubation in FCS (A-C) and after 4 days stored at 37 °C in FCS (D-F). A,D: excitation at 480 nm; B,E: bright-field mode; C,F: overlay of fluorescence image and bright-field image.

the released F-mAb amount at day 0 and day 4 on incubation in PBS underlined the results outlined in section 3.2.5 that the mAb-loaded vesicles show a high stability over time, even at 37 °C (figure 4-23). Vesicles incubated in FCS were initially stable but released 18.9 ± 2.6 % of the content during 4 days of incubation at 37 °C.

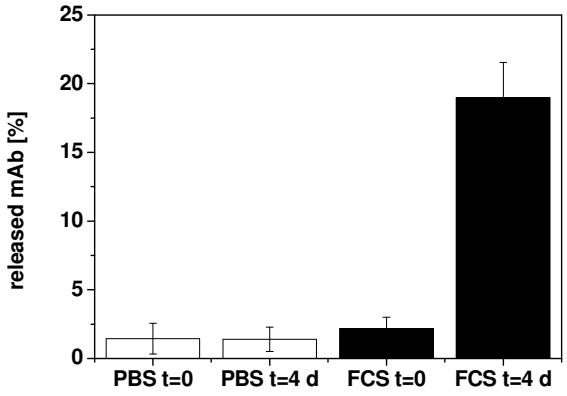

Figure 4-23 Percentage of mAb released from PL-mAb vesicles upon incubation in PBS (reference) and FCS for 0 and 4 days at 37 °C.

Aggregation of PL vesicles in the presence of serum is described in literature to occur as a consequence of serum protein adsorption on the vesicle membrane [221] and presumably serum albumin leads to gap formation in the lipid membrane followed by phase separation [222]. This agglomerate formation may even be advantageous for IA application as synovial clearance is known to be decelerated with increasing vesicle size. In the present study, 80 % of encapsulated mAb were retained by the vesicle membrane after 4 days, which can be seen as an adequate release rate for the intended purpose. In order to improve vesicle stability, potentially cholesterol could be incorporated into the lipid bilayer [223].

3.2.8 *In vivo* mAb release from PL-mAb vesicles after separation of non-encapsulated mAb

As described in section 3.2.3, prolonged synovial mAb retention after IA application of the initial vesicular PL-mAb formulation in comparison to a PL-free mAb solution was not seen. It was hypothesized that the low EE of only 15 % was the reason for the similar pharmacokinetic profiles as the high amount of free mAb was rapidly cleared from the synovial space. Thus, an effect of mAb encapsulation on synovial mAb retention could not be identified during the observation period of 48 hrs. Consequently, the non-encapsulated portion was separated from the mAb-loaded vesicles and the mAb recovery in serum upon IA administration was investigated during 10 days. Besides the purified PL-mAb vesicles, empty

vesicles with spiked mAb and a mAb solution of the same concentration were used as controls.

Mean serum mAb concentrations after IA administration of the PL-mAb vesicles were drastically lower compared to the references (figure 4-24). After 4 hrs, the mean mAb serum concentration of the vesicle formulation was only 6 % of the concentration of both controls. All formulations reached the c_{max} after one day. Animals, dosed with mAb solution and empty vesicles with spiked mAb, revealed maximal mAb serum concentrations of 1.4 ± 0.3 µg/mL and 1.6 ± 0.2 µg/mL respectively. The c_{max} after dosing with PL-mAb vesicles was only 0.2 ± 0.03 µg/mL. After one day, mean serum mAb concentrations of all groups slightly decreased. Both references revealed highly similar pharmacokinetic profiles. After 10 days, SF of all animals was analyzed with respect to the remaining mAb concentration. All sample concentrations were found to be below the lower limit of quantification and therefore no relevant information concerning the remaining mAb could be obtained (data not shown).

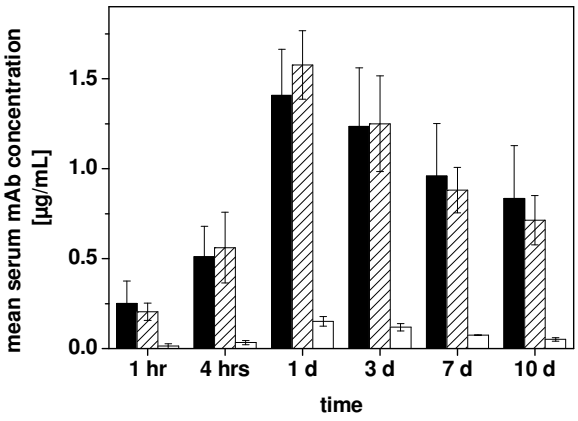

Figure 4-24 Mean serum mAb concentrations after IA administration of PL-mAb vesicles separated from non-encapsulated mAb (white) in comparison to mAb solution (black) and empty vesicles with spiked mAb (striped).

The observed lower mean serum mAb concentrations upon application of the PL-mAb vesicles compared to the references show that mAb encapsulation drastically reduced the systemic exposure which is in good accordance with the literature [35, 37]. The fact that no vesicles were detectable in SF at the end of the study might be due to vesicle migration into the surrounding tissue. Similar observations were reported by Edwards *et al.* who identified extra-articular liposome distribution after IA administration of iohexol-loaded liposomes in sheep [39]. Another possible explanation could be that the vesicles were adsorbed to the articular cartilage surface and thus were not removable by synovial wash. Moreover, vesicle clearance from the synovial space and subsequent accumulation in the liver could also be hypothesized. Until day one, increased mAb concentrations were found in the systemic

circulation which can be ascribed to mAb release from the PL vesicles and underlines the findings of section 3.2.7 where it was shown that vesicle stability in serum is limited. In order to gain insight into the potential fate of the mAb-loaded vesicles following IA administration, an additional experiment with near infrared fluorescent dye-labeled mAb incorporated into vesicles was performed in rats and the fluorescence intensity of the knee joint and of the gastrointestinal tract was studied using a near infrared fluorescence camera. This experiment was performed in collaboration with the Preformulation Group (Dr. Michael Siedler, Dr. Vishwesh A Patil) and the Pharmacology Department (Dr. Bradford McRae, Grace Lynch) at the Abbott Bioresearch Center. Three days after IA injection, high fluorescence intensity of the knee joint was detectable (figure 4-25 A) indicating that at least the labeled protein was still present at the site of injection. From previous studies it is known that free mAb is rapidly cleared from the synovial cavity (section 3.2.3). Hence, the fluorescence intensity in the right joint after 3 days can be ascribed to the presence of mAb-loaded vesicles that are retained at the site of injection. Protein accumulation at the injection site due to formation of large protein aggregates is not expected based on foregoing experiments showing the excellent formulation stability. Moreover, also the control formulation in the aforementioned *in vivo* study containing empty vesicles with spiked mAb showed a rapid mAb release from the joint without evidence of protein aggregation. After 3 days, no fluorescence intensity was found in the liver (figure 4-25 B) which demonstrates that the mAb-loaded vesicles are not cleared

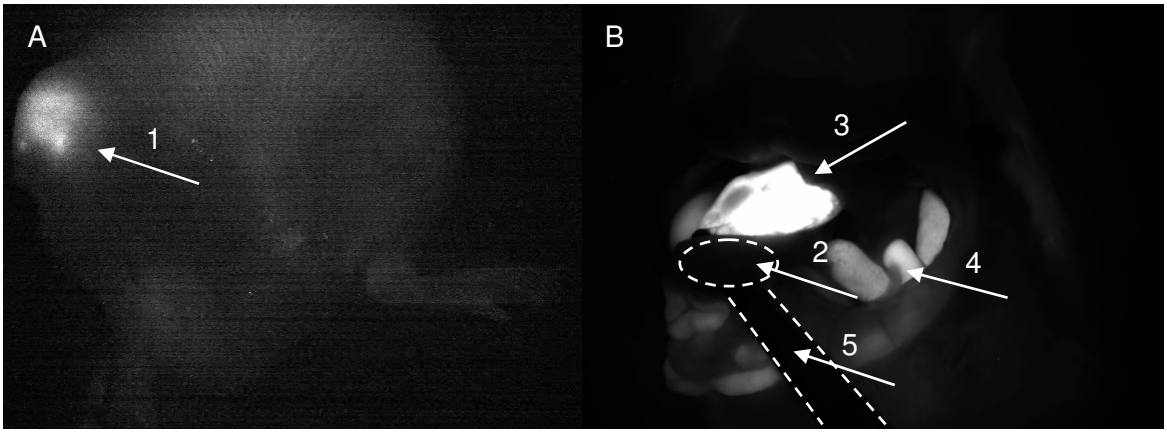

Figure 4-25 Fluorescence images of right joint (A, arrow 1) and gastrointestinal tract after laparotomy (B) 3 days after IA administration of near infrared fluorescent dye-labeled mAb encapsulated in PL vesicles in rats. Arrow 2, dashed boundary: liver; arrow 3: stomach; arrow 4: intestine, arrow 5, dashed boundary: forceps. The experiment was performed in collaboration with the Preformulation group (Dr. Michael Siedler, Dr. Vishwesh A Patil) and the Pharmacology Department (Dr. Bradford McRae and Grace Lynch) at the Abbott Bioresearch Center.

from the joint as such. In literature it is described that liposomes that enter into the systemic circulation are commonly phagocytosed by the reticuloendothelial system which is mainly located in liver and spleen [224]. The high fluorescence intensity observed in figure 4-25 B can be ascribed to the auto-fluorescence of the stomach and intestine content and is not attributed to the mAb-vesicles.

The above findings indicate that IA injected mAb-loaded vesicles show a high residence time at the site of injection. Based on the fact that at the end of the previous study residual mAb was undetectable in the SF, it can be presumed that vesicle adsorption to the articular cartilage takes place which would be beneficial for the intended purpose. In order to substantiate this presumption, histological cross-sections of the joint would provide a detailed understanding concerning the synovial behavior of the mAb-loaded vesicles. Additionally, the efficacy of IA application of mAb-loaded vesicles in reducing arthritic disorder would provide important information. The overall promising results outlined above underline the importance of mAb entrapment in vesicles for the prolongation of the synovial mAb residence time.

4 SUMMARY AND CONCLUSIONS

The aim of this chapter was the development of a biocompatible PL-based vesicular mAb formulation for IA administration. This formulation was intended to provide prolonged synovial residence time and thus therapeutic action at the site of injection. Within this scope, two different formulations were developed and characterized and their suitability for the intended purpose was evaluated. In a first approach, sd mAb was suspended at a concentration of 50 mg/g in a non-aqueous PL solution containing propylene glycol as organic solvent. Upon contact with body fluid, sd mAb was to be dissolved and subsequently entrapped within *in situ* formed PL vesicles. For assessment of the mAb stability after incorporation in the PL solution and the subsequent vesicle formation in contact with the aqueous medium, mAb was extracted from the PL matrix. It was shown that insoluble aggregates were formed and that both secondary and tertiary protein structure were drastically altered. The detected protein instabilities were identified to be induced by the organic solvent (propylene glycol) that was used to dissolve the PL component. The destabilizing influence of propylene glycol was shown to occur only at high organic solvent concentrations. Analysis of mAb in the presence of 50 % propylene glycol/water mixtures did not lead to any precipitation and no alteration in secondary and tertiary protein structure were detectable. In order to exclude the destabilizing effect of propylene glycol, the formulation was modified with respect to the organic solvent. PEG 300 was identified to show excellent mAb compatibility and solubility properties for the PL component. After suspension of sd mAb particles in the PL-PEG 300 solution, injection into PBS and subsequent extraction of mAb, the conformational mAb stability was maintained. Cryo-TEM analysis revealed a broad vesicle size distribution ranging from ~100 nm to 1000 nm with the presence of ULVs, BLVs and MLVs. By analysis of the EE it became evident that the complete mAb amount was present outside of the vesicles. Apparently, vesicle formation occurred more rapidly than dissolution of the sd mAb particles causing the formation of empty vesicles that were surrounded by a highly-concentrated mAb solution. As non-encapsulated mAb was reported to be rapidly cleared from the synovial space, the use of this approach appeared unsuitable for the intended purpose.

In a second approach, the vesicular PL-mAb formulation was prepared *ex vivo* by mixing a highly-concentrated mAb solution with a non-aqueous PL solution consisting of 50 % PL dissolved in propylene glycol. Analysis of mAb stability after incorporation into the vesicular

PL matrix and subsequent extraction revealed excellent mAb stability as assessed by various analytical methods. Moreover, the mAb bioactivity was shown to be maintained. The formulation exhibited shear thinning behavior that enabled easy injection through thin syringe needles. The maximal injection forces using 26 G syringe needles did not exceed 4 N and did not differ significantly from the placebo formulation. These results indicated that the physical formulation characteristics were not altered by the presence of mAb. Cryo-TEM analysis revealed a broad vesicle size distribution ranging from ~100 nm to 800 nm with the presence of ULVs, BLVs and MLVs. These findings were consistent with DLS measurements where a mean vesicle size of 520.4 ± 28.6 nm with a polydispersity index of 0.5 ± 0.04 was detected. By analysis of the EE it became apparent that ~15 % of mAb were entrapped in the vesicles. The encapsulation of mAb in the vesicles was confirmed by fluorescence microscopy analysis after labeling of both mAb and PL vesicles. In order to gain an insight into the pharmacokinetic profile of the formulation upon IA administration, an *in vivo* study with healthy Lewis rats was performed. The mean serum and SF mAb concentration levels of the vesicular PL-mAb formulation were compared to a PL-free mAb solution as reference. An initially slightly lower mAb absorption rate into the systemic circulation was observed for the PL formulation during the first 12 hrs. At later time points no or only marginal differences between PL formulation and reference were observed. This indicates that the EE of 15 % was too low to detect differences compared to the reference. In order to increase the EE, the lipid content of the formulation was modified. It was shown that the EE was raised from 15.9 ± 1.0 % to 31.5 ± 4.4 % when increasing the lipid content from 152 mg/g to 236 mg/g. A further increase of the lipid content did not affect the EE. The addition of cholesterol in a molar ratio of 1:9 (cholesterol:PL) at a lipid content of 236 mg/g increased the EE up to 43.4 ± 2.2 %. A further increase of the cholesterol content, however, led to a decrease in the EE. The application of 5 freeze-thaw cycles as well as the formulation homogenization by means of an ultra-turrax® had no impact on the EE. Formulation preparation by means of a DAC significantly increased the EE up to 53.3 ± 5.4 % at a centrifugation time of 60 min. All modifications led to a decrease of vesicle size. In order to keep the preparation of the dosage system as convenient as possible, the formulation preparation by means of a dual-syringe system was maintained and an increased lipid content of 236 mg/g was chosen for further experiments, providing an EE of 31.5 ± 4.4 % and a mean vesicle size of ~300 nm. To study the physical stability of the PL-mAb vesicles in phosphate buffer, the non-encapsulated mAb amount was removed from the vesicles. While the encapsulated mAb remained completely entrapped during one week of storage at 2-8 °C, a marginal decrease of HP-SEC monomer recovery to 98.7 ± 0.03 % at day 1 and 97.1 ± 0.9 % at day 14 was observed. For assessment of the vesicle stability upon contact with body fluid, fluorescence-labeled mAb

containing PL vesicles, separated from non-encapsulated mAb, were incubated in FCS and stored for 4 days at 37 °C. Fluorescence microscopy images demonstrated that the vesicles formed large agglomerates in the presence of FCS while no changes were observed in phosphate buffer. After 4 days, 18.9 ± 2.6 % of the encapsulated mAb were released indicating that FCS did slightly affect the vesicle stability. In order to study the pharmacokinetic profile of PL-mAb vesicles in the absence of non-encapsulated drug, an *in vivo* study was performed on healthy rats. Analysis of the mean serum mAb concentrations upon IA administration during an observation period of 10 days revealed significantly lower serum levels in comparison to a mAb solution and placebo vesicles with non-encapsulated mAb as references. Due to the fact that at the end of the study residual mAb could not be recovered in the SF, an additional study was performed that was intended to provide information concerning the fate of the vesicles *in vivo*. Near infrared fluorescent dye-labeled mAb was encapsulated into the PL vesicles and 3 days after IA injection the rat was examined using a near infrared fluorescence camera. It was shown that the PL-mAb vesicles remained at the site of injection and no mAb-related fluorescence intensity was observed in liver. Based on these results it was presumed that PL-mAb vesicles that remain at the injection site adsorb to the cartilage surface and are therefore not removable by synovial wash. The results lead to the conclusion that this vesicular drug delivery system is a highly potent formulation for the sustained IA delivery of mAb and subsequent efficacy studies should be envisaged.

CHAPTER 5

SUMMARY OF THE THESIS

The objective of the present thesis was the development of sustained release formulations for the IA delivery of a therapeutic mAb. In Chapter 1 the reader is introduced to the IA route of application and the respective literature is reviewed with regards to the current status of IA drug delivery strategies. Within this scope, it became apparent that despite numerous promising studies published in literature the application of IA drug delivery systems to therapeutic proteins was not investigated in detail up to now. Based on the unique physiological conditions prevailing in the joint and the current knowledge concerning the IA route of application, the requirements on the mAb-containing depot formulation to be developed were defined. This comprised the injectability through small size syringe needles that are commonly applied for IA injection. Moreover, an adequate viscosity after injection had to be provided in order to permit entire joint mobility. On account of the limited injection frequency, the restricted injection volume and the rapid clearance of drugs from the synovial space, a high drug load and a prolonged residence time at the injection site were envisaged. The preservation of the mAb stability after incorporation into the formulation and after release was of utmost importance. Furthermore, a high physiological compatibility of the formulation components was aspired.

The focus of Chapter 2 lay on the development of an *in situ* forming PLGA formulation for the IA delivery of the mAb. This concept encompassed the dispersion of the sd mAb in a non-aqueous PLGA solution. After contact with SF the PLGA formulation was intended to precipitate, leading to a solidified matrix and entrapment of the mAb. Release of mAb was meant to occur simultaneously to polymer degradation over a prolonged period of time. For formulation preparation, the polymer was dissolved in PEG 300 and triacetin. As no mAb instabilities were detected with the help of various analytical methods, these solvents were identified as protein-compatible. Excellent conformational mAb stability was demonstrated after extraction from the non-aqueous PLGA formulation. Analysis of the protein stability after release, performed with the murine mAb variant, revealed a slight decrease in HP-SEC monomer recovery, but preserved binding affinity to the target. *In vitro* mAb release experiments pointed out that the mAb release can be tailored by the amount of the

hydrophobic solvent triacetin used. With increasing amounts of triacetin employed, the initial burst was reduced and therefore higher amounts of mAb were entrapped in the solidifying matrix. The observed *in vitro* release characteristics could however not be confirmed *in vivo*. This was ascribed to the distinct mechanical impact on mAb release induced by the movement of the animals which leads to rapid mAb release. Modification of the *in vitro* release model enabled simulation of the physiological conditions prevailing in the joint. However, a promising formulation composition that might provide a high mAb entrapment rate after injection could not be identified with the help of a formulation screening. In addition, considerable protein aggregate formation became apparent after application of the modified *in vitro* release model. Based on these results, it was concluded that the *in situ* forming PLGA formulation has limited applicability for the IA delivery of mAb.

In Chapter 3, the suitablity of polysaccharides as carrier for the local IA delivery of mAb was investigated. The main focus was on the development of a HA-mAb gel with high protein concentration, high gel viscosity but adequate injectability through thin syringe needles. The HA material with a MW of 2 MDa at a concentration of 1 % provided the most suitable gel characteristics. Excellent compatibility with the incorporated mAb at a concentration of 50 mg/mL was shown using a variety of analytical methods. SPR measurements demonstrated the presence of slight interactions between HA and mAb. However, a distinct impact of these interactions on both the *in vitro* and *in vivo* mAb release from the HA gel could not be observed. Overall, a significantly slower *in vitro* mAb release from the gel compared to the HA-free mAb solution was identified during the first day. This was ascribed to the initially dense gel network causing a restricted mobility and a reduced diffusion rate of mAb. After day one, the mAb release rates from buffer and HA gel became identical. *In vivo* experiments in rats revealed comparable results as slightly lower mAb serum levels were achieved for the gel system compared to the HA-free mAb solution during the first 12 hrs only. This was explained by the continuous dissolution and dilution of the HA gel followed by synovial clearance of the HA molecules, leading to enhanced mAb release. An additional aim of this chapter was to evaluate if the use of polysaccharides with a higher charge density than HA might lead to more pronounced mAb retention at the site of application. Within this scope, sodium alginate was employed to study the conditions at which insoluble charge complexes with mAb are formed. It was demonstrated that complex formation between mAb and alginate depends on the pH and the mAb-alginate ratio. The presence of increasing concentrations of calcium ions induced gelation of alginate but simultaneously caused mAb redissolution via shielding effects. At physiological conditions 96 % of mAb were dissolved. Based on these results, it was concluded that enhanced mAb retention in the synovial cavity,

induced by HA at a concentration of 1 % or by using sodium alginate, was expected to be less effective.

The development of PL-based formulations for the IA delivery of mAb is outlined in Chapter 4. In a first approach, an *in situ* forming PL-mAb formulation was to be developed. This formulation consisted of sd mAb particles suspended in a non-aqueous PL solution. Upon contact with SF, sd mAb was to be dissolved and subsequently entrapped within the *in situ* formed PL vesicles. After detailed protein analysis upon extraction from the formulation, the vesicular structure was characterized with the help of cryo-TEM analysis. The presence of mainly MLVs in the size range of ~100 nm to 1 µm became apparent. Analysis of the EE elucidated that vesicle formation occurred more rapidly than dissolution of the sd mAb particles. This caused the formation of empty vesicles that were surrounded by a highly-concentrated mAb solution. As non-encapsulated mAb is reported to be rapidly cleared from the synovial cavity, the use of this formulation appeared unsuitable for the intended purpose. In a second approach, the vesicular PL-mAb formulation was prepared *ex vivo* by mixing a highly-concentrated mAb solution with a non-aqueous PL solution using a dual-syringe system. Excellent mAb stability and preserved bioactivity were proven with the help of several analytical methods. Moreover, adequate injectability and a broad vesicle size distribution were demonstrated. Analysis of the EE revealed that 15 % of the mAb were vesicularly encapsulated. However, results of an *in vivo* study demonstrated that a higher EE needed to be achieved in order to realize the beneficial effect of drug encapsulation in vesicles. Several attempts were made to increase the EE. This included the increase of the lipid content, the addition of cholesterol, the application of freeze-thaw cycles as well as the use of preparation methods such as ultra-turrax® homogenization or dual asymmetric centrifugation. As these approaches did not lead to EE values higher than 53 %, non-encapsulated mAb was separated from the drug-loaded vesicles for further experiments. The purified vesicles provided a high physical stability in phosphate buffer. After incubation in FCS, distinct vesicle agglomeration was identified, accompanied by mAb release (18 % during 4 days). *In vivo* administration of the mAb-loaded vesicles induced drastically lower serum mAb levels compared to the reference. Vesicle visualization in the animal after IA administration of near infrared fluorescent dye-labeled mAb-vesicles after 3 days using a near infrared fluorescence camera revealed that the vesicles remained at the application site and accumulation in the liver could not be detected. These promising results led to the conclusion that this vesicular drug delivery system presents a highly potent formulation for the sustained IA delivery of mAb.

REFERENCES

1. Sangha O., Epidemiology of rheumatic diseases. Rheumatology (2000), 39(2), 3-12.
2. Hunter D.J., McDougall J.J., Keefe F.J., The symptoms of osteoarthritis and the genesis of pain. Rheumatic Disease Clinics of North America (2008), 34(3), 623-643.
3. Lawrence R.C., Helmick C.G., Arnett F.C., Deyo R.A., Felson D.T., Giannini E.H., Heyse S.P., Hirsch R., Hochberg M.C., Hunder G.G., Liang M.H., Pillemer S.R., Steen V.D., Wolfe F., Estimates of the prevalence of arthritis and selected musculoskeletal disorders in the United States. Arthritis & Rheumatism (1998), 41(5), 778-799.
4. Hochberg M.C., Altman R.D., Brandt K.D., Clark B.M., Dieppe P.A., Griffin M.R., Moskowitz R.W., Schnitzer T.J., Guidelines for the medical management of osteoarthritis Part I. Osteoarthritis of the hip. Arthritis & Rheumatism (1995), 38(11), 1535-1540.
5. El Desoky E.S., Pharmacotherapy of rheumatoid arthritis: an overview. Current Therapeutic Research (2001), 62(2), 92-112.
6. Saag K.G., Teng G.G., Patkar N.M., Anuntiyo J., Finney C., Curtis J.R., Paulus H.E., Mudano A., Pisu M., Elkins-Melton M., Outman R., Allison J.J., Almazor M.S., Bridges S.L., Chatham W.W., Hochberg M., Maclean C., Mikuls T., Moreland L.W., O´Dell J., Turkiewicz A.M., Furst D.E., American College of Rheumatology 2008 Recommendations for the use of nonbiologic and biologic disease-modifying antirheumatic drugs in rheumatoid arthritis. Arthritis & Rheumatism (Arthritis Care & Research) (2008), 59(6), 762-784.
7. Zhang W., Moskowitz R.W., Nuki G., Abramson S., Altman R.D., Arden N., Bierma-Zeinstra S., Brandt K.D., Croft P., Doherty M., Dougados M., Hochberg M., Hunter D.J., Kwoh K., Lohmander L.S., Tugwell P., OARSI recommendations for the management of hip and knee osteoarthritis, Part II: OARSI evidence-based, expert consensus guidelines. Osteoarthritis and Cartilage (2008), 16(2), 137-162.
8. Tarner I.H., Müller-Ladner U., Drug delivery systems for the treatment of rheumatoid arthritis. Expert Opinion on Drug Delivery (2008), 5(9), 1027-1037.
9. Grainger D.W., Controlled-release and local delivery of therapeutic antibodies. Expert Opinion on Biological Therapy (2004), 4(7), 1029-1044.
10. Abramson S., Drug delivery in degenerative joint disease: Where we are and where to go?. Advanced Drug Delivery Reviews (2006), 58(2), 125-127.
11. Ayral X., Injections in the treatment of osteoarthritis. Best Practice & Research Clinical Rheumatology (2001), 15(4), 609-626.
12. Roughley P.J., Lee E.R., Cartilage proteoglycans: Structure and potential functions. Microscopy Research and Technique (1994), 28(5), 385-397.
13. Gerwin N., Hops C., Lucke A., Intraarticular drug delivery in osteoarthritis. Advanced Drug Delivery Reviews (2006), 58(2), 226-242.
14. Allison N., Fremont-Smith F., Dailey M.E., Kennard M.A., Comparative studies between synovial fluid and plasma. The Journal of Bone & Joint Surgery (1926), 8(4), 758-765.
15. Larsen C.,Ostergaard J., Larsen S.W., Jensen H., Jacobsen S., Lindegaard C., Andersen P.H., Intra-articular depot formulation principles: Role in the management of postoperative pain and arthritic disorders. Journal of Pharmaceutical Sciences (2008), 97(11), 4622-4654.

16. Rodnan G.P., Maclachlan M.J., The absorption of serum albumin and gamma globulin from the knee joint of man and rabbit. Arthritis & Rheumatism (1960), 3(2), 152-157.
17. Weinberger A., Simkin P.A., Plasma proteins in synovial fluids of normal human joints. Seminars in Arthritis and Rheumatism (1989), 19(1), 66-76.
18. Schumacher H.R., Aspiration and injection therapies for joints. Arthritis & Rheumatism (Arthritis Care & Research) (2003), 49(3), 413-420.
19. Owen S.G., Francis H.W., Roberts M.S., Disappearance kinetics of solutes from synovial fluid after intra-articular injection. British journal of clinical pharmacology (1994), 38(4), 349-355.
20. Chevalier X., Goupille P., Beaulieu A.D., Burch F.X., Bensen W.G., Conrozier T., Loeuille D., Kivitz A.J., Silver D., Appleton B.E., Intraarticular injection of anakinra in osteoarthritis of the knee: A multicenter, randomized, double-blind, placebo-controlled study. Arthritis & Rheumatism (Arthritis Care & Research) (2009), 61(3), 344-352.
21. Rungseevijitprapa W., Bodmeier R., Injectability of biodegradable in situ forming microparticle systems (ISM). European Journal of Pharmaceutical Sciences (2009), 36(4-5), 524-531.
22. Fields T.R., Berman J.R., Stern R., HSS Manual Chapter 8 - Arthrocentesis, intraarticular injection and synovial fluid analysis. Hospital for Special Surgery Manual of Rheumatology and Outpatient Orthopedic Disorders (2005), 5, 47-54.
23. Volon A - prescribing information (2012), Rote Liste Online, FachInfo Service.
24. Lipotalon - prescribing information (2012), Rote Liste Online, FachInfo Service.
25. Balazs E.A., Denlinger J.L., Viscosupplementation: a new concept in the treatment of osteoarthritis. The Journal of Rheumatology, Supplement (1993), 39, 3-9.
26. Lee J.Y., Spicer A.P., Hyaluronan: a multifunctional, megaDalton, stealth molecule. Current Opinion in Cell Biology (2000), 12(5), 581-586.
27. Liang L.S., Wong W., Burt H.M., Pharmacokinetic study of methotrexate following intra-articular injection of methotrexate loaded poly(L-lactic acid) microspheres in rabbits. Journal of Pharmaceutical Sciences (2005), 94(6), 1204-1215.
28. Thakkar H., Sharma R.K., Mishra A.K., Chuttani K., Murthy R.S.R., Celecoxib incorporated chitosan microspheres: In vitro and in vivo evaluation. Journal of Drug Targeting (2004), 12(9-10), 549-557.
29. Mierisch C.M., Cohen S.B., Jordan L.C., Robertson P.G., Balian G., Diduch D.R., Transforming growth factor-β in calcium alginate beads for the treatment of articular cartilage defects in the rabbit. Arthroscopy: The Journal of Arthroscopic and Related Surgery (2002), 18(8), 892-900.
30. Kim M.-J., Kim S.-J., Kwon O.-R., Sustained-release composition of drugs encapsulated in microparticles of hyaluronic acid, US Patent 7,276,251 B2 (2007).
31. Sayed Aly M.N., Intra-articular drug delivery: A fast growing approach. Recent Patents on Drug Delivery & Formulation (2008), 2(3), 231-237.
32. Rote Liste Online, Arzneimittelinformationen für Deutschland (einschließlich EU-Zulassungen und bestimmter Medizinprodukte), 2012.
33. Shaw I.H., Knight C.G., Dingle J.T., Liposomal retention of a modified anti-inflammatory steroid. Biochemical Journal (1976), 158(2), 473-476.
34. Dingle J.T., Gordon J.L., Hazleman B.L., Knight C.G., Page Thomas D.P., Phillips N.C., Shaw I.H., Fildes F.J.T., Oliver J.E., Turner E.H., Lowe J.S., Novel treatment for joint inflammation. Nature (1978), 271, 372-373.
35. Bonanomi M.H., Velvart M., Stimple M., Roos K.M., Fehr K., Weder H.G., Studies of pharmacokinetics and therapeutic effects of glucocorticoids entrapped in liposomes after intraarticular application in healthy rabbits and in rabbits with antigen-induced arthritis. Rheumatology International (1987), 7(5), 203-212.

36. Williams A.S., Camilleri J.P., Goodfellow R.M., Williams B.D., A single intra-articular injection of liposomally conjugated methotrexate suppresses joint inflammation in rat antigen-induced arthritis. British Journal of Rheumatology (1996), 35(8), 719-724.
37. Hou S.M., Yu H.Y., Comparison of systemic absorption of aqueous and liposomal lidocain following intra-articular injection in rabbits. Journal of the Formosan Medical Association (1997), 96(2), 141-143.
38. Trif M., Guillen C., Vaughan D.M., Telfer J.M., Brewer J.M., Roseanu A., Brock J.H., Liposomes as possible carriers for lactoferrin in the local treatment of inflammatory diseases. Experimental Biology and Medicine (2001), 226(6), 559-564.
39. Edwards S.H.R., Cake M.A., Spoelstra G., Read R.A., Biodistribution and clearance of intra-articular liposomes in a large animal model using a radiographic marker. Journal of Liposome Research (2007), 17(3-4), 249-261.
40. López-García F., Vásquez-Autón J.M., Gil F., Latoore R., Moreno F., Villalaín J., Gómez-Fernández J.C., Intra-articular therapy of experimental arthritis with a derivative of triamcinolone acetonide incorporated in liposomes. Journal of Pharmacy and Pharmacology (1993), 45(6), 576-578.
41. Zalutsky M.R., Noska M.A., Gallagher P.W., Shortkroff S., Sledge C.B., Use of liposomes as carriers for radiation synovectomy. International Journal of Radiation Applications and Instrumentation. Part B. Nuclear Medicine and Biology (1988), 15(2), 151-156.
42. Chowdhary R.K., Ratkay L.G., Canaan A.J., Waterfield J.D., Richter A.M., Levy J.G., Uptake of Verteporfin® by articular tissues following systemic and intra-articular administration. Biopharmaceutics & Drug Disposition (1998), 19(6), 395-400.
43. Tanaka H., Sugita T., Yasunaga Y., Shimose S., Deie M., Kubo T., Murakami T., Ochi M., Efficiency of magnetic liposomal transforming growth factor-beta 1 in the repair of articular cartilage defects in a rabbit model. Journal of Biomedical Materials Research Part A (2005), 73(3), 255-263.
44. Butoescu N., Jordan O., Burdet P., Stadelmann P., Petri-Fink A., Hofmann H., Doelker E., Dexamethasone-containing biodegradable superparamagnetic microparticles for intra-articular administration: Physicochemical and magnetic properties, in vitro and in vivo drug release. European Journal of Pharmaceutics and Biopharmaceutics (2009), 72(3), 529-538.
45. Packhaeuser C.B., Schnieders J., Oster C.G., Kissel T., In situ forming parenteral drug delivery systems: an overview. European Journal of Pharmaceutics and Biopharmaceutics (2004), 58(2), 445-455.
46. Tang L., Persky A.M., Hochhaus G., Meibohm B., Pharmacokinetic aspects of biotechnology products. Journal of Pharmaceutical Sciences (2004), 93(9), 2184-2204.
47. Jiskoot W., Randolph T.W., Volkin D.B., Middaugh C.R., Schöneich C., Winter G., Friess W., Crommelin D.J.A., Carpenter J.F., Protein instability and immunogenicity: Roadblocks to clinical application of injectable protein delivery systems for sustained release. Journal of Pharmaceutical Sciences (2012), 101(3), 946-954.
48. Stolnik S., Shakesheff K., Formulations for delivery of therapeutic proteins. Biotechnology Letters (2009), 31(1), 1-11.
49. Van Tomme S.R., Hennink W.E., Biodegradable dextran hydrogels for protein delivery applications. Expert Review of Medical Devices (2007), 4(2), 147-164.
50. Daugherty A.L., Mrsny R.J., Formulation and delivery issues for monoclonal antibody therapeutics. Advanced Drug Delivery Reviews (2006), 58(5-6), 686-706.
51. Pisal D.S., Kosloski M.P., Balu-Iyer S.V., Delivery of therapeutic proteins. Journal of Pharmaceutical Sciences (2010), 99(6), 2557-2575.
52. Cleland J.L., Daugherty A., Mrsny R., Emerging protein delivery methods. Current Opinion in Biotechnology (2001), 12(2), 212-219.

53. Crommelin D.J., Storm G., Verrijk R., de Leede L., Jiskoot W., Hennink W.E., Shifting paradigms: biopharmaceuticals versus low molecular weight drugs. International Journal of Pharmaceutics (2003), 266(1–2), 3-16.
54. Rosenberg A., Effects of protein aggregates: An immunologic perspective. The AAPS Journal (2006), 8(3), E501-E507.
55. Cai L., Okumu F.W., Cleland J.L., Beresini M., Hogue D., Lin Z., Filvaroff E.H., A slow release formulation of insulin as a treatment for osteoarthritis. Osteoarthritis and Cartilage (2002), 10(9), 692-706.
56. Eswaramoorthy R., Chang C.C., Wu S.C., Wang G.J., Chang J.K., Ho M.L., Sustained release of PTH(1–34) from PLGA microspheres suppresses osteoarthritis progression in rats. Acta Biomaterialia (2012), 8(6), 2254-2262.
57. Lambert W.J., Peck K.D., Development of an in situ forming biodegradable poly-lactide-coglycolide system for the controlled release of proteins. Journal of Controlled Release (1995), 33(1), 189-195.
58. Brodbeck K.J., Pushpala S., McHugh A.J., Sustained release of human growth hormone from PLGA solution depots. Pharmaceutical Research (1999), 16(12), 1825-1829.
59. Eliaz R.E., Kost J., Characterization of a polymeric PLGA-injectable implant delivery system for the controlled release of proteins. Journal of Biomedical Materials Research (2000), 50(3), 388-396.
60. Li L., Okada H., Takemura G., Esaki M., Kobayashi H., Kanamori H., Kawamura I., Maruyama R. Fujiwara T., Fujiwara H., Tabata Y., Minatoguchi S., Sustained release of erythropoietin using biodegradable gelatin hydrogel microspheres persistently improves lower leg ischemia. Journal of the American College of Cardiology (2009), 53(25), 2378-2388.
61. Özbaş-Turan S., Akbuğa J., Aral C., Controlled release of interleukin-2 from chitosan microspheres. Journal of Pharmaceutical Sciences (2002), 91(5), 1245-1251.
62. Wells L.A., Sheardown H., Extended release of high pI proteins from alginate microspheres via a novel encapsulation technique. European Journal of Pharmaceutics and Biopharmaceutics (2007), 65(3), 329-335.
63. Kim H.K., Park T.G., Microencapsulation of human growth hormone within biodegradable polyester microspheres: Protein aggregation stability and incomplete release mechanism. Biotechnology and Bioengineering (1999), 65(6), 659-667.
64. van de Weert M., Hennink W.E., Jiskoot W., Protein instability in poly(lactic-co-glycolic acid) microparticles. Pharmaceutical Research (2000), 17(10), 1159-1167.
65. Houchin M.L., Topp E.M., Chemical degradation of peptides and proteins in PLGA: A review of reactions and mechanisms. Journal of Pharmaceutical Sciences (2008), 97(7), 2395-2404.
66. Vermonden T., Censi R., Hennink W.E., Hydrogels for protein delivery. Chemical Reviews (2012), 112(5), 2853-2888.
67. Trif M., Roseanu A., Brock J.H., Brewer J.M., Designing lipid nanostructures for local delivery of biologically active macromolecules. Journal of Liposome Research (2007), 17(3-4), 237-248.
68. Tian W., Schulze S., Brandl M., Winter G., Vesicular phospholipid gel-based depot formulations for pharmaceutical proteins: Development and in vitro evaluation. Journal of Controlled Release (2010), 142(3), 319-325.
69. Meyer J., Whitcomb L., Collins D., Efficient encapsulation of proteins within liposomes for slow release in vivo. Biochemical and Biophysical Research Communications (1994), 199(2), 433-438.
70. Herrmann S., Mohl S., Siepmann F., Siepmann J., Winter G., New insight into the role of polyethylene glycol acting as protein release modifier in lipidic implants. Pharmaceutical Research (2007), 24(8), 1527-1537.

71. Almeida A.J., Souto E., Solid lipid nanoparticles as a drug delivery system for peptides and proteins. Advanced Drug Delivery Reviews (2007), 59(6), 478-490.
72. Vorauer-Uhl K., Wagner A., Katinger H., Long term stability of rh-Cu/Zn-superoxide dismutase (SOD)-liposomes prepared by the cross-flow injection technique following International Conference on Harmonisation (ICH)-guidelines. European Journal of Pharmaceutics and Biopharmaceutics (2002), 54(1), 83-87.
73. Siepmann J., Elkharraz K., Siepmann F., Klose D., How autocatalysis accelerates drug release from PLGA-based microparticles: A quantitative treatment. Biomacromolecules (2005), 6(4), 2312-2319.
74. Makadia H.K., Siegel S.J., Poly lactic-co-glycolic acid (PLGA) as biodegradable controlled drug delivery carrier. Polymers (2011), 3(3), 1377-1397.
75. Astaneh R., Moghimi H.R., Erfan M., Mobedi H., Formulation of an injectable implant for peptide delivery and mechanistic study of the effect of polymer molecular weight on its release behavior. DARU Journal of Pharmaceutical Sciences (2006), 14(2), 65-70.
76. Chhabra S., Sachdeva V., Singh S., Influence of end groups on in vitro release and biological activity of lysozyme from a phase-sensitive smart polymer-based in situ gel forming controlled release drug delivery system. International Journal of Pharmaceutics (2007), 342(1-2), 72-77.
77. Dong W.Y., Körber M., López Esguerra V., Bodmeier R., Stability of poly(D,L-lactide-co-glycolide) and leuprolide acetate in in-situ forming drug delivery systems. Journal of Controlled Release (2006), 115(2), 158-167.
78. Göpferich A., Mechanisms of polymer degradation and erosion. Biomaterials (1996), 17(2), 103-114.
79. Friess W., Schlapp M., Sterilization of gentamicin containing collagen/PLGA microparticle composites. European Journal of Pharmaceutics and Biopharmaceutics (2006), 63(2), 176-187.
80. Athanasiou K.A., Niederauer G.G., Agrawal C.M., Sterilization, toxicity, biocompatibility and clinical applications of polylactic acid/ polyglycolic acid copolymers. Biomaterials (1996), 17(2), 93-102.
81. Grayson A.C.R., Cima M.J., Langer R., Size and temperature effects on poly(lactic-co-glycolic acid) degradation and microreservoir device performance. Biomaterials (2005), 26(14), 2137-2145.
82. Brodbeck K.J., DesNoyer J.R., McHugh A.J., Phase inversion dynamics of PLGA solutions related to drug delivery: Part II. The role of solution thermodynamics and bath-side mass transfer. Journal of Controlled Release (1999), 62(3), 333-344.
83. Dunn R., Application of the ATRIGEL implant drug delivery technology for patient-friendly, cost-effective product development. Drug Development & Delivery (2003), 3(6).
84. Morlock M., Koll H., Winter G., Kissel T., Microencapsulation of rh-erythropoietin, using biodegradable poly(D,L-lactide-co-glycolide): protein stability and the effects of stabilizing excipients. European Journal of Pharmaceutics and Biopharmaceutics (1997), 43(1), 29-36.
85. Dunn R.L., English J.P., Cowsar D.R., Vanderbilt D.P., Biodegradable in-situ forming implants and methods of producing the same, US Patent 5,990,194 (1999).
86. Dunn R.L., English J.P., Biodegradable polymer composition, US Patent 6,461,631 B1 (2002)
87. Hatefi A., Amsden B., Biodegradable injectable in situ forming drug delivery systems. Journal of Controlled Release (2002), 80(1-3),. 9-28.
88. Chen G., Junnarkar G., ALZAMER® Depot™ Bioerodible Polymer Technology, Modified-Release Drug Delivery Technology (2008), 2(2), 215-226.

89. Astaneh R., Erfan M., Moghimi H., Mobedi H., Changes in morphology of in situ forming PLGA implant prepared by different polymer molecular weight and its effect on release behavior. Journal of Pharmaceutical Sciences (2009), 98(1), 135-145.
90. Butoescu N., Jordan O., Doelker E., Intra-articular drug delivery systems for the treatment of rheumatic diseases: A review of the factors influencing their performance. European Journal of Pharmaceutics and Biopharmaceutics (2009), 73(2), 205-218.
91. Tunçay M., Calis S., Kas H.S., Ercan M.T., Peksoy I., Hincal A.A., Diclofenac sodium incorporated PLGA (50:50) microspheres: formulation considerations and in vitro/in vivo evaluation. International Journal of Pharmaceutics (2000), 195(1-2), 179-188.
92. Fernández-Carballido A., Herrero-Vanrell R., Molina-Martínez I.T., Pastoriza P., Biodegradable ibuprofen-loaded PLGA microspheres for intraarticular administration: Effect of Labrafil addition on release in vitro. International Journal of Pharmaceutics (2004), 279(1-2), 33-41.
93. Liang L.S., Jackson J., Min W., Risovic V., Wasan K.M., Burt H.M., Methotrexate loaded poly(L-lactic acid) microspheres for intra-articular delivery of methotrexate to the joint. Journal of Pharmaceutical Sciences (2004), 93(4), 943-956.
94. Liggins R.T., Cruz T., Min W., Liang L., Hunter W.L., Burt H.M., Intra-articular treatment of arthritis with microsphere formulations of paclitaxel: biocompatibility and efficacy determinations in rabbits. Inflammation Research (2004), 53(8), 363-372.
95. Butoescu N., Seemayer C.A., Foti M., Jordan O., Doelker E., Dexamethasone-containing PLGA superparamagnetic microparticles as carriers for the local treatment of arthritis. Biomaterials (2009), 30(9), 1772-1780.
96. Cilurzo F., Selmin F., Minghetti P., Adami M., Bertoni E., Lauria S., Montanari L., Injectability evaluation: An open issue. AAPS PharmSciTech (2011), 12(2), 604-609.
97. Schmid K., Arpagaus C., Friess W., Evaluation of the Nano Spray Dryer B-90 for pharmaceutical applications. Pharmaceutical Development and Technology (2011), 16(4), 287-294.
98. Rungseevijitprapa W., Brazeau G.A., Simkins J.W., Bodmeier R., Myotoxicity studies of O/W-in situ forming microparticle systems. European Journal of Pharmaceutics and Biopharmaceutics (2008), 69(1), 126-133.
99. Strickley R.G., Solubilizing excipients in oral and injectable formulations. Pharmaceutical Research (2004), 21(2), 201-230.
100. Bailey J.W., Haymond M.W., Miles J.M., Triacetin: A potential parenteral nutrient. Journal of Parenteral and Enteral Nutrition (1991), 15(1), 32-36.
101. Kueltzo L.A., Wang W., Randolph T.W., Carpenter J.F., Effects of solution conditions, processing parameters, and container materials on aggregation of a monoclonal antibody during freeze–thawing. Journal of Pharmaceutical Sciences (2008), 97(5), 1801-1812.
102. Mach H., Middaugh R., Simultaneous monitoring of the environment of tryptophan, tyrosine, and phenylalanine residues in proteins by near-ultraviolet second-derivative spectroscopy. Analytical Biochemistry (1994), 222(2), 323-331.
103. Kueltzo L.A., Ersoy B., Ralston J.P., Middaugh C.R., Derivative absorbance spectroscopy and protein phase diagrams as tools for comprehensive protein characterization: A bGCSF case study. Journal of Pharmaceutical Sciences (2003), 92(9), 1805-1820.
104. Faisant N., Siepmann J., Benoit J.P., PLGA-based microparticles: elucidation of mechanisms and a new, simple mathematical model quantifying drug release. European Journal of Pharmaceutical Sciences (2002), 15(4), 355-366.
105. Shively M.L., Coonts B.A., Renner W.D., Southard J.L., Bennett A.T., Physico-chemical characterization of a polymeric injectable implant delivery system. Journal of Controlled Release (1995), 33(2), 237-243.

106. Graham P.D., Brodbeck K.J., McHugh A.J., Phase inversion dynamics of PLGA solutions related to drug delivery. Journal of Controlled Release (1999), 58(2), 233-245.
107. Yeo Y., Park K., Control of encapsulation efficiency and initial burst in polymeric microparticle systems. Archives of Pharmacal Research (2004), 27(1), 1-12.
108. Körber M., Bodmeier R., Development of an in situ forming PLGA drug delivery system: I. Characterization of a non-aqueous protein precipitation. European Journal of Pharmaceutical Sciences (2008), 35(4), 283-292.
109. Karlsson R., Michaelsson A., Mattsson L., Kinetic analysis of monoclonal antibody-antigen interactions with a new biosensor based analytical system. Journal of Immunological Methods (1991), 145(1-2), 229-240.
110. Richter W., Bhansali S.G., Morris M.E., Mechanistic determinants of biotherapeutics absorption following SC administration. The AAPS Journal (2012), 14(3), 559-570.
111. Larsen C., Larsen S.W., Jensen H., Yaghmur A., Ostergaard J., Role of in vitro release models in formulation development and quality control of parenteral depots. Expert Opinion on Drug Delivery (2009), 6(12), 1283-1295.
112. Frost A.B., Larsen F., Ostergaard J., Larsen S.W., Lindegaard C., Hansen H.R., Larsen C., On the search for in vitro in vivo correlations in the field of intra-articular drug delivery: Administration of sodium diatrizoate to the horse. European Journal of Pharmaceutical Sciences (2010), 41(1), 10-15.
113. Jain R.A., Rhodes C.T., Railkar A.M., Malick A.W., Shah N.H., Controlled delivery of drugs from a novel injectable in situ formed biodegradable PLGA microsphere system. Journal of Microencapsulation (2000), 17(3), 343-362.
114. Liu Z., Jiao Y., Wang Y., Zhou C., Zhang Z., Polysaccharides-based nanoparticles as drug delivery systems. Advanced Drug Delivery Reviews (2008), 60(15), 1650-1662.
115. Chen J., Jo S., Park K., Polysaccharide hydrogels for protein drug delivery. Carbohydrate Polymers (1995), 28(1), 69-76.
116. Reddy K., Mohan G.K., Satla S., Gaikwad S., Natural polysaccharides: versatile excipients for controlled drug delivery systems. Asian Journal of Pharmaceutical Sciences (2011), 6(6), 275-286.
117. della Valle F., Romeo A., Cross-linked esters of hyaluronic acid, US Patent 4,957,744 (1990).
118. Park Y.D., Tirelli N., Hubbell J.A., Photopolymerized hyaluronic acid-based hydrogels and interpenetrating networks. Biomaterials (2003), 24(6), 893-900.
119. Bettelheim F.A., Laurent T.C., Pertoft H., Interaction between serum albumin and acidic polysaccharides. Carbohydrate Research (1966), 2(5), 391-402.
120. Zhao Y., Li F., Carvajal M.T., Harris M.T., Interactions between bovine serum albumin and alginate: An evaluation of alginate as protein carrier. Journal of Colloid and Interface Science (2009), 332(2), 345-353.
121. Jin Y.-J., Ubonvan T., Kim D.-D., Hyaluronic acid in drug delivery systems. Journal of Pharmaceutical Investigation (2010), 40, 33-43.
122. Illum L., Farraj N.F., Fisher A.N., Gill I., Miglietta M., Benedetti L.M., Hyaluronic acid ester microspheres as a nasal delivery system for insulin. Journal of Controlled Release (1994), 29(1–2), 133-141.
123. Prisell P.T., Camber O., Hiselius J., Norstedt G., Evaluation of hyaluronan as a vehicle for peptide growth factors. International Journal of Pharmaceutics (1992), 85(1-3), 51-56.
124. Meyer J., Whitcomb L., Treuheit M, Collins D., Sustained in vivo activity of recombinant human granulocyte colony stimulating factor (rHG-CSF) incorporated into hyaluronan. Journal of Controlled Release (1995), 35(1), 67-72.
125. Cascone M.G., Sim B., Downes S., Blends of synthetic and natural polymers as drug delivery systems for growth hormone. Biomaterials (1995), 16(7), 569-574.

126. Tian W.M., Zhang C.L., Hou S.P., Yu X., Cui F.Z., Xu Q.Y., Sheng S.L., Cui H., Li H.D., Hyaluronic acid hydrogel as Nogo-66 receptor antibody delivery system for the repairing of injured rat brain: in vitro. Journal of Controlled Release (2005), 102(1), 13-22.
127. Schellekens H., Immunogenicity of therapeutic proteins: Clinical implications and future prospects. Clinical Therapeutics (2002), 24(11), 1720-1740.
128. Lyons R.T., Robinson M.R., Trogden J.T., Whitcup S.M., Peripherally administered viscuous formulations, US Patent 2008/0044476 A1 (2008).
129. Tanaka K., Pharmaceutical composition containing viscoelastic substance and medicaiton, US Patent 2004/0038936 A1 (2004).
130. Thompson J., Gosiewska A., Niemiec S., Dhanaraj S., Composition comprising glycosaminoglycans and hyaluronidase inhibitors for the treatment of arthritic joints, European Patent 1423081 A2 (2004).
131. de Kruif C.G., Weinbreck F., de Vries R., Complex coacervation of proteins and anionic polysaccharides. Current Opinion in Colloid & Interface Science (2004), 9(5), 340-349.
132. Shank J.L., Cunningham W.H., Precipitation of proteins from whey using sodium alginate, US Patent 3,404,142 (1968).
133. Easton I.A., Gorham S.D., Protein/Polysaccharide complexes, US Patent 4,614,794 (1986).
134. Zaffagnini S., Allen A.A., Suh J.-K., Fu F.H., Temperature changes in the knee joint during arthroscopic surgery. Knee Surgery, Sports Traumatology, Arthroscopy (1996), 3(4), 199-201.
135. Balazs E.A., The physical properties of synovial fluid and the special role of hyaluronic acid. Disorders of the Knee, T.B. Lippincott Company, Philadelphia (1974), 63-75.
136. Fouissac E., Milas M., Rinaudo M., Borsali R., Influence of the ionic strength on the dimensions of sodium hyaluronate. Macromolecules (1992), 25(1), 5613-5617.
137. Lapcík L., Lapcík L., Hyaluronan: Preparation, structure, properties, and applications. Chemical Reviews (1998), 98(8), 2663-2684.
138. Fraser J.R.E., Laurent T.C., Laurent U.B.G., Hyaluronan: its nature, distribution, functions and turnover. Jounal of Internal Medicine (1997), 242(1), 27-33.
139. Mendichi R., Šoltés L., Schieroni A.G., Evaluation of radius of gyration and intrinsic viscosity molar mass dependence and stiffness of hyaluronan. Biomacromolecules (2003), 4(6), 1805-1810.
140. Krause W.E., Bellomo E.G., Colby R.H., Rheology of sodium hyaluronate under physiological conditions. Biomacromolecules (2001), 2(1), 65-69.
141. Alfrey T., Bartovics A., Mark H., The effect of temperature and solvent type on the intrinsic viscosity of high polymer solutions. Journal of the American Chemical Society (1942), 64(7), 1557-1560.
142. Fraser J.R.E., Foo W.K., Maritz J.S., Viscous interactions of hyaluronic acid with some proteins and neutral saccharides. Annals of the Rheumatic Diseases (1972), 31(6), 513-520.
143. Bos G.W., Verrijk R., Franssen O., Bezemer J.M., Hennink W.E., Crommelin D.J.A., Hydrogels for the controlled release of pharmaceutical proteins. Pharmaceutical Technology (2001), 25(10), 110-119.
144. Matheus S., Friess W., Mahler H.-C., FTIR and nDSC as analytical tools for high-concentration protein formulations. Pharmaceutical Research (2006), 23(6), 1350-1363.
145. Cleland R.L., Wang J.L., Detweiler D.M., Polyelectrolyte properties of sodium hyaluronate. 2. Potentiometric titration of hyaluronic acid. Macromolecules (1982), 15(2), 386-395.

146. Brown M., Jones S., Hyaluronic acid: a unique topical vehicle for the localized delivery of drugs to the skin. European Academy of Dermatology and Venereology (2005), 19(3), 308-318.
147. Comper W.D., Laurent T.C., Physiological function of connective tissue polysaccharides. Physiological Reviews (1978), 58(1), 255-315.
148. Lenormand H., Deschrevel B., Tranchepain F., Vincent J.C., Electrostatic interactions between hyaluronan and proteins at pH 4: How do they modulate hyaluronidase activity. Biopolymers (2008), 89(12), 1088-1103.
149. Van Damme M.P., Moss J.M., Murphy W.H., Preston B.N., Binding properties of glycosaminoglycans to lysozyme-effect of salt and molecular weight. Archives of Biochemistry and Biophysics (1994), 310(1), 16-24.
150. Yu H., Munoz E.M., Edens R.E., Linhardt R.J., Kinetic studies on the interactions of heparin and complement proteins using surface plasmon resonance. Biochimica et Biophysica Acta (BBA) - General Subjects (2005), 1726(2), 168-176.
151. Van der Merwe P.A., Surface plasmon resonance, journal name and year of publication not indicated.
152. Mathes J., Protein adsorption to vial surfaces - quantification, structural and mechanistic studies. Thesis (2010).
153. Yadav S., Laue T.M., Kalonia D.S., Singh S.N., Shire S.J., The influence of charge distribution on self-association and viscosity behavior of monoclonal antibody solutions. Molecular Pharmaceutics (2012), 9(4), 791-802.
154. Gelman R.A., Blackwell J., Interactions between mucopolysaccharides and cationic polypeptides in aqueous solution: Hyaluronic acid, heparitin sulfate, and keratan sulfate. Biopolymers (1974), 13(1), 139-156.
155. Brown T.J., Laurent U.B., Fraser J.R., Turnover of hyaluronan in synovial joints: elimination of labelled hyaluronan from the knee joint of the rabbit. Experimental Physiology (1991), 76(1), 125-134.
156. Lindholm A., Ronéus B., Lindblad G., Jones B., Hyaluronan turnover in the synovial fluid in metacarpophalangeal- and middle carpal joints in standardbred horses. Acta veterinaria Scandinavica (1996), 37(2), 147-151.
157. De Smedt S.C., Lauwers A., Demeester J., Structural information on hyaluronic acid solutions as studied by probe diffusion experiments. Macromolecules (1994), 27(1), 141-146.
158. Laurent T.C., Björk I., Pietruszkiewicz A., Persson H., On the interaction between polysaccharides and other macromolecules: II. The transport of globular particles through hyaluronic acid solutions. Biochimica et Biophysica Acta (1963), 78, 351-359.
159. Kushner I., Somerville J.A., Permeability of human synovial membrane to plasma proteins. Arthritis and Rheumatism (1971), 14(5), 560-570.
160. Larsen N.E., Dursema H.D., Pollak C.T., Skrabut E.M., Clearance kinetics of a hylan-based viscosupplement after intra-articular and intravenous administration in animal models. Journal of Biomedical Materials Research Part B: Applied Biomaterials (2012), 100B(2), 457-462.
161. Knight A.D., Levick J.R., Morphometry of the ultrastructure of the blood-joint barrier in the rabbit knee. Quarterly Journal of Experimental Physiology (1984), 69(2), 271-288.
162. Gombotz W.R., Wee S.F., Protein release from alginate matrices. Advanced Drug Delivery Reviews (1998), 31(3), 267-285.
163. Pillay V., Dangor C.M., Govender T., Moopanar K.R., Hurbans N., Drug release modulation from cross-linked calcium alginate microdiscs, 1: Evaluation of the concentration dependency of sodium alginate on drug entrapment capacity, morphology, and dissolution rate. Drug Delivery (1998), 5(1), 25-34.
164. Barry J.J., Higham P.A., Aberman H.M., In situ modification of alginate, US Patent 5,266,329 (1993).

165. Storm G., Koppenhagen F., Heeremans A., Vingerhoeds M., Woodle M.C., Crommelin D.J.A., Novel developments in liposomal delivery of peptides and proteins. Journal of Controlled Release (1995), 36(1-2), 19-24.
166. Olson F., Hunt C.A., Szoka F.C., Vail W.J., Papahadjopoulos D., Preparation of liposomes of defined size distribution by extrusion through polycarbonate membranes. Biochimica et Biophysica Acta (BBA) - Biomembranes (1979), 557(1), 9-23.
167. du Plessis J., Ramachandran C., Weiner N., Müller D.G., The influence of lipid composition and lamellarity of liposomes on the physical stability of liposomes upon storage. International Journal of Pharmaceutics (1996), 127(2), 273-278.
168. Cagdas F.M., Ertugral N., Bucak S., Atay N.Z., Effect of preparation method and cholesterol on drug encapsulation studies by phospholipid liposomes. Pharmaceutical Development and Technology (2011), 16(4), 408-414.
169. Kirby C., Clarke J., Gregoriadis G., Effect of the cholesterol content of small unilamellar liposomes on their stability in vivo and in vitro. Biochemical Journal (1980), 186(2), 591-598.
170. Anderson P.M., Katsanis E., Sencer S.F., Hasz D., Ochoa A.C., Bostrom B., Depot characteristics and biodistribution of interleukin-2 liposomes: importance of route of administration. Journal of Immunotherapy (1992), 12(1), 19-31.
171. Stevenson R.W., Patel H.M., Parsons J.A., Ryman B.E., Prolonged hypoglycemic effect in diabetic dogs due to subcutaneous administration of insulin in liposomes. Diabetes (1982), 31(6), 506-511.
172. Postma N.S., Boerman O.C., Oyen W.J.G., Zuidema J., Storm G., Absorption and biodistribution of ^{111}indium-labelled desferrioxamine (^{111}In-DFO) after subcutaneous injection of ^{111}In-DFO liposomes. Journal of Controlled Release (1999), 58(1), 51-60.
173. Oussoren C., Storm G., Liposomes to target the lymphatics by subcutaneous administration. Advanced Drug Delivery Reviews (2001), 50(1-2), 143-156.
174. Weiner A.L., Liposomes for protein delivery: selecting manufacture and development processes. ImmunoMethods (1994), 4(3), 201-209.
175. Brandl M., Vesicular phospholipid gels: A technology platform. Journal of Liposome Research (2007), 17(1), 15-26.
176. Nuernberg E., Gassenmeier T., Beutler R.D., Ebinger J., Bade- und Duschzusaetze mit vesikelbildenden Eigenschaften, ihre Herstellung und Verwendung, European Patent 0557825 A2 (1993).
177. Massing U., Cicko S., Ziroli V., Dual asymmetric centrifugation (DAC)—A new technique for liposome preparation. Journal of Controlled Release (2008), 125(1), 16-24.
178. Talsma H., Özer A.Y., van Bloois L., Crommelin D.J.A., The size reduction of liposomes with a high pressure homogenizer (Microfluidizer™). Characterization of prepared dispersions and comparison with conventional methods. Drug Development and Industrial Pharmacy (1989), 15(2), 197-207.
179. Sharma A. Sharma U.S., Liposomes in drug delivery: Progress and limitations. International Journal of Pharmaceutics (1997), 154(2), 123-140.
180. Zhang Z., Huang G., Micro- and nano-carrier mediated intra-articular drug delivery systems for the treatment of osteoarthritis. Journal of Nanotechnology (2012), 1-11
181. Alexa Fluor 488 Monoclonal Antibody Labeling Kit, Molecular Probes (2011), Manuals & Protocols, MP20181.
182. XenoLight CF680 Fluorescent Dye Kits for In Vivo Imaging, Caliper Life Sciences (2009), Technical information.
183. Kong J., Yu S., Fourier transform infrared spectroscopic analysis of protein secondary structures. Acta Biochimica et Biophysica Sinica (2007), 39(8), 549-559.

184. Schüle S., Frieß W., Bechtold-Peters K., Garidel P., Conformational analysis of protein secondary structure during spray-drying of antibody/mannitol formulations. European Journal of Pharmaceutics and Biopharmaceutics (2007), 65(1), 1-9.
185. Dong A., Kendrick B., Kreilgard L., Matsuura J., Spectroscopic study of secondary structure and thermal denaturation of recombinant human factor XIII in aqueous solution. Archives of Biochemistry and Biophysics (1997), 347(2), 213-220.
186. Ahmad A., Salahuddin A., Effect of organic solvents on lysozyme-antilysozyme precipitin reaction. Comparative Biochemistry and Physiology Part C: Pharmacology, Toxicology and Endocrinology (1996), 114(2), 119-121.
187. Rehan M., Younus H., Effect of organic solvents on the conformation and interaction of catalase and anticatalase antibodies. International Journal of Biological Macromolecules (2006), 38(3–5), 289-295.
188. Scharnagl C., Reif M., Friedrich J., Stability of proteins: Temperature, pressure and the role of the solvent. Biochimica et Biophysica Acta (2005), 1749(2), 187-213.
189. Griebenow K., Klibanov A.M., On protein denaturation in aqueous–organic mixtures but not in pure organic solvents. Journal of the American Chemical Society (1996), 118(47), 11695-11700.
190. van de Weert M., Hoechstetter J., Hennink W.E., Crommelin D.J.A., The effect of a water/organic solvent interface on the structural stability of lysozyme. Journal of Controlled Release (2000), 68(3), 351-359.
191. Brandl M., Drechsler M., Bachmann D., Tardi C., Schmidtgen M, Bauer K.H., Preparation and characterization of semi-solid phospholipid dispersions and dilutions thereof. International Journal of Pharmaceutics (1998), 170(2), 187-199.
192. Marrink S.J., Mark A.E., Molecular dynamics simulation of the formation, structure, and dynamics of small phospholipid vesicles. Journal of the American Chemical Society (2003), 125(49), 15233-15242.
193. Colletier J.P., Chaize B., Winterhalter M., Fournier D., Protein encapsulation in liposomes: efficiency depends on interactions between protein and phospholipid bilayer. BMC Biotechnology (2002), 2, 9.
194. Zhao Y.Z., Lu C.T., Increasing the entrapment of protein-loaded liposomes with a modified freeze–thaw technique: A preliminary experimental study. Drug Development and Industrial Pharmacy (2009), 35(2), 165-171.
195. Xu X., Costa A., Burgess D.J., Protein encapsulation in unilamellar liposomes: High encapsulation efficiency and a novel technique to assess lipid-protein interaction. Pharmaceutical Research (2012), 29(7), 1919-1931.
196. Laloy E., Vuillemard J.C., Preparation of liposomes by a simple emulsification technique. Biotechnology Techniques (1994), 8(10), 717-722.
197. Shew R.L., Deamer D.W., A novel method for encapsulation of macromolecules in liposomes. Biochimica et Biophysica Acta, (1985), 816(1), 1-8.
198. Jain M.K., Ramirez F., McCaffrey T.M., Ioannou P.V., Marecek J.F., Leunissen-Bijvelt J., Phosphatidylcholesterol bilayers. A model for phospholipid-cholesterol interaction. Biochimica et Biophysica Acta (1980), 600(3), 678-688.
199. Tseng L.P., Liang H.J., Chung T.W., Huang Y.Y., Liu D.Z., Liposomes incorporated with cholesterol for drug release triggered by magnetic field. Journal of Biological Engineering (2007), 27(1), 29-34.
200. Chan Y.H., Chen B.H., Chiu C.P., Lu Y.F., The influence of phytosterols on the encapsulation efficiency of cholesterol liposomes. International Journal of Food Science & Technology (2004), 39(9), 985-995.
201. Shimizu M., Miwa Y., Hashimoto K., Goto A., Encapsulation of chicken egg yolk immunoglobulin G (IgY) by liposomes. Bioscience, Biotechnology, and Biochemistry (1993), 57(9), 1445-1449.
202. Ramana L., Sethuraman S., Ranga U., Krishnan U.M., Development of a liposomal nanodelivery system for nevirapine. Journal of Biomedical Science (2010), 17(1), 57.

203. Deniz A., Sade A., Severcan F., Keskin D., Tezcaner A., Banerjee S., Celecoxib-loaded liposomes: effect of cholesterol on encapsulation and in vitro release characteristics. Bioscience Reports (2010), 30(5), 365-373.
204. Hsu M.J., Juliano R.L., Interactions of liposomes with the reticuloendothelial system: II. Nonspecific and receptor-mediated uptake of liposomes by mouse peritoneal macrophages. Biochimica et Biophysica Acta (BBA) - Molecular Cell Research (1982), 720(4), 411-419.
205. Mayer L.D., Hope M.J., Cullis P.R., Janoff A.S., Solute distributions and trapping efficiencies observed in freeze-thawed multilamellar vesicles. Biochimica et Biophysica Acta (BBA) - Biomembranes (1985), 817(1), 193-196.
206. Crowe J.H., Crowe L.M., Induction of anhydrobiosis: Membrane changes during drying. Cryobiology (1982), 19(3), 317-328.
207. Castile J.D., Taylor K.M.G., Factors affecting the size distribution of liposomes produced by freeze–thaw extrusion. International Journal of Pharmaceutics (1999), 188(1), 87-95.
208. Kasper J.C., Friess W., The freezing step in lyophilization: Physico-chemical fundamentals, freezing methods and consequences on process performance and quality attributes of biopharmaceuticals. European Journal of Pharmaceutics and Biopharmaceutics (2011), 78(2), 248-263.
209. Cao E., Chen Y., Cui Z., Foster P.R., Effect of freezing and thawing rates on denaturation of proteins in aqueous solutions. Biotechnology and Bioengineering (2003), 82(6), 684-690.
210. Talsma H., van Steenbergen M.J., Salemink P.M., Crommelin D.J.A., The cryopreservation of liposomes. 1. A differential scanning calorimetry study of the thermal behavior of a liposome dispersion containing mannitol during freezing/thawing. Pharmaceutical Research (1991), 8(8), 1021-1026.
211. Crowe J.H., Crowe L.M., Carpenter J.F., Rudolph A.S., Wistrom C.A., Spargo B.J., Anchordoguy T.J., Interactions of sugars with membranes. Biochimica et Biophysica Acta (1988), 947(2), 367-384.
212. Koster K.L., Webb M.S., Lynch D.V., Interactions between soluble sugars and POPC (1-palmitoyl-2-oleoylphosphatidylcholine) during dehydration: vitrification of sugars alters the phase behavior of the phospholipid. Biochimica et Biophysica Acta (BBA) - Biomembranes (1994), 1193(1), 143-150.
213. Ozaki K., Hayashi M., Effect of cycloinulohexaose with additives on the freeze-drying of liposome. International Journal of Pharmaceutics (1998), 160(2), 219-227.
214. Cavatur R.K., Vemuri N.M., Pyne A., Chrzan Z., Toledo-Velasquez D., Suryanarayanan R., Crystallization behavior of mannitol in frozen aqueous solutions. Pharmaceutical Research (2002), 19(6), 894-900.
215. Kiese S., Pappenberger A., Friess W., Mahler H.C., Shaken, not stirred: mechanical stress testing of an IgG1 antibody. Journal of Pharmaceutical Sciences (2008), 97(10), 4347-4366.
216. Bresseleers G.J.M., Goderis H.L., Tobback P.P., Measurement of the glucose permeation rate across phospholipid bilayers using small unilamellar vesicles Effect of membrane composition and temperature. Biochimica et Biophysica Acta (BBA) - Biomembranes (1984), 772(3), 374-382.
217. Allen T.M., Cleland L.G., Serum-induced leakage of liposome contents. Biochimica et Biophysica Acta (BBA) - Biomembranes (1980), 597(2), 418-426.
218. Scherphof G., Roerdink F., Waite M., Parks J., Disintegration of phosphatidylcholine liposomes in plasma as a result of interaction with high-density lipoproteins. Biochimica et Biophysica Acta (BBA) - General Subjects (1978), 542(2), 296-307.
219. Kalie L., Einfluss des Serum-Komplementsystems auf die Permeabilität von Liposomenmembranen, Thesis (2006).

220. Kim C.K., Kim H.S., Lee B.J., Han J.H., Effect of bovine serum albumin on the stability of methotrexate-encapsulated liposomes. Archives of Pharmacal Research (1991), 14(4), 336-341.
221. Schenkman S., Araujo P.S., Dijkman R., Quina F.H., Chaimovich H., Effects of temperature and lipid composition on the serum albumin-induced aggregation and fusion of small unilamellar vesicles. Biochimica et Biophysica Acta (BBA) - Biomembranes (1981), 649(3), 633-641.
222. Yokouchi Y., Tsunoda T., Imura T., Yamauchi H., Yokoyama S., Sakai H., Abe M., Effect of adsorption of bovine serum albumin on liposomal membrane characteristics. Colloids and Surfaces B: Biointerfaces (2001), 20(2), 95-103.
223. Senior J., Gregoriadis G., Stability of small unilamellar liposomes in serum and clearance from the circulation: The effect of the phospholipid and cholesterol components. Life Sciences (1982), 30(24), 2123-2136.
224. Papahadjopoulos D., Fate of liposomes in vivo: A brief introductory review. Journal of Liposome Research (1996), 6(1), 3-17.
225. Tian W., The development of sustained release formulation for pharmaceutical proteins based on vesicular phospholipid gels, Thesis (2010).

LIST OF ABBREVIATIONS

A	absorbance
ATR	attenuated total reflection
AUC	area under the curve
BLV	bilamellar vesicle
BSA	bovine serum albumin
Cryo-TEM	cryo-transmission electron microscopy
DAC	dual asymmetric centrifuge
DLS	dynamic light scattering
DMARD	disease-modifying anti-rheumatic drug
DMSO	dimethylsulfoxide
DSC	differential scanning calorimetry
EA	ethyl acetate
EE	encapsulation efficiency
ELISA	enzyme-linked immunosorbent assay
FCS	fetal calf serum
FDA	Food and Drug Administration
FITC	fluorescein isothiocyanate
F-mAb	fluorescence-labeled monoclonal antibody
FT	freeze-thaw
FTIR	Fourier transform infrared spectroscopy
GH	growth hormone
GRAS	generally recognized as safe
HA	hyaluronic acid
HEC	hydroxyethyl cellulose
HP-IEC	high performance ion exchange chromatography

HPLC	high performance liquid chromatography
HP-SEC	high performance size exclusion chromatography
I	ionic strength
IA	intra-articular
IgG1	immunoglobulin 1
Ile	isoleucine
IV	intravenous
K_D	dissociation constant
mAb	monoclonal antibody
MLV	multilamellar vesicle
mu	murine
MW	molecular weight
NMP	*N*-methyl-2-pyrrolidone
OA	osteoarthritis
OG	octyl glycoside
PBS	phosphate buffered saline
PdI	polydispersity index
PEG	polyethylene glycol
PG	propylene glycol
Phe	phenylalanine
pI	isoelectric point
pKa	acid dissociation constant
PL	phospholipid
PLA	polylactide
PLGA	poly(lactide-co-glycolide)
P/T	PEG 300/triacetin
PVDF	polyvinylidene difluoride
RA	rheumatoid arthritis
rhG-CSF	recombinant human granulocyte colony stimulating factor
rhTNF	recombinant human tumor necrosis factor

RM	residual moisture
RT	room temperature
SC	subcutaneous
sd	spray-dried
SEM	scanning electron microscopy
SF	synovial fluid
SPIONs	superparamagnetic iron oxide nanoparticles
SPR	surface plasmon resonance
TGF-β	transforming growth factor-β
T_{in}/T_{out}	spray drying inlet/outlet temperature
T_m	melting temperature
TNF	tumor necrosis factor
Trp	tryptophane
Tyr	tyrosine
ULV	unilamellar vesicle
UV	ultraviolet
vs.	versus
w/w	weight per weight